Epigenetic mechanisms regulating epithelial-mesenchymal plasticity in breast cancer

Inauguraldissertation

zur
Erlangung der Würde eines Doktors der Philosophie
vorgelegt der
Philosophisch-Naturwissenschaftlichen Fakultät
der Universität Basel

von

Ayse Nihan Kilinc

aus Istanbul, Turkei

Basel, 2017

Genehmigt von der Philosophisch-
Naturwissenschaftlichen Fakultät
auf Antrag von

Prof. Dr. Gerhard M. Christofori, Prof. Dr. Dirk Schübeler

Basel, 20th June 2017

Prof. Dr. Martin Spiess

Table of contents

Summary

An epithelial-mesenchymal transition (EMT) is a fundamental example of cell plasticity, involving a reversible switch from epithelial to mesenchymal cell states. An EMT endows stationary epithelial cells with migratory and invasive potential, leads to intravasation into the blood circulation and extravasation to the distant organ. To promote metastatic outgrowth, mesenchymal cells undergo a reverse process of mesenchymal-epithelial transition (MET). Therefore, it is important to understand the underlying mechanisms of epithelial-mesenchymal plasticity to design effective therapeutic approaches that revert EMT and prevent tumor cell invasion and metastasis.

The dynamic cell state transitions during EMT imply a role for chromatin rearrangements that are established by epigenetic regulators. However, we still do not fully understand the differences between the epigenetically regulated mechanisms defining the transient cell state transitions of a reversible EMT and the fixed cell status of an irreversible EMT. To delineate these differences, we have generated from murine mammary epithelial cancer cells a novel *in vitro* irreversible EMT model as compared to a reversible EMT model. Reversible EMT is induced by TGF-β, a potent inducer of EMT. Upon removal of TGF-β, mesenchymal cells undergo a MET and revert to the epithelial state. In contrast, *in vitro* irreversible EMT cells maintain their mesenchymal state even after removal of the EMT-inducing growth medium. These EMT systems have provided us a unique opportunity to identify the *de novo* established epigenetic modifiers which maintain the mesenchymal state.

Gene expression analysis has revealed a remarkable difference between the reversible and the irreversible EMT systems. Interestingly, irreversible EMT cells exhibit a highly aggressive phenotype in terms of tumor growth rate and metastasis formation as compared to the reversible EMT cells. To identify the epigenetic regulators contributing to the maintenance of the mesenchymal cell state and the aggressive phenotype of irreversible EMT cells, we have used several pharmacological inhibitors targeting various

epigenetic modifiers. We have found that histone deacetylase (HDAC) inhibitors partially revert irreversible EMT cells into an epithelial cell state. Due to the merely partial contribution of HDACs to an irreversible EMT, we have further explored additional contributors to the maintenance of the mesenchymal cell state. HDACs are involved in several corepressor complexes to exert their specific functions. The Mbd3/NuRD complex is one of the corepressor complexes containing HDAC1/2. It plays an important role in the generation of induced pluripotent stem (iPS) cells from mouse embryonic fibroblasts (MEFs), indicating a key role in cellular plasticity. Notably, Mbd3 is the only methyl binding domain protein which is not able to bind to the methylated cytosines due to an amino acid substitution in the methyl binding domain. Instead, it is thought that it recognizes the DNA demethylation intermediate 5-hydroxymethyl cytosine which is generated by Tet hydroxylases.

Using loss of function experiments, we demonstrate that the Mbd3/NuRD complex, involving histone deacetylases (HDACs) and Tet2 hydroxylase, acts as an epigenetic block in epithelial-mesenchymal plasticity. Interestingly, these epigenetic factors keep the mesenchymal cells in a stable state and promote the aggressive cancer cell phenotype by regulating a wide-range of gene networks. The pharmacological inhibition of HDACs and ablation of Mbd3 and/or Tet2 leads to a MET as well as to diminished tumor growth and metastasis formation. These results provide important insights into the epigenetic regulation of epithelial-mesenchymal plasticity and identify novel therapeutic targets to interfere with primary tumor growth and metastasis formation. In particular, the development of specific inhibitors of Tet hydroxylases and their combinatorial use with HDAC inhibitors may be an effective therapeutic approach to prevent tumor progression and metastasis.

1 Introduction

1.1 Epithelial to mesenchymal transition

Epithelium is the one of the most common and abundant type of tissue. It is found really early in the embryonic development and forms the lining of most tissues. Epithelial cells are converted to mesenchymal cells through “epithelial-mesenchymal transformation”. Elizabeth Hay first observed this process during the primitive streak formation in the chick embryos, with dramatic morphological changes of the epithelial cells (Hay, 1995). However, after the discovery of reverse mechanism of mesenchymal to epithelial transition, the term “transformation” was replaced by “transition”, thereby reflecting the reversibility of the process (Thiery, 2002). (Wicki et al., 2006)

1.1.1 Basics of EMT

The epithelium is a highly organized tissue consisting of single layered squamous or single/multilayered sheets of cuboidal and columnar cells. Simple epithelium is formed by epithelial cells characterized by apical-basal polarity, cell-cell junctions and their attachment to the basal lamina. These structures maintain the tissue integrity and stabilize the epithelial cells within a restricted area (Baum et al., 2008). Upon induction of EMT, epithelial cells undergo morphological and functional changes by disruption of the cell junctions and apical-basal polarity, and reorganizing their actin cytoskeleton that gives rise to motile cells which invades the basement membrane (Thiery et al., 2009). The hallmarks of EMT are discussed below (Figure 1).

i) Disruption of cell-cell junctions during EMT: The polarized epithelial cells are tightly connected through specialized intercellular junctions such as tight junctions, adherens junctions, desmosomes and gap junctions (Thiery and Sleeman, 2006). Tight junctions provide a physical intercellular barrier and prevent the fluid exchange between the luminal and stromal compartments. They reside at the boundary between the apical and lateral surface. Claudins and zona occludens (ZO-1, ZO-2 and ZO-3) are the most important components of the tight junctions (Giepmans and van Ijzendoorn, 2009). Upon induction of EMT, claudins/zona occludens are downregulated

and ZO-1 translocates to the cytoplasm (Huang et al., 2012). Adherens junctions reside at the lateral surface and mediate the cell-cell contact along with tight junctions. E-cadherin is a calcium-dependent, single-span transmembrane glycoprotein, which belongs to the classical cadherins family (Yilmaz and Christofori, 2009). E-cadherin binds to β-catenin through its cytoplasmic domain and β-catenin binds to α-catenin, which mediates the interaction with actin microfilaments (Huang et al., 2012). EMT induces loss of E-cadherin and gain of N-cadherin, known as cadherin switch involved during development and tumor cell invasion (Cavallaro et al., 2002; Christofori, 2003). Desmosomes, adhesive junction components interacting with the intermediate cytokeratin filaments are disrupted during EMT (Huang et al., 2012). Gap junctions mediate the exchange of ions and small molecules between the cells through hemi-channels. Reducing connexin levels diminish the integrity of gap junctions (Lamouille et al., 2014).

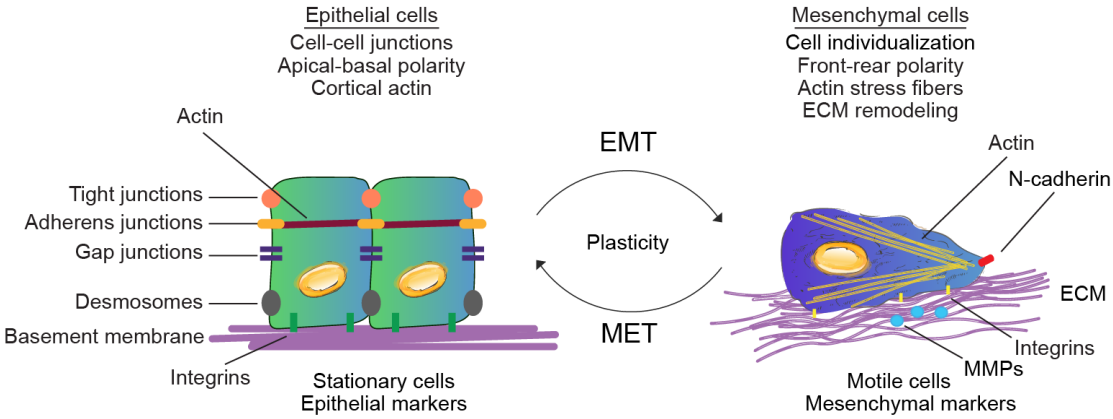

Figure 1: Hallmarks of EMT. The initial steps of epithelial-mesenchymal transition (EMT) are the disassembly of cell–cell contacts, tight junctions, adherens junctions, desmosomes and gap junctions and E-cadherin switch to N-cadherin. Apical-basal polarity turns into front-rear polarity. The expression of epithelial genes is repressed, accompanied by mesenchymal gene activation. Further, cortical actin is reorganized into stress fibers, cells secrete matrix metalloproteinases (MMPs) leads to remodeling of extracellular matrix (ECM) and drive migration and invasion by the formation of cell-matrix adhesions through, integrins. EMT is able to undergo reverse process mesenchymal–epithelial transition (MET) and revert to the epithelial state.

ii) Loss of apical-basal polarity: The apical-basal polarity of the epithelial cells leads to the vectorial transportation of soluble factors and cellular components. Upon EMT, the apical-basal polarity turns into front-rear polarity to provide directional migration (Nelson, 2009). Epithelial polarity is mediated by several group of proteins such as partitioning defective (Par), Crumbs, and Scribble, and lipids such as phosphoinositides and Rho GTPases (Cdc42, Rac1 and RhoA). The Crumbs complex leads to immature apical junction by acting with the Cdc42-Par3-Par6-atypical protein kinase C (aPKC) and the Scribble complexes, which matures into tight junctions and adherens junctions (Jaffe and Hall, 2005; Rodriguez-Boulan and Macara, 2014).

iii) Cytoskeletal rearrangements: Cytoskeleton provides tissue integrity and mechanical strength via actin cytoskeleton, microtubules and intermediate filaments. Cytoskeleton is rearranged during EMT and act as a driving force for cell migration and invasion (Sun et al., 2015). In epithelial cells, actin is localized cortically, whereas in mesenchymal cells actin is reorganized into stress fibers (Thiery et al., 2009). Actin machinery is mainly regulated by Rho GTPase family which conduct signals from chemokines, growth factors and adhesion receptors to actin remodeling. RhoA, Rac1, Cdc42 belonging to RhoGTPase family are important regulators of cell migration and invasion. RhoA is responsible of actin stress fiber formation, Rac1 and Cdc42 mediate lamellipodia and filopodia formation, respectively (Yilmaz and Christofori, 2009). Microtubules are also regulated during EMT induced cell migration. Upon EMT, microtubules that are uniformly distributed in cytoplasm translocate mainly to the protrusions and drive cell migration. Intermediate filaments are dramatically rearranged during EMT, exhibiting a switch between different types of intermediate filaments. For example, epithelial cells are rich with type I keratin, while mesenchymal cells are enriched with type III vimentin (Sun et al., 2015).

iv) *ECM remodeling:* Extracellular matrix (ECM) provides a 3D structure to a cell to regulate tissue homeostasis, cell proliferation, differentiation and migration. Basal lamina is a specialized type of ECM, which segregates epithelium from the surrounding stroma. Epithelial tissue interacts

with the basal lamina through integrins (Bonnans et al., 2014; Yilmaz and Christofori, 2009). Integrins are transmembrane proteins that are composed by α and β chains and different combinations of α/β subunits can form 24 different integrins in a cell-type or a stage-specific manner (Hynes, 2002), though a handful of them are specific to the basal lamina. During EMT, epithelial cells lose their contact with the basal lamina. Mesenchymal cells remodel the basal lamina by secreting new components of ECM, downregulating some epithelial integrins and upregulating/synthesizing new integrins (Radisky, 2005; Yilmaz and Christofori, 2009). For example, epithelial-specific $\alpha_6\beta_4$ integrin is epigenetically silenced during EMT (Yang et al., 2009), while $\alpha_5\beta_1$ integrin is induced in mesenchymal cells which regulates the cell adhesion to fibronectin, increased during EMT and promotes cell migration (Maschler et al., 2005). Interaction of $\alpha_1\beta_1$ or $\alpha_2\beta_1$ integrins with collagen type 1 induces EMT by downregulating E-cadherin and $\alpha_5\beta_8$ integrin induces the matrix metallaproteinases (MMPs) expression and liberate/activate TGF-β, a potent inducer of EMT (Araya et al., 2006; Yilmaz and Christofori, 2009).

1.1.2 EMT in physiological contexts

EMT is classified in three different subgroups. Type 1 EMT is associated with the developmental EMT, which leads to the formation of different tissue types with various functions. Type 2 EMT involved in physiological context such as wound healing, tissue remodeling, and pathological processes such as organ fibrosis. Type 3 EMT is characterized in the pathological context such as cancer with the uncontrolled systemic invasion of cancer cells. Although, these three types of EMT share common features, they also exhibit distinct characteristics according to the cellular context (Figure 2) (Kalluri and Weinberg, 2009; Nieto, 2013).

Type 1 EMT is involved at different stages of embryonic development, including mesoderm formation, neural crest and heart valve development, as well as secondary plate formation. The transition between epithelial and mesenchymal cells is not necessarily an irreversible commitment. Several rounds of EMT and MET are required during organ formation referred to as primary, secondary and tertiary EMT events. During gastrulation, epithelial

cells of the single layer epiblast undergo primary EMT and migrate from the primitive streak to form the mesoderm and endoderm. Later, the

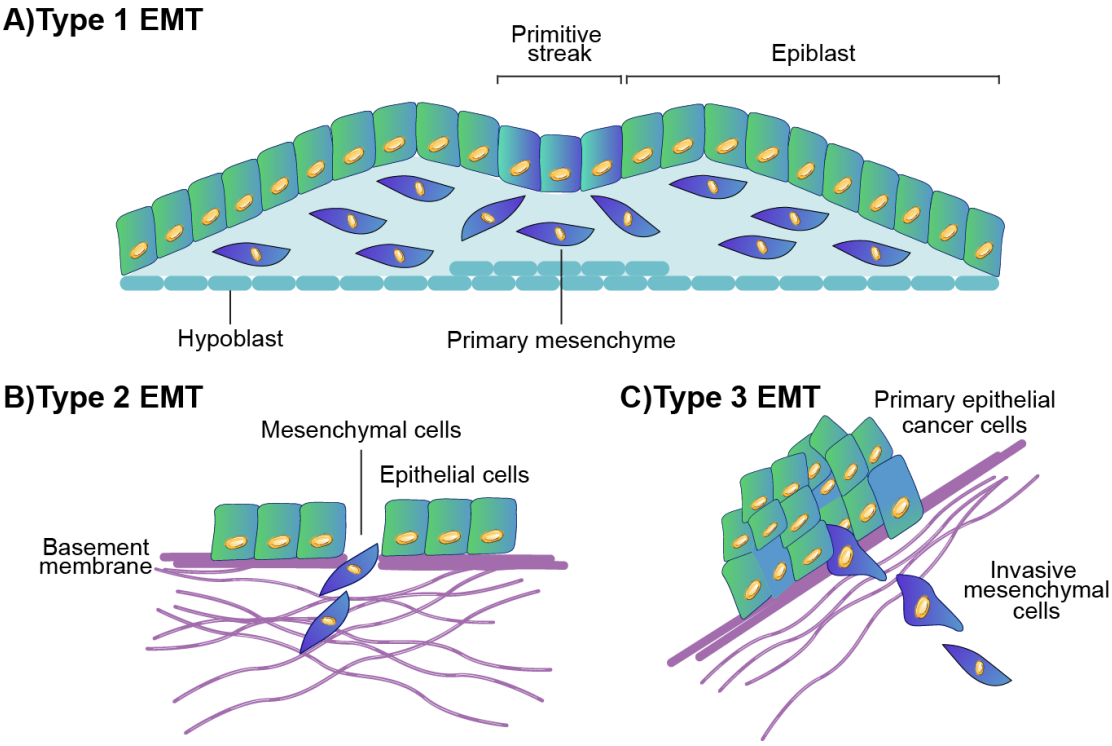

Figure 2: Different types of EMT. A) Type 1 EMT is associated with developmental EMT. During gastrulation, the primitive epithelium, specifically the epiblast, undergoes primary EMT and migrates from the primitive streak, giving rise to primary mesenchyme. Further lineage specifications are established by MET and with several rounds of EMT. B) Type 2 EMT involved in the physiological context such as wound healing. C) Type 3 EMT is characterized in the pathological context such as cancer. Primary epithelial cancer cells undergo an EMT which endows cells with migratory and invasive potential to invade their basement membrane (Adapted from (Kalluri and Weinberg, 2009)).

mesenchymal cells revert to a transient epithelial state, which forms the notochord, the somites, primordia of the urogenital system, the somatopleure and splanchnopleure. Except the notochord, a second round of EMT is observed to give rise to more differentiated cell types. For instance, the dorsal part of the somites give rise to dermis and muscle satellite cells while the ventral somites generate the vertebrae, tendons and ribs. Somatopleure generates the connective tissue of body wall muscle, while the

Splanchnopleure gives rise to haematopoietic, endocardial progenitors and later to the endocardial cushions which are the progenitors of heart valves via tertiary EMT. In neural crest formation, neural crest cells undergo EMT and gain migratory capacity for long distances and generate the peripheral nervous system, some endocrine cells and melanocytes (Thiery et al., 2009; Yang and Weinberg, 2008) (Nieto, 2013).

Type 2 EMT plays a role during wound healing. Keratinocytes undergo an EMT-like process at the border of the wound as a physiological response to injury. In addition, EMT is not only involved in the physiological condition, but also during pathological organ fibrosis. In fibrosis, epithelial cells undergo an EMT and give rise to myofibroblast cells in renal tissue (Iwano et al., 2002). The same mechanism is also observed in lens epithelium, endothelium, hepatocytes and cardiomyocytes during tissue fibrosis. Myofibroblasts together with the immune cells deposit excessive amount of ECM components such as collagens, laminins, elastins and tenacins which leads to organ failure (Kalluri and Weinberg, 2009; Thiery et al., 2009).

Type 3 EMT accompanies cancer progression in epithelial tumors. Upon EMT, stationary epithelial cells lose their cell-cell junctions and acquire motility to invade their basement membrane. EMT process induces the dissemination of tumor cells and intravasation into the blood circulation and extravasation into a distant organ. It is proposed that the reverse process MET in the distant tissue is crucial to promote metastatic colonization. EMT is also implicated in acquisition of stem-like properties, drug resistance and immune surveillance (Thiery et al., 2009). The role of EMT in tumor progression and the contribution of EMT/MET plasticity to tumor metastasis will be discussed in detail in the next chapters (1.1.3) and (1.1.4), respectively.

1.1.3 EMT in tumor progression and metastasis

Carcinomas, derived from epithelial tumor cells are the cause of 90% mortality in human cancers (Mehlen and Puisieux, 2006). Tumor progression and metastasis is proposed as a multistep process of morphological aberrations accompanied by genetic and epigenetic alterations. Only a subset of cells that have accomplished full malignant transformation can leave the

primary tumor site and seed for metastasis. This is referred to as the linear progression model and it is based on the observations of the association of the primary tumor size with high metastatic incidence. However, there is also another model, termed as the parallel progression model, suggesting the neoplastic cells might disseminate long before the detectable tumors due to the growth rates of primary tumors (Klein, 2009).

The metastatic cascade as shown in Figure 3 involves several steps from the formation of the primary tumor until the successful colonization of the tumor cells at the distant site. Tumor cells exhibit an excessive proliferation rate in the epithelial primary tumors and require blood vessels to survive, a process called angiogenesis. Subpopulation of stationary epithelial tumor cells gains migratory and invasive capacity, migrate through the basement membrane into the blood circulation. Only a subset of cells that are able to survive in the blood circulation extravasate into the distant organ. It is proposed that mesenchymal cells revert back to the epithelial state in the distant organ to form the metastatic colonization (Chambers et al., 2002; Hanahan and Weinberg, 2011).

EMT is proposed as a crucial mechanism in different stages of cancer progression from benign adenoma to malignant carcinoma. It has been shown that EMT endows epithelial tumor cells with migratory and invasive properties *in vitro* and *in vivo* (Tiwari et al., 2012). Epithelial tumor cell de-differentiation is observed at the invasive front with loss of epithelial markers and gain of mesenchymal phenotype (Kirchner and Brabletz, 2000). Additionally, loss of E-cadherin, a profound marker of EMT correlates with poor patient survival rate in many carcinomas (Berx et al., 2007). However, a full EMT phenomenon is rarely observed in the clinical samples, thus involvement of EMT during tumor cell invasion is still under debate (Christofori, 2006). On the contrary, partial EMT, the coexistence of epithelial and mesenchymal markers is a more frequently observed event *in vivo* (Berx et al., 2007). Difficulties to observe partial EMT can be circumvented by *in vivo* lineage tracing experiments (Beck and Blanpain, 2013).

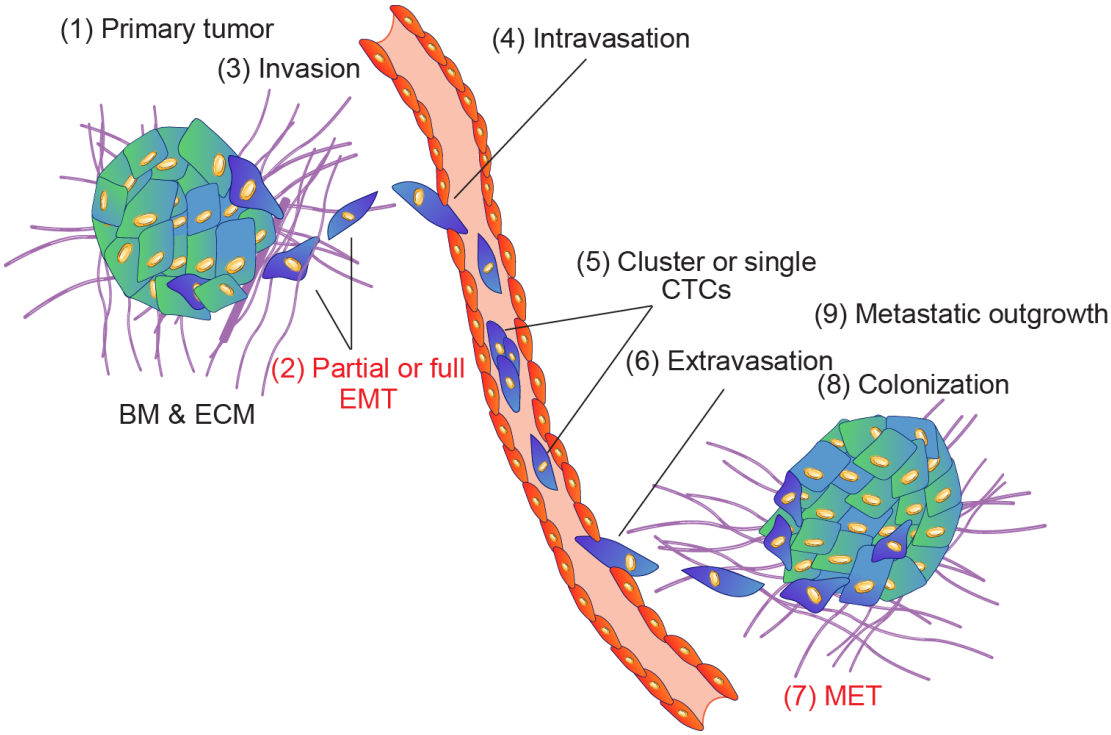

Figure 3: EMT/MET plasticity in metastatic cascade. (1) Primary epithelial tumor cells (green) exhibit high proliferation (2) Epithelial cells undergo either partial or full EMT (blue) and gain migratory potential (3) Migratory mesenchymal cells invade through the basement membrane (4) intravasate into the blood circulation (5) as clusters or single circulating tumor cells (CTCs) with mesenchymal characteristics (6) extravasate to the distant organ (7) invade parenchyma, enter a dormant state or undergo MET (8) start colonizing (9) form metastatic outgrowth.

Single or clusters of circulating tumor cells (CTCs) from breast cancer patients exhibit EMT phenotype (Yu et al., 2013) which is highly correlated with the metastatic disease, indicating the involvement of EMT in the metastatic outgrowth (Kallergi et al., 2011). However, distant metastases mostly exhibit an epithelial phenotype brought the idea of dynamic regulation of EMT process. It is proposed that EMT program is activated during invasion, dissemination process and upon arrival of tumor cells to the distant site, the reverse process MET takes place to form metastatic outgrowth (Thiery, 2002). Even though the contribution of EMT/MET plasticity has been demonstrated in several studies (Ocaña et al., 2012; Tsai et al., 2012), the role of EMT to promote metastatic outgrowth is still hotly debated (Tarin, 2005; Thomson et

al., 2005). Epithelial-mesenchymal plasticity will be further discussed in detail in the next chapter.

1.1.4 Plasticity of EMT

Plasticity of a cell refers to the reversible changes in phenotypic cell states such as EMT. EMT is a fundamental example of cell plasticity that involves a reversible switch within a spectrum of fully epithelial and mesenchymal cell states by involving partial EMT/MET cell states. Partial EMT/MET cell states are often accompanied by a higher degree of cell plasticity due to the acquired flexibility for rapid transition between cell states. The plastic nature of EMT is a shared mechanism between physiological and pathological conditions, such as development and cancer, respectively (Figure 4) (Nieto et al., 2016; Tsai and Yang, 2013).

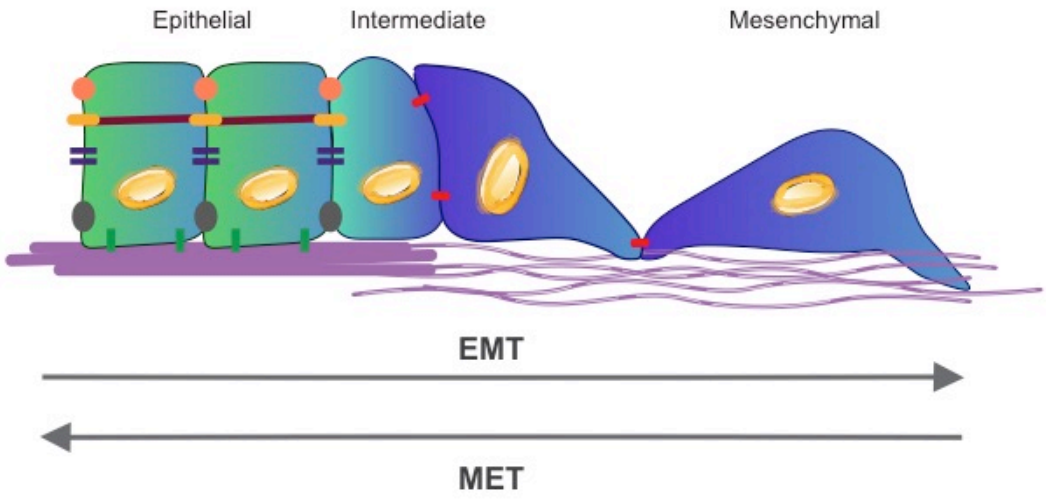

Figure 4: Plasticity of EMT. EMT is a reversible switch within a spectrum of the fully epithelial and mesenchymal cell states by involving the intermediate cell states. The color transitions represent hypothetical transitions.

The crucial role of EMT/MET plasticity is observed in early embryonic development (Nieto, 2013). (See chapter: EMT in physiological context). The best-studied example of MET is during kidney development. During this process, excretory tubules undergo MET which is induced by collecting duct system invasion through area of mesenchymal cells. The cells start polarizing

and establishing cell-cell contacts to form the kidney tubules (Yang and Weinberg, 2008).

EMT plasticity is also involved in induced pluripotent stem cells (iPSCs) generation, a cell-reprogramming process established by the overexpression of Oct4 (Pou5f1), Klf4, Sox2, and c-Myc (OKSM) in somatic cells (Apostolou and Hochedlinger, 2013). It has been shown that MET is a prerequisite in the initiation phase of the reprogramming of MEFs to iPS cells (Fu et al., 2011; Samavarchi-Tehrani et al., 2010). MET is observed with the upregulation of epithelial markers E-cadherin and Epcam, accompanied by downregulation of mesenchymal markers Snail and N-cadherin during cell reprogramming (Samavarchi-Tehrani et al., 2010). It has been also suggested that overexpression of Snail, and the depletion of E-cadherin suppresses MET dramatically impairing the cell reprogramming process (Li et al., 2010). Additionally, Klf4, one of the reprogramming factors, which is responsible in the maintenance of epithelial phenotype, binds directly to the E-cadherin promoter, thereby inducing a MET during iPSC formation (Polo and Hochedlinger, 2010).

The dynamic transitions from epithelial to mesenchymal cell states have been proposed as a crucial mechanism promoting tumor invasion and metastatic dissemination (Baum et al., 2008; Thiery, 2002). However, the role of EMT/MET plasticity in the formation of secondary tumors at the metastatic site is still under debate. As it has been shown in the metastatic squamous cell carcinoma model, the “reversible” EMT cells with the Twist1 inactivation at the metastatic site has higher metastatic colonization in the lungs compared to the “irreversible” EMT cells that constitutively express Twist1. Depletion of Twist1 led to a MET with increased proliferation rate. Twist1 activation irrespective of the “reversible” or “irreversible” condition led to an increase in the number of CTCs and extravasated tumor cells into the lungs, indicating the role of EMT during dissemination (Tsai et al., 2012). This study provides *in vivo* evidence to the necessity of MET during metastatic colonization. Requirement of MET in the metastatic colonization has been also suggested by downregulation of EMT activator transcription factor Prrx1 at the metastatic site (Ocaña et al., 2012). Several reports suggested that re-differentiation through MET is required for the switch from EMT-associated growth arrest to

the higher proliferating epithelial cells to form the metastatic outgrowth (Brabletz, 2012). It can be argued that some therapeutic approaches may lead to the reversion of EMT that enhances the metastatic outgrowth.

It is proposed that mesenchymal state is induced and maintained by continuous microenvironmental signals. Removal of those signals brings the cells to their default epithelial state (Tam and Weinberg, 2013). For instance, upon adding TGF-β, epithelial cells undergo an EMT and with the removal of TGF-β, mesenchymal cells revert back to their epithelial state (Waldmeier et al., 2012). However, it is important to note that we still do not have enough evidence to understand whether MET-driven epithelial cells are identical with their initial epithelial counterparts. It is more likely that MET-derived epithelial cells are different than their ancestors, which is implicated during developmental processes.

1.1.5 EMT in breast cancer

Breast cancer is the most commonly diagnosed cancer in women. 90% of the breast cancer mortality is due to the local invasion and metastasis (Wang and Zhou, 2011). Breast cancer is heterogeneous disease with different subtypes characterized among different individuals as well as within the same tumors (Ellsworth et al., 2017). Characterization of the diversity of breast cancers is important for better prognosis and to apply appropriate therapy (Schnitt, 2010).

Initially, breast cancer subtypes were classified according to their morphology. Later on, immunopathological differences were also taken into account to assess them by estrogen receptor (ER), progesterone receptor (PR), and human epidermal receptor 2 (HER2). ER+ tumors are targeted with ER antagonists or aromatase inhibitors, which are anti-estrogen therapy (Jordan and Brodie, 2007). PR status does not add any benefit to endocrine therapy. HER2+ tumors are treated with monoclonal antibody trastuzumab which binds to HER2, inhibits HER2 signaling, significantly improving the overall outcome of the disease. ER+ tumors are associated with the best therapeutic outcome, whereas triple negative (TN) breast cancer (ER-/PR-/HER2-) correlate with the worst prognosis (Bertos and Park, 2011).

Gene expression profiling studies added another layer to the characterization of breast cancer subtypes. They are classified as Luminal A, Luminal B, HER2-enriched basal-like, normal breast-like, and claudin-low. Claudin-low tumors exhibit mesenchymal phenotypes that are characterized by low expression of epithelial markers (E-cadherin, claudins and occludins), triple-negative status of luminal markers, and hormone receptors. However, in contrast to the expected poor prognosis predicted by the presence of EMT which causes tumor cell invasion and metastasis, claudin-low tumors are not associated with worse prognosis compared to luminal B, HER2-enriched or basal-like. Yet, claudin-low tumors are more resistant to chemotherapy, in line with the contribution of EMT to therapy resistance (Bill and Christofori, 2015).

It has been shown that in some cases of triple-negative breast tumors exhibit simultaneous expression of epithelial and mesenchymal markers in the core of the tumor which is histologically indistinguishable from neighboring epithelial cells (Yu et al., 2013). Co-expression of epithelial and mesenchymal markers is also implicated in claudin-low and basal-like breast cancers, indicating a “partial EMT” phenotype (Prat et al., 2010). These findings are consistent with the implicated role of partial EMT in cancer stemness and aggressiveness which indicates that partial EMT is more likely to occur rather than a full EMT in breast cancers (Davis et al., 2014; Tsai and Yang, 2013).

1.2 Inducers of EMT

A plethora of extracellular stimuli can activate an EMT program during development, wound healing and malignant tumor progression. An EMT is triggered by soluble growth factors such as transforming growth factor-β (TGF-β), fibroblast growth factor (FGF), epidermal growth factor (EGF), insulin-like growth factor (IGF), hepatocyte growth factor (HGF), platelet-derived growth factor (PDGF) and vascular endothelial growth factor (VEGF) in a context-dependent manner (Lamouille et al., 2014). Epithelial cells respond to these ligands by activating receptor-mediated intracellular signaling pathways, such as TGF-β, EGF, FGF, Wnt, Notch and many others and cross-talk between these pathways regulate EMT process. For example, TGF-β/Smad pathway regulate EMT by cooperating with activated Ras kinase

pathway through receptor tyrosine kinases (RTKs) is required for maintenance of complete EMT (Zavadil and Bottinger, 2005). EMT can also be induced by hypoxia, cytokines and mechanical stress (Gjorevski et al., 2012).

1.2.1 TGF-β signaling in EMT

TGF-β signaling controls cell behavior in many diverse processes, including cell proliferation, differentiation, apoptosis, hence tissue homeostasis during development and tissue regeneration. Upon TGF-β ligand binding, type I and type II TGF-β receptors interact and form a heterotetrameric complex, followed by phosphorylation of type I receptor. Activated type I TGF-β receptor leads to phosphorylation of receptor regulated Smad (R-Smad) proteins, Smad2 and Smad3. R-Smads form a complex with common-mediator Smad (Co-Smad), Smad4 and translocate to the nucleus to regulate the target gene expression by interacting with other transcriptional cofactors (Shi and Massagué, 2003; Zavadil and Bottinger, 2005).

The role of TGF-β in induction of EMT is shown in normal mammary epithelial cells with phenotypic change from cuboidal morphology to fibroblast-like phenotype, with concomitant decrease of epithelial and upregulation of mesenchymal markers, with increased motility. This EMT is reversed upon removal of TGF-β (Miettinen et al., 1994). Further, it has been shown that TGF-β/Smad signaling induce transcription factor Snail (Hoot et al., 2008), which in return interacts with Smad3 and Smad4 to repress epithelial genes E-cadherin and occludin (Vincent et al., 2009). TGF-β leads to a gradual increase of Zeb1 and Zeb2, which are required to repress E-cadherin expression during EMT, which is further controlled by MAPK signaling (Shirakihara et al., 2007).

TGF-β can also induce EMT through RhoGTPases, Pi3K and MAPK pathways, named as non-canonical TGF-β signaling. RhoGTPases such as RhoA, Rac1 and Cdc42 drive cell migration and invasion by rearranging actin cytoskeleton and forming lamellipodia and filopodia, respectively (Yilmaz and Christofori, 2009). TGF-β induces mammalian TOR complex 1 and 2 (mTORC1 and mTORC2) via activating AKT/PI3K pathway during EMT,

required for cell size, migration and an EMT phenotype, respectively (Lamouille et al., 2014). Additionally, TGF-β can activate Erk/MAPK pathway, which drives disassembly of adherens junctions and cell motility during EMT (Zavadil and Bottinger, 2005).

1.3 Transcriptional and post-transciptional control in EMT

EMT is regulated by highly orchestrated networks of alternative spicing and transcriptional control mechanisms. The cooperation between transcriptional and post-transcriptional machinery contributes to the epithelial mesenchymal plasticity and deregulation drives malignant tumor progression (Lamouille et al., 2014).

1.3.1 Transcriptional control of EMT

Extracellular signals activate an EMT program, regulate switches from epithelial to mesenchymal cell states through contribution of many transcription factors in tissue-specific manner. The transcription factor families such as Snail, includes zinc finger proteins (Snail and Slug), Zeb1 family (zinc-finger E-box binding Zeb1 and Zeb2) and Twist (basic helix-loop-helix proteins Twist1, Twist2, Id, E12, E47) are referred to as the master regulators of EMT process. These transcription factors are activated by various microenvironmental signals such as TGF-β, Wnt family proteins and Notch. These ligands activate several signaling pathways to regulate the initiation and maintenance phases of an EMT (Lamouille et al., 2014).

Snail1, Zeb1 and Twist1 can repress epithelial genes by interacting with the E-box DNA sequences, acting as an early inducer of EMT. They mediate transcriptional repression of E-cadherin, the most crucial step during EMT, by recruiting several epigenetic complexes (Dong et al., 2013; Dong et al., 2012; Herranz et al., 2008; Lin et al., 2010a; Peinado et al., 2004; Wang et al., 2007; Yang et al., 2010) (See chapter: Histone modifications during EMT). Further, they regulate EMT and cell motility through repression of other epithelial genes such as claudins and occludins and activate mesenchymal

gene expression such N-cadherin and several ECM proteins (Lamouille et al., 2014).

Transcription factors are aberrantly induced during cancer progression. Snail and Twist1 are highly expressed, associated with repression of E-cadherin in breast carcinoma (Cheng et al., 2001). High expression levels of Snail and Zeb2, correlated with low expression levels of E-cadherin in breast cancer (Elloul et al., 2005). Increased expression levels of Slug is associated with metastasis in human breast cancers (Martin et al., 2005). Zeb1 promotes metastasis in colorectal cancers by repressing cell polarity gene, Lgl2 (Spaderna et al., 2008).

In addition to these transcription factors, large number of transcription factors are implicated in EMT and malignant tumor progression such as Sox4 (Tiwari et al., 2013b), Prrx1 (Ocaña et al., 2012), Klf4 (Tiwari et al., 2013a) and many others.

1.3.2 Alternative splicing in EMT

Alternative splicing of mRNAs is a post-transcriptional mechanism, which leads to generation of different mRNA and protein isoforms. Extensive isoform changes are also implicated during EMT with alternative splice variants mutually exclusive to the epithelial and mesenchymal cell states during EMT (Brown et al., 2011; Eswarakumar et al., 2002; Pino et al., 2008).

Fibroblast growth factor 2 (FGFR2) is spliced into two isoforms, exon FGFRIIIb is associated with the epithelial cells, while exon FGFRIIIc is specific to the mesenchymal cells, which are both tightly regulated during development (De Moerlooze et al., 2000; Eswarakumar et al., 2002). A switch from variant isoforms (CD44v) to the standard isoform (CD44s) of CD44, a cell surface marker, is required to drive EMT process. In addition, the CD44s isoform is highly expressed in high-grade human breast tumors (Brown et al., 2011). A member of the Ena/VASP family, hMena (ENAH) spliced to hMena^{+11a} is implicated as an epithelial marker in human pancreatic cancer cell lines (Pino et al., 2008). In addition, cadherin-associated protein p120 catenin regulates RhoGTPases and cell motility by cell state specific splice variants. Epithelial cells expess short-length p120 isoforms, lack N-terminal domain, while mesenchymal cells express the full length transcript to repress

RhoA activity (Yanagisawa et al., 2008). It is shown that splicing of FGFR2, CD44, ENAH and p120-Catenin (CTNND1) is regulated by Epithelial Splicing Regulatory Proteins 1 and 2 (ESRP1 and ESRP2), master regulators of the epithelial-specific splicing process. The depletion of ESRP1 and ESRP2 induced a switch from epithelial-specific isoforms to the mesenchymal state associated transcript variant induced an EMT, is rescued with ectopic expression of ESRP1 (Warzecha et al., 2009). In addition, RBFOX2 is a crucial regulator of the mesenchymal-specific splicing events (Venables et al., 2013) and the ratio between ESRP1 or ESRP2 and RBFOX2 which is decreased during EMT, correlated with higher risk of metastasis in early breast cancer patients, indicating a potential biomarker for metastasis in breast cancer (Fici et al., 2017). In summary, highly coordinated events during mutually exclusive regulation of splicing variants in epithelial and mesenchymal cells provide important insights in the regulation of reversible cell states.

1.4 Epigenetic regulation of EMT

In 1942, Waddington defined the term “epigenetics” as changes in phenotype without an effect on genotype. Later on, it was further clarified that inheritance of gene expression is transmitted by epigenetic mechanisms by modifying chromatin without any alterations to the genomic sequence. Enzymatic changes in the chromatin state may dictate a cell to alter its gene expression as well as epigenetic regulators. Euchromatin (open-chromatin) is associated with gene activity and heterochromatin (closed-chromatin) is correlated with gene repression. The epigenetic regulators refers to the covalent modifications on DNA or histones which can regulate gene expression and chromatin stability in a reversible manner (Allis and Jenuwein, 2016). During EMT, cells can undergo multiple phenotypic transitions between epithelial and mesenchymal cell states regulated by genetic and epigenetic changes (Tam and Weinberg, 2013).

1.4.1 DNA methylation/demethylation during EMT

DNA methylation is a crucial epigenetic process that regulates gene expression. DNA methylation is catalyzed by DNA methyltransferases

(DNMTs) by covalent transfer of methyl group to the 5th carbon position of the cytosine residues in CpG islands, called as 5mC (Bird, 2002). DNA methylation generally represses transcription exerting its function by interfering with the binding of transcription factors to their target sites or by regulating the recruitment of the methyl-CpG-binding proteins with their associated chromatin remodeling complexes (Robertson, 2005; Schubeler, 2015). DNA methylation is a relatively stable epigenetic modification once it is established in somatic cells. However, it is dynamically regulated during early embryonic development and in tumor cells (Wolffe et al., 1999).

It has been shown that the promoter of the E-cadherin was silenced by hypermethylation in human breast and prostate carcinomas. Treatment with the demethylating agent 5-aza-2'-deoxycytidine partially restored the E-cadherin expression levels (Graff et al., 1995). The inhibition of E-cadherin expression with the promoter hypermethylation, is restored by 5-aza-2'-deoxycytidine in hereditary diffused gastric cancer (Grady et al., 2000). Similarly, loss of estrogen receptor α (ERα) gene was dependent on the hypermethylation of promoter regions in breast cancer cell lines and in primary human breast cancers (Lapidus et al., 1996; Ottaviano et al., 1994). It has been suggested that alterations of methylation levels on E-cadherin and ERα gene promoters start prior to the invasion and increase during later stages of tumor progression in human ductal breast carcinomas (Nass et al., 2000). In addition, hypermethylation of miR-200 family promoter leads to upregulation of Zeb1 and Zeb2, associated with the mesenchymal phenotype and metastasis (Davalos et al., 2012) (Neves et al., 2010; Vrba et al., 2010).

It has been reported that during TGF-β-induced EMT, E-cadherin and collagen 1A1 genes indicated aberrant methylation patterns that can be reversed by the removal of TGF-β. In addition, TGF-β contributed to the induction of DNMTs. Inhibition of DNMTs reversed TGF-β-induced EMT in ovarian cancer cells (Cardenas et al., 2014). However, it has been suggested that genome-wide DNA methylation patterns are not altered dramatically during EMT in AML12 mouse hepatocytes. Rather, it is the histone modifications which exhibited significant changes (McDonald et al., 2011).

These reports provided evidence for the role of DNA methylation and the removal of methylation by DNA demethylating agents that target DNMTs leads to passive dilution of methyl groups during replication. However, DNA methylation can be either passively lost during several rounds of replication in the absence of DNA methylation maintenance machinery or by the active DNA demethylation enzymes. Ten-eleven translocation (TET) family enzymes contribute to active DNA demethylation by sequentially oxidizing 5-methylcytosine (5mC) to 5-hydroxymethylcytosine (5hmC), 5-formylcytosine (5fC), and 5-carboxylcytosine (5caC). Decarboxylation of 5caC, followed by conversion to unmethylated cytosines is mediated by TDG/BER pathway (Cimmino et al., 2011). It has been suggested that the depletion of TET family enzymes and TDG act as molecular blocks in MET by inhibiting demethylation of miR-200 family and impairs iPSC reprogramming from MEFs (Hu et al., 2014). It has been shown that miR-22 overexpression leads to hypermethylation of miR-200 promoter via repressing TET hydroxylases which in return induces Zeb1/2 and promoting EMT, stemness and metastasis (Song et al., 2013).

Further, developing new methods to detect genome-wide DNA-methylation turnover kinetics can be important to interpret the stability of modified cytosines which might be regulated by active DNA demethylation machinery (Schubeler, 2015) and can give important insights especially in establishing cell plasticity mechanism such as EMT.

1.4.2 Histone modifications during EMT

Histones serve as the basic components of chromatin structure together with DNA (nucleosome), regulate heritable chromatin states and gene expression by chemical modifications on the histone tails. Histones are modified by various covalent modifications at different aminoacid residues such as acetylation and methylation of lysines, methylation of arginines, and phosphorylation of serines and threonines (Turner, 2007). These modifications are dynamically regulated and reversed by deacetylases, demethylases and phosphatases. In general terms, acetylation of histones is associated with the active gene transcription and deacetylation is implicated in the gene repression, whereas, methylation and demethylation can act as the

activator or repressor of gene transcription depending on the amino acid residue (Bannister and Kouzarides, 2011).

1.4.2.1 Histone methylation

Histones are methylated by histone methyltransferases (HMTs) which are classified according to their substrate specificity as lysine or arginine methyltransferases. Lysines that are mainly methylated on histone H3 (K4, K36, K79) are associated with the active gene transcription, and H3 (K9, K27, and K20) are correlated with transcriptional repression (Kouzarides, 2007). Lysine residues on histones can be mono-, di-, or tri-methylated by SET (SU(VAR) 3-9, the Polycomb-group (PcG) protein Enhancer of Zeste and the trithorax-group (TrxG) protein Trithorax) domain containing enzymes such as G9a, EZH1/2, and SUV39H1/H2 and others (Zhang and Reinberg, 2001).

Polycomb group (PcG) complexes

PcG complexes that are involved in transcriptional repression consist of two major complexes, polycomb repressor complex 1 (PRC1) and 2 (PRC2). The mammalian PRC2 contains three core components: enhancer of zeste 1 or 2 (EZH1/2), embryonic ectoderm development (EED), and suppressor of zeste 12 (SUZ12). EZH1 and EZH2 catalyze mono-, di- and trimethylation of H3K27 residues. The deposition of H3K27me3 recruits the PRC1 complex which contributes to the maintenance of the gene silencing by catalyzing monoubiquitination of H2A on K119 (H2AK119ub1) (Di Croce and Helin, 2013).

The elevated expression levels of Ezh2 is implicated in many carcinomas such as breast cancer (Collett et al., 2006; Kleer et al., 2003), BRCA1-deficient breast cancer (Puppe et al., 2009), prostate cancer (Varambally et al., 2002) which are associated with tumor invasiveness, metastasis and correlated with an EMT gene signature. PRC2 is involved in EMT and tumor progression by repressing the E-cadherin expression (Cao et al., 2008). Additionally, it has been suggested that PRC2 contributes to the silencing of the E-cadherin expression thereby inducing EMT by direct interaction with several EMT-associated transcription factors. For example, transcription factor Snail recruits the PRC2 complex by directly interacting with Suz12 and Ezh2 on the E-cadherin promoter. Increased H3K27me3 mark

on the E-cadherin promoter leads to the repression of the E-cadherin expression (Herranz et al., 2008). Snail can repress E-cadherin by recruiting G9a and SUV39H1 methyltransferases (Dong et al., 2013; Dong et al., 2012). It has been shown that Ezh2 is the direct target of Sox4 and is upregulated during TGF-β-induced EMT. The depletion of Ezh2 blocked TGF-β-induced EMT and metastatic colonization. Interestingly, Ezh2 can deposit H3K27me3 marks on many EMT-related gene promoters that are associated with the tumor invasiveness and distant metastasis (Figure 5) (Tiwari et al., 2013b). Suz12 overexpression is also indicated in the induction of EMT and metastasis by regulating transcriptional repression of epithelial genes such as E-cadherin and Klf2 in human gastric cancers (Xia et al., 2015). In addition, another core component of the PRC2 complex, EED is upregulated during TGF-β-induced EMT through recruitment of Ezh2 and H3K27me3 marks. The depletion of EED antagonized the expression of EMT-relevant genes such as E-cadherin, Zeb1, Zeb2 and miR-200 family in lung and colon cancer cells (Figure 5) (Oktyabri et al., 2014). However, functional role of PRC2 is highly context-dependent due to the cooperation of the PRC2 components with oncogenic signaling factors in several cancers (De Raedt et al., 2014). For instance, KRAS-driven tumors undergo autonomous EMT, with the simultaneous inactivation of the PRC2 components (Ezh2 and EED) and Trp53 gene, which shows a barrier function by PRC2 during EMT (Serresi et al., 2016).

It is important to note the co-existence of the repressive and active methylation marks such as H3K27me3 and H3K4me3 creates poised chromatin (bivalent domains) which maintains repression as the default state and activates with the appropriate signals in embryonic stem cells (Bernstein et al., 2006). These bivalent domains can contribute to EMT/MET plasticity by enabling rapid changes in chromatin states in response to the EMT inducing signals. Indeed, it has been indicated that plastic non-cancer stem cell (CSC) populations generate CSC populations that exhibit more mesenchymal phenotype by maintaining the poised chromatin state of the Zeb1 promoter that is activated upon TGF-β induction (Chaffer et al., 2013). It has been also shown that Twist1-induced EMT leads to the increased bivalent domains on

the important EMT-related gene promoters and contributes stemness (Malouf et al., 2013).

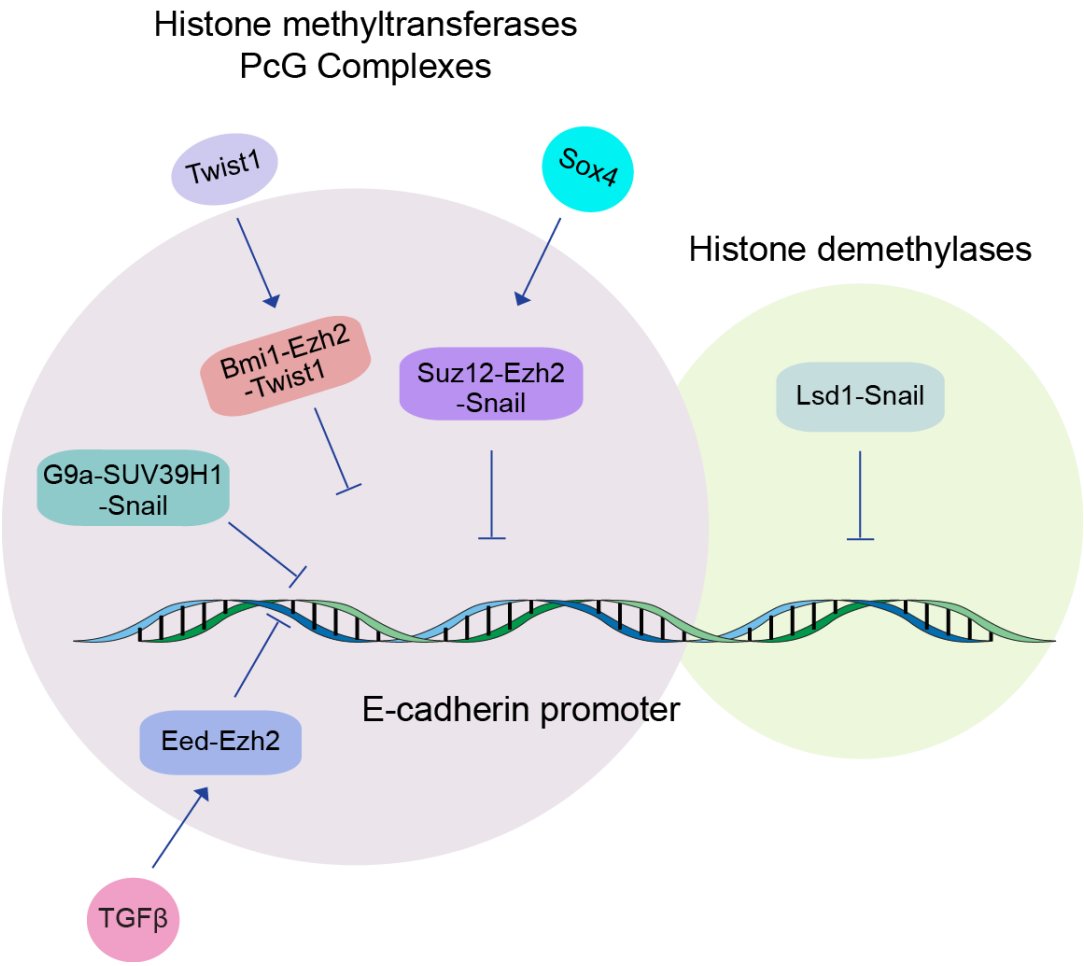

Figure 5: Cooperation of histone modifiers with transcription factors to modify E-cadherin expression. Polycomb group complexes (PcG) (pink), histone demethylases (yellow), cooperate with transcription factors to regulate the E-cadherin promoter.

Initial deposition of H3K27me3 marks by the PRC2 complex signals for the recruitment of PRC1 complex to maintain the inactive state and transcriptional memory. H3K27me3 marks are recognized by the chromobox homologue (CBX) proteins and nuclear localization is mediated by the RING finger domain containing proteins BMI1, RING1 and RNF2 of PRC1 complex (Mills, 2010). It has been reported that BMI1 overexpression induces EMT and stemness. The depletion of BMI1 leads to the reversion of EMT, reduced stemness and increased drug sensitivity in breast cancer cells (Paranjape et

al., 2014). In addition, it has been shown that Twist1 induced EMT and stemness by directly regulating the BMI1 in head and neck squamous cell carcinoma (HNSCC) (Figure 5) (Yang et al., 2010).

These findings indicate that interaction between the PRC1 and PRC2 complexes with various EMT-relevant factors can contribute to the EMT, stemness and tumor aggressiveness by changing the chromatin conformations.

1.4.2.2 Histone demethylation

Histone methylation has been long interpreted as a stable modification. It has been unclear whether the histone methylation is a dynamically regulated process through the antagonizing enzymes. Later on, it was shown that the Lysine specific demethylase (Lsd1) acts as a transcriptional corepressor by catalyzing the removal of mono- and di-methylation marks on H3K4 (Shi et al., 2004). After the discovery of the dynamic regulation of histone methylation by counteracting histone demethylases, a plethora of experiments showed the involvement of these enzymes in cellular plasticity such as EMT (Lin et al., 2010a; Lin et al., 2010b). It has been revealed that Snail represses the epithelial gene promoters such as E-cadherin, CLDN7, and KRT8 via direct interaction with Lsd1. Lsd1 reduces the active H3K4m2 mark, thereby contributes to the maintenance of the transcriptional repression of these epithelial genes (Lin et al., 2010a). Snail1 suppresses E-cadherin with its SNAG domain that has a similarity with the histone H3 tail to interact with the amine oxidase domain of Lsd1 and form a complex together with CoREST (Figure 5) (Lin et al., 2010b). It has been shown that Lsd1 along with Snail is required in the SLUG mediated mammary epithelial cell plasticity, lineage commitment by contributing to the repression of lineage-specific gene promoters (Phillips et al., 2014). Indeed, Lsd1 inhibitor Parnate, blocked the interaction of Lsd1 with the SNAG domain of Slug, reverted EMT, reduced tumor cell motility and invasiveness both *in vitro* and *in vivo* (Ferrari-Amorotti et al., 2014; Ferrari-Amorotti et al., 2013).

High expression levels of Lsd1 were observed in ER- and PR- breast cancers and correlates with tumor aggressiveness (Lim et al., 2010). This implicates a possible role for the deregulation of Lsd1 during EMT. Indeed, it

has been shown that Lsd1 induces EMT by catalyzing the removal of H3K4me3 mark from the E-cadherin promoter, which causes an induction in the mesenchymal markers N-cadherin, Vimentin and MMP-2 in ovarian cancer cells (Li et al., 2016). In addition, the inhibition of Lsd1 by Pargyline (Lsd1 inhibitor) inhibits EMT by restoring the E-cadherin expression and downregulating N-cadherin and Vimentin in prostate cancer (Wang et al., 2015).

Lsd1 is a component of various corepressor complexes (Lee et al., 2005; Shi et al., 2005; Wang et al., 2007). Lsd1 also forms a complex with the Mi-2/nucleosome remodeling and deacetylase (NuRD), inhibits *in vitro* tumor cell invasion, and metastasis *in vivo* by negatively regulating EMT via inhibiting TGF-β as a downstream target (Wang et al., 2009). In another study it has been shown that Lsd1 is upregulated during TGF-β-induced EMT, accompanied by genome-wide loss of the repressive marks H3K9me2 and gain of the active marks H3K4me3 in a reversible manner depending in part on Lsd1. However, the depletion of Lsd1 did not affect the initiation of EMT in AML12 hepatocytes, hence Lsd1 was regulated as the downstream of the TGF-β-induced EMT (McDonald et al., 2011). This finding is in concert with the functional role of Lsd1 in the removal of repressive H3K9 methylation marks and the activation of target genes depending on the interaction partner (Metzger et al., 2005). These results suggest that Lsd1 is a crucial player during EMT by interacting with several transcription factors and corepressor complexes to either supress or to activate EMT-related target genes.

1.4.2.3 Histone acetylation

Histone acetylation leads to a switch between permissive and repressive chromatin states (Eberharter and Becker, 2002). Histone acetyltransferases (HATs) catalyze the acetylation of lysine residues, which neutralizes the positive charges of histones and leads to open chromatin configuration by reducing its binding potential with the negatively charged DNA (Glozak and Seto, 2007). Several multiprotein complexes of coactivators with HAT activity catalyze the acetylation of histones. They are mainly classified into 3 groups, GNAT, CBP/p300, and MYST (Kouzarides, 2007; Roth et al., 2001).

HATs are mostly associated with the induction of EMT and cancer cell metastasis by acetylating the transcription factor Snail (Chang et al., 2017; Hsu et al., 2011). The induction of EMT in lung tumor-associated osteoblast cells enhances the Runx2 and Snail expression. Further, it has been shown that the increased Runx2 recruits p300 to the Snail promoter, which has a binding site for p300, hence induces the Snail expression (Hsu et al., 2011). The acetylation of Snail by p300 is also known to induce an EMT in lung cancer cells (Chang et al., 2017). In addition, p300 is overexpressed in 47% of the HCC patient samples, accompanied with an EMT-like process. Further, depletion of p300 in HCC cell lines led to an increase in E-cadherin, associated with the Snail, Twist1 and HIF-1α downregulation, indicating a MET phenotype (Yokomizo et al., 2011). However, it has been suggested that p300 positively regulates the E-cadherin expression by interacting with the E-cadherin promoter together with the other factors and suppresses the metastatic potential of breast cancer cells (Liu et al., 2005). MOF, a member of MYST family is associated with the epithelial state and is downregulated during EMT. MOF can acetylate Lsd1 only in epithelial cells, interfering with the Lsd1-mediated methylation of the epithelial gene promoter thereby blocking EMT and tumor invasion (Luo et al., 2016).

Although, Snail is mostly associated with the transcriptional repression of the E-cadherin (Cano et al., 2000; Herranz et al., 2008; Peinado et al., 2004). It has been indicated that Snail can act as a transcriptional activator of its target genes during EMT. Snail mediates the acetylation and induction of its target genes such as ERCC1 and IL8 by recruiting the CREB-binding protein (CBP) to their promoters. Interestingly, this result indicates that Snail contributes to EMT and metastasis by being not only as a transcriptional repressor of the adhesion proteins, but also by activating the genes which are involved in tumor microenvironment remodeling (Hsu et al., 2014).

1.4.2.4 Histone deacetylation

Acetylation of histones is a reversible process mediated by histone deacetylases (HDACs). HDACs remove the acetyl groups, allowing compaction of the chromatin and prevent accessibility of transcriptional machinery, mostly correlates with the transcriptional repression (Glozak and

Seto, 2007). HDACs are divided into two families and four classes according to their sequence similarities and cofactor dependencies. In humans, HDAC1, -2, -33 and 8 (class I); HDAC4, -5,-6,-7,-9 and -10 (class II); and HDAC11 (class IV) belong to the classical HDAC family. The second family is NAD^+-dependent sirtuins (SIRT1-7, class III) which have no sequence similarities with the classical HDAC family (Yang and Seto, 2007). HDACs mostly exert their function within the multimeric complexes, often with the other family members. For example, HDAC1 and HDAC2 are involved in NuRD, Sin3a and CoREST complexes. Complexes are crucial to bring stability and recruit the HDACs to the specific target genes for the transcriptional regulation (Bannister and Kouzarides, 2011).

HDAC inhibitors interfere with the enzymatic activity of HDACs, induce hyperacetylation of histones and therefore transcriptional activation of the target genes. HDAC inhibitors gained great attention in cancer therapy due to their pro-apoptotic, anti-proliferative and anti-angiogenic effects (Mottamal et al., 2015). In addition, several studies showed the effect of HDAC inhibitors during EMT. Some reports showed that pan-HDAC inhibitors such as Trichostatin A (TSA) and Suberoylanilide hydroxamic acid (SAHA) induced an EMT phenotype associated with the increased mesenchymal genes vimentin, N-cadherin and fibronectin in the prostate cancer cells (Kong et al., 2012). Similar results were observed in the nasopharygeal, colon and liver carcinoma cell lines (Jiang et al., 2013). However, it has been implicated that HDAC inhibition led to a significant inhibition on the hepatocellular carcinoma metastasis (Coradini et al., 2004). In addition, the inhibition of HDACs has been implicated in the reversion of mesenchymal cells to the epithelial state, either partially in triple negative breast cancer (TNBC) cell lines (Jiang et al., 2013) or fully in breast (Srivastava et al., 2010), ovarian, bladder and pancreatic cancer cells (Luo et al., 2016). Interestingly, the intermediate EMT state reverted back to the epithelial state as detected by increased E-cadherin promoter activity and more potently by HDAC class I inhibitors (Luo et al., 2016), indicating EMT states may dictate the differences in response to the HDAC inhibition during EMT. Additionally, E-cadherin expression was restored with the concomitant decrease in Zeb1, with the increased drug

sensitivity to the gemcitabine treatment by HDAC class I inhibitor (mocetinostat) in pancreatic cancer cells (Meidhof et al., 2015). The contradictory findings about the effect of HDAC inhibitors on EMT can be due to the pleiotropic effects of pan-HDAC inhibitors. In addition, the given findings of the potency of HDAC class I inhibitors in reverting the mesenchymal state to the epithelial state can give a hint that the regulation of EMT may depend on more to the activity of HDACs within the corepressor complexes.

HDACs, in particular, HDAC1 and HDAC2 predominantly function as part of the several stable multimeric complexes such as CoREST, Sin3a and NuRD, enabling the recruitment of HDACs to the specific target sites (Denslow and Wade, 2007; Grozinger and Schreiber, 2002; Hayakawa and Nakayama, 2011). Indeed, Snail silences E-cadherin by recruiting corepressor complex Sin3a/HDAC1 and HDAC2. In addition, the recruitment of HDAC1/2-containing Mi-2/nucleosome remodeling and deacetylase (NuRD) complex by master regulators of EMT, such as Snail (Fujita et al., 2003) and Twist (Bannister and Kouzarides, 2011), to the E-cadherin gene promoter contributes to the silencing of the E-cadherin (Figure 6).

NuRD complexes can be formed by various combinations of different subunits to provide functional specificity, such as HDAC1 and HDAC2 containing Methyl-CpG-binding domain 3 (Mbd3)/NuRD complex or Mbd2/NuRD. (Hendrich and Tweedie, 2003; Lai and Wade, 2011). Mbd3 lacks the ability to bind methylated DNA regions might indicate that different combinations of NuRD complex can contribute to an EMT due to the different substrate specificities.

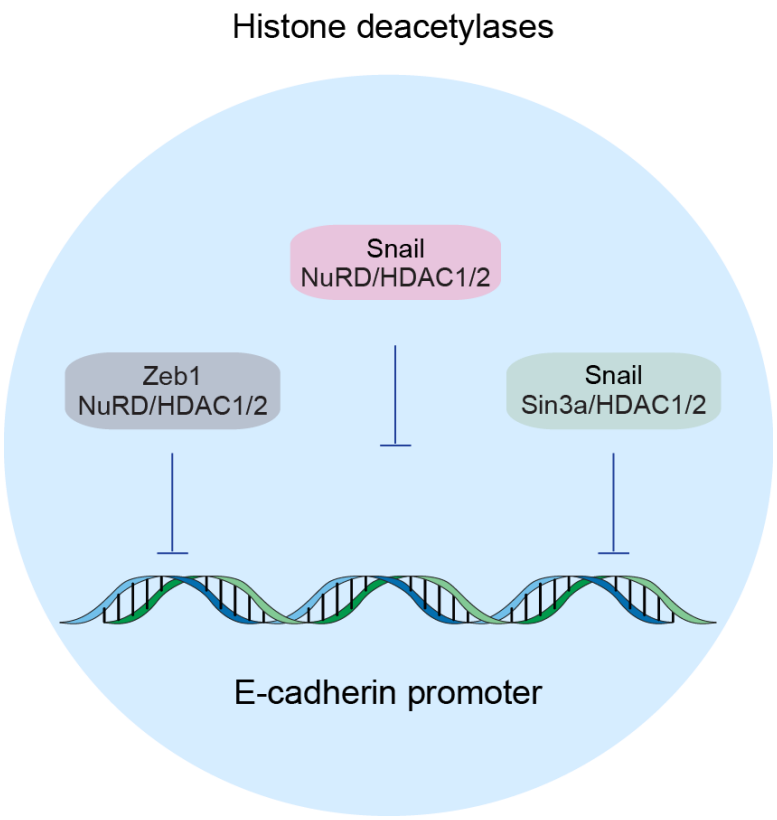

Figure 6: Cooperation of histone modifiers with transcription factors to modify E-cadherin expression. Histone deacetylases (blue) cooperate with transcription factors to regulate the E-cadherin promoter.

1.4.2.5 miRNAs and lncRNAs in EMT

MicroRNAs are approximately 22 nucleotide long non-coding RNAs (lncRNAs) that post-transcriptionally regulate gene expression (Bartel, 2004). Different mRNAs can be targeted by one miRNA, yet several miRNAs can target the same mRNA as well (Friedman et al., 2009). miRNAs act as molecular switches to regulate developmental processeses (Mendell, 2005) and EMT (Gregory et al., 2008). miR-200 family is associated with the epithelial phenotype, blocks TGF-β-induced EMT and the induced overexpression of the miR-200 family converts mesenchymal canine kidney cells (MDCK) to the epithelial state (Gregory et al., 2008). In addition, the enhanced expression of the miR-200 family induced a MET, identified by the upregulation of E-cadherin and the downregulation of Zeb1 and Zeb2 in the mesenchymal 4TO7 cells (Korpal et al., 2008). However, Zeb1 can also

suppress miR-200 family by binding to the specific sites on their promoters during TGF-β-induced EMT and this reciprocal feedback loops are important regulators of the cell migration and invasion in breast cancer cell lines (Burk et al., 2008). These results indicate that reciprocal feedback loops between miRNAs and transcription factors can regulate the plasticity of EMT process. In addition to miRNAs, long non-coding RNAs (lncRNAs), length of more than 200 nucleotides, are implicated during EMT. LncRNA HOTAIR is highly expressed in many different cancer types and correlated with the lymph node metastasis, depletion of lncRNA HOTAIR induces a MET (Xu et al., 2013). LncRNA-ATB is induced by TGF-β in normal liver cell line as well as in breast and colorectal cancer cell lines. LncRNA-ATB can physically interact with the miR-200 family, acts as a competitive endogenous RNA to regulate Zeb1 and Zeb2, leads to the induction of EMT and tumor cell invasion and metastasis. However, lncRNA-ATB induces metastasis by partially depending on the interaction with the miR-200 family. LncRNA-ATB regulates the metastatic colonization through IL-11/STAT3 pathway by causing the autocrine induction of IL-11 (Yuan et al., 2014). It is also reported that lncRNA-LET prevents EMT and Wnt/β-catenin pathway as well as cell migration and invasion (Liu et al., 2016).

2 Aim of the study

Epithelial-mesenchymal transition (EMT) and its reverse process mesenchymal-epithelial transition (MET) is an example of cell plasticity which is implicated as a crucial mechanism during tumor invasion and metastatic dissemination. However, the underlying mechanisms that regulate dynamic switches between epithelial and mesenchymal cell states during tumor progression are still poorly understood. The plastic nature of EMT implies a key role for the rearrangement of chromatin states that are regulated by epigenetic modifiers. Therefore, in this study, we aimed to elucidate the key epigenetic players which contributed to the epithelial-mesenchymal plasticity as well as tumor progression and metastatic outgrowth.

To answer these questions, we generated an *in vitro* irreversible EMT model by manipulating specific medium conditions to identify the *de novo* established epigenetic modifications that induce and maintain the mesenchymal cell state. We compared these irreversible EMT cells to the transforming growth factor β (TGF-β)-induced reversible EMT cells to understand the epigenetic differences between transient and fixed mesenchymal cell states.

This study will provide us important understandings to discover new therapeutic approaches to target cell state transitions during breast cancer progression. Hence, by interfering with several epigenetic modifiers, we will be able to target wide-range of gene networks that are responsible in tumor growth and metastasis formation.

3 Results

3.1 A critical role of histone deacetylases, Mbd3/NuRD and Tet2 hydroxylase in epithelial-mesenchymal cell plasticity and tumor metastasis

Ayse Nihan Kilinc[1], Ravi Kiran Reddy Kalathur[1], Helena Antoniadis[1], Huseyin Birogul[1], and Gerhard Christofori[1]*

[1] Department of Biomedicine, University of Basel, 4058 Basel, Switzerland

-Submitted-

3.1.1 Summary

While a critical role of epigenetic modifiers and their specific chromatin modifications has been demonstrated during an EMT, it has remained elusive whether epigenetic control differs between the dynamic cell state transitions of a reversible EMT and the fixed differentiation status of an irreversible EMT. We have employed varying EMT models of murine breast cancer cells to identify the key players establishing cell state transitions during a reversible and an irreversible EMT. We demonstrate that the Mbd3/NuRD complex and the activities of histone deacetylases (HDACs) and Tet2 hydroxylase keep the cancer cells in a mesenchymal state. Their pharmacological inhibition and/or RNAi-mediated ablation lead to a mesenchymal-epithelial transition (MET) and the repression of metastasis formation by mesenchymal breast cancer cells.

3.1.2 Significance

An epithelial-mesenchymal transition (EMT) represents a basic morphogenetic process of high cell plasticity underlying embryogenesis, wound healing and cancer metastasis and drug resistance. It involves a profound transcriptional reprogramming of cells, however, the role of epigenetic regulation in differentiating a reversible EMT from an irreversible EMT has remained elusive. Here, we demonstrate a critical role of the Mbd3/NuRD complex together with histone deacetylases (HDACs) and Tet2 hydroxylase in maintaining a stable mesenchymal phenotype of murine breast cancer cells. Combinatorial interference with their functions represses primary tumor growth and breast cancer metastasis, making these epigenetic modifiers attractive targets for cancer therapy.

3.1.3 Highlights

- Reversible and irreversible EMT differ in gene expression and epigenetic regulation
- HDACs, Mbd3 and Tet2 maintain an irreversible EMT
- HDACs, Mbd3 and Tet2 act in an additive manner to maintain a mesenchymal cell state

- Inhibition of HDACs and/or Mbd3 and Tet2 represses tumor growth and metastasis

3.1.4 Introduction

An epithelial-mesenchymal transition (EMT) is a critical morphogenetic process during embryonic development and wound healing (Baum et al., 2008; Hanahan and Weinberg, 2011; Kalluri and Weinberg, 2009; Nieto, 2011; Thiery, 2002; Yang and Weinberg, 2008). The dynamic transitions from an epithelial to a mesenchymal cell state have also been shown to promote cancer cell stemness and tumorigenicity, cancer cell invasion, metastatic dissemination and drug resistance (Baum et al., 2008; Diepenbruck and Christofori, 2016; Kalluri and Weinberg, 2009; Nieto, 2011; Thiery, 2002). The profound changes in gene expression and the high cell plasticity accompanying the dynamic processes of an EMT and its reversion, a mesenchymal-epithelial transition (MET), imply a key role of the rearrangement of chromatin states by epigenetic modifications, including changes in gene-specific histone acetylation, histone methylation and DNA methylation (Bedi et al., 2014; McDonald et al., 2011; Tam and Weinberg, 2013). While the importance of epigenetic modifications and the respective chromatin modifying enzymes has been documented (McDonald et al., 2011; Tam and Weinberg, 2013), the actual contribution of epigenetic changes to epithelial-mesenchymal cell plasticity, notably to the reversibility or irreversibility of an EMT, is poorly understood.

Histone deacetylases (HDACs) catalyze the removal of acetyl groups from lysine residues of histones, leading to chromatin condensation and repression of gene expression (Glozak and Seto, 2007; Haberland et al., 2009). The inhibition of HDAC activity has been implicated in the conversion of mesenchymal cells into an epithelial state in breast, ovarian, bladder and pancreatic cancer cells (Srivastava et al., 2010; Tang et al., 2016; Tate et al., 2012). HDACs, in particular HDAC1 and HDAC2, predominantly function as components of stable multi-protein complexes, including CoREST, Sin3a and NuRD, and thereby are recruited to specific target genes (Denslow and Wade, 2007; Grozinger and Schreiber, 2002; Hayakawa and Nakayama, 2011). In the context of an EMT, the HDAC1/2-containing NuRD complex is bound by

the EMT transcription factors Snail and Twist and directed to the promoter region of the E-cadherin (Cdh1) gene to silence its expression (Fu et al., 2011; Fujita et al., 2003).

NuRD complexes can be formed by various combinations of different subunits to provide functional specificity, an example being the HDAC1 and HDAC2-containing Methyl-CpG-binding domain 3 (Mbd3)/NuRD complex (Hendrich and Tweedie, 2003; Lai and Wade, 2011). Mbd3 is a non-enzymatic component of the Mbd3/NuRD complex with critical functions; its genetic deletion in mice causes early embryonic lethality (Hendrich et al., 2001) and defects in lineage commitment of embryonic stem (ES) cells (Kaji et al., 2006; Kaji et al., 2007). Underscoring its crucial function in regulating cell plasticity, the Mbd3/NuRD complex serves as a molecular block in the rather inefficient reprogramming of mouse embryonic fibroblasts (MEFs) to induced pluripotent stem (iPS) cells; the depletion of Mbd3 allows a more efficient conversion of MEFs into iPS cells (Rais et al., 2013).

Mammalian Mbd3 is the only Mbd family protein that is not able to recognize methylated CpG dinucleotides due to an amino acid change in the Mbd domain (Fraga et al., 2003; Hendrich and Tweedie, 2003; Saito and Ishikawa, 2002). It has been reported that Mbd3 is able to recognize 5-hydroxymethylcytosine (5hmC) sites and recruit Mbd3/NuRD to these sites in mouse ES cells by binding to Tet1 (Yildirim et al., 2011), a member of the Tet hydroxylase family. Tet1, 2 and 3 hydroxylases contribute to active DNA demethylation by catalyzing the sequential oxidation of methylated cytosines (5mC) to 5-hydroxymethylcytosine (5hmC) to 5-formylcytosine (5fC) to 5-carboxylcytosine (5caC), followed by the latter's decarboxylation to unmodified cytosine (Tahiliani et al., 2009); (Cimmino et al., 2011). However, it has been also suggested that Mbd3-binding to DNA does not depend on 5hmC (Baubec et al., 2013). On the other hand, Tet hydroxylases have been implicated in the initiation of a MET that is a prerequisite for MEFs to undergo iPS cell reprogramming (Hu et al., 2014); (Li et al., 2010; Samavarchi-Tehrani et al., 2010). However, the details of the functional contributions of the Mbd3/NuRD complex and Tet hydroxylases to pathophysiological cell state transitions and to an EMT remain largely unknown. Here, using cellular

models of an irreversible and a reversible EMT we have delineated the central role of the Mbd3/NuRD complex and of Tet2 hydroxylase in the maintenance of the mesenchymal state of murine breast cancer cells *in vitro* and primary tumor growth and metastasis *in vivo*. The results underscore a critical role of the Mbd3/NuRD complex and Tet hydroxylases in regulating epithelial-mesenchymal plasticity and highlight them as therapeutic targets to interfere with metastatic breast cancer.

3.1.5 Results

3.1.5.1 Generation of an irreversible EMT system

To investigate the dynamic transitions underlying a reversible EMT as compared to an irreversible EMT, we set out to establish an *in vitro* model system, which after undergoing an EMT lacked the ability to revert to an epithelial cell state. As a model for a reversible EMT we used Py2T murine epithelial breast cancer cells which upon treatment with TGFβ for >10 days undergo a full EMT, while when depleted of TGFβ readily convert back to their epithelial state (Waldmeier et al., 2012). Starting with Py2T cells, an irreversible EMT system was established by culturing them for 3 months in mammary epithelial growth medium (MEGM) in the presence of different concentrations of fetal bovine serum (FBS) (adapted from (Dumont et al., 2008). Over time, a subset of Py2T cells acquired a mesenchymal cell morphology and, upon serial passaging, these subsets of cells retained their mesenchymal cell morphology. Individual mesenchymal phenotype cells were then isolated and expanded as cell clones that stably maintained their mesenchymal phenotype in basal medium (referred to as M clone cells M1, M2, and M3; Figure 1A,B). In contrast, long-term TGFβ-treated Py2T cells (referred to as Py2T-LT cells) reverted back to their epithelial state when TGFβ was withdrawn from the culture medium (referred to as Py2T-LT MET cells; Figure 1B).

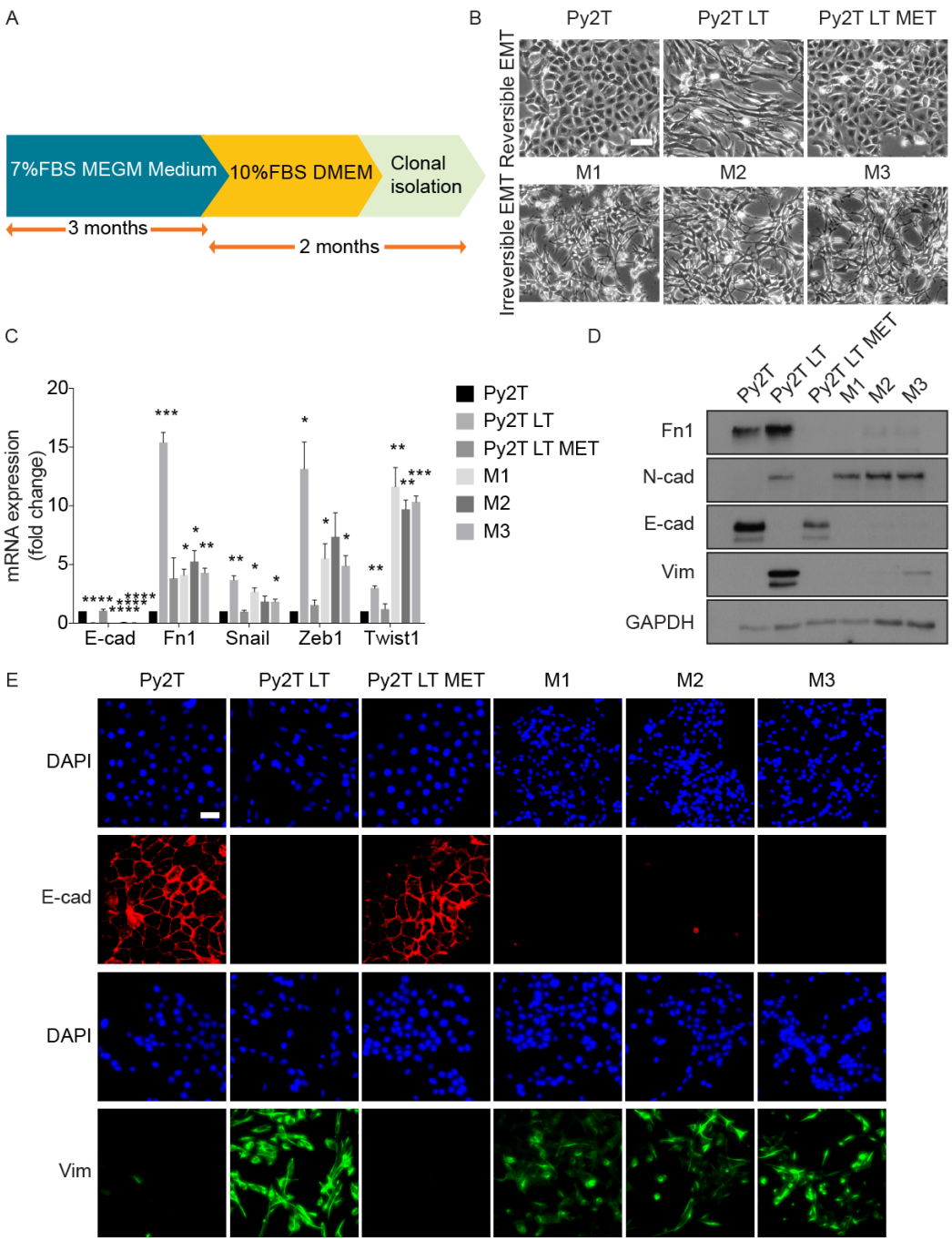

Figure 1. In vitro characterization of irreversible EMT cells (M clone cells) (A) Scheme of the generation of an irreversible EMT system (M clone cells). **(B)** Phase-contrast microscopy of Py2T cells, Py2T cells treated for >20days with TGFβ (Py2T-LT), Py2T-LT cells upon TGFβ withdrawal (Py2T-LT MET), and M1, M2, and M3 clone cells. Scale bar, 100µm. **(C)** Expression of E-cadherin (E-cad), fibronectin (Fn1), Snail, Zeb1, Twist1 was determined by quantitative RT-PCR in Py2T, Py2T-LT, and Py2T-LT MET cells and in M1, M2, and M3 clone cells. Fold changes are related to expression levels in Py2T cells. **(D)** Expression of fibronectin (Fn1), N-

cadherin (N-cad), E-cadherin (E-cad), and Vimentin (Vim) was determined by immunoblotting in Py2T, Py2T-LT, and Py2T-LT MET cells and in M1, M2, and M3 clone cells. Immunoblotting for GAPDH was used as a loading control. **(E)** Immunoflorescence microscopy analysis of changes in the localization and expression levels of marker proteins in Py2T, Py2T-LT, and Py2T-LT MET cells and M1, M2, and M3 clone cells. Cells were stained with antibodies against the epithelial marker E-cadherin (E-cad) and the mesenchymal marker vimentin (Vim). DAPI was used to visualize nuclei. Scale bar, 50μm. Data are displayed as mean ± SEM. Statistical values were calculated using a paired, two-tailed t-test. *, $P < 0.05$; **, $P < 0.01$, ***; $P < 0.001$; ****, $P < 0.0001$.

To characterize whether M clone cells had undergone a *bona fide* EMT, we examined the expression of EMT markers by quantitative RT-PCR in irreversible EMT cells (M clones) compared to reversible EMT cells (Py2T-LT). In M clone cells, the mRNA levels of genes associated with a mesenchymal state, such as fibronectin (Fn1), Snail, Zeb1 and Twist1, were continuously expressed at high levels, whereas epithelial genes, such as E-cadherin (E-cad), were found at low levels throughout. In contrast, upon TGFβ withdrawal Py2T-LT cells regained the expression of E-cad and lost the expression of Fn1, Snail, Zeb1 and Twist1 (Figures 1C). Immunoblotting analysis further confirmed the hallmarks of an EMT in M clone cells. The protein levels of the mesenchymal markers Fn1, N-cadherin (N-cad) and vimentin (Vim) were high, while the protein levels of E-cad were low. In Py2T cells treated with TGFβ, expression of the mesenchymal marker proteins was high, whereas removal of TGFβ led to a loss of mesenchymal marker expression and an upregulation of E-cad protein expression (Figure 1D). Finally, immunofluorescence microscopy analysis revealed that M clone cells maintained their mesenchymal state by expressing Vim and lacking E-cad at the cell membranes, as did Py2T-LT cells. Py2T-LT MET cells lost Vim expression and re-expressed E-cad at the cell membranes (Figures 1E). Altogether, these results show that TGFβ-induced Py2T-LT cells revert from a mesenchymal state back to an epithelial state upon withdrawal of TGFβ, while M clone cells sustain their mesenchymal phenotype in basal culture conditions.

Next generation RNA sequencing identified 6624 genes differentially expressed between Py2T-LT cells and M clone cells, suggesting that the irreversible M clone cells significantly differ from reversible Py2T-LT cells, although they both originated from Py2T cells (data not shown).

3.1.5.2 M clone cells are highly tumorigenic and metastatic

Next, we assessed the tumorigenic potential of Py2T-LT and M clone cells by orthotopic transplantation into the mammary fat pads of immunodeficient NOD scid gamma (NSG) mice. M1 and M3 clone cells showed a significantly faster tumor growth rate than Py2T-LT cells (Figure 2A). Immunofluorescence microscopy analysis showed a low E-cad and high Vim expression (Figure 2B), indicating that both Py2T-LT and M clone cells formed mesenchymal phenotype tumors. Almost all mice transplanted with M clone cells developed macroscopic lung metastases, while only 50% of the mice transplanted with Py2T-LT cells showed few microscopic metastatic lesions (Figure 2C). Upon tail vein injection of Py2T-LT, M1 and M3 clone cells, all mice developed metastasis, however, the M clone cells seeded a strikingly higher number of metastases and larger metastatic lesions in the lungs compared to Py2T-LT cells (Figure 2D,E).

We next assessed the tumor initiation potential of the M clone cells and Py2T-LT cells by orthotopic injection of limiting dilutions of cells into immunodeficient BALB/c $Rag2^{-/-}$ common γ $receptor^{-/-}$ (RG) mice. M clone cells exhibited a significantly higher and faster tumor-forming capability than Py2T-LT cells (Figure 2F), and all tumors arisen from M clone cells could be serially transplanted (Figure 2G). Taken together, the data demonstrate a higher ability of irreversible EMT cells to initiate tumors and to colonize the lung as compared to reversible EMT cells.

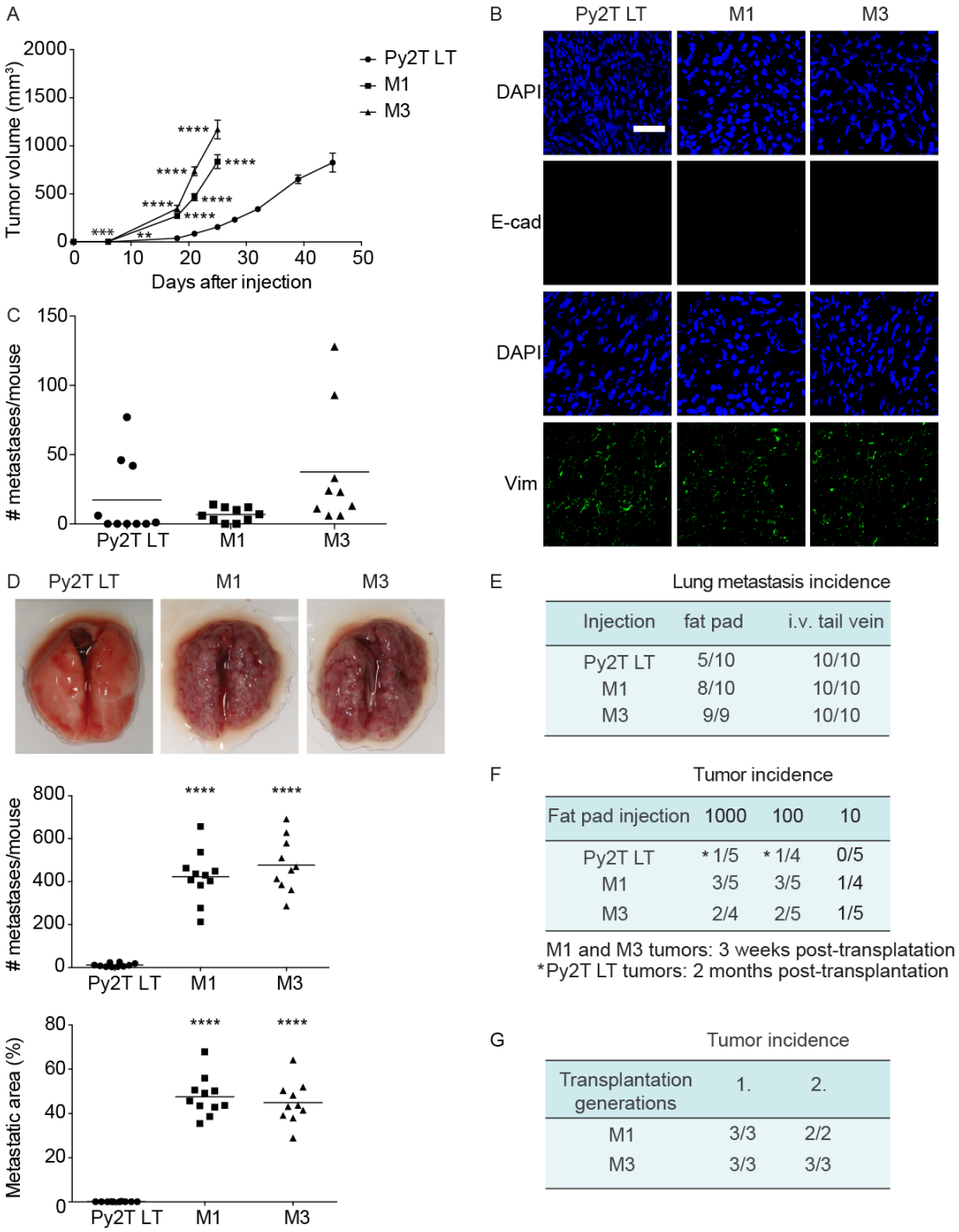

E

Lung metastasis incidence

Injection	fat pad	i.v. tail vein
Py2T LT	5/10	10/10
M1	8/10	10/10
M3	9/9	10/10

F

Tumor incidence

Fat pad injection	1000	100	10
Py2T LT	*1/5	*1/4	0/5
M1	3/5	3/5	1/4
M3	2/4	2/5	1/5

M1 and M3 tumors: 3 weeks post-transplatation
*Py2T LT tumors: 2 months post-transplantation

G

Tumor incidence

Transplantation generations	1.	2.
M1	3/3	2/2
M3	3/3	3/3

Figure 2. Tumorigenicity of irreversible M clone cells (A) Primary tumor growth in the mammary fat pad of female immunodeficient NOD scid gamma (NSG) mice transplanted with 10^5 cells of Py2T-LT cells and M1 and M3 clone cells. Data are displayed as mean tumor volumes ± SEM. **(B)** Immunoflorescence staining of tumors formed by Py2T-LT cells and M1 and M3 clone cells for E-cadherin (E-cad) and vimentin. DAPI staining was used to visualize nuclei. Scale bar, 50µm. **(C)** Numbers of lung metastases per mouse transplanted orthotopically with Py2T-LT cells and M1

and M3 clone cells as described in (A). **(D)** Representative macroscopic photographs of lungs taken 17 days post injection of 10^5 Py2T-LT cells or M1 and M3 clone cells into the tail vein of NSG mice. Means of the numbers of metastases and the percentages of the metastasis area per lung tissue area per mouse were quantified. **(E)** Quantification of the incidence of lung metastasis in the mice described in C and D. **(F)** Tumor incidence assessed by transplantation of Py2T-LT cells or M1 and M3 clone cells in limiting dilutions (1000, 100, 10 cells) into the mammary fat pads of RG mice. * represents the delayed tumor formation by Py2T-LT cells as compared to tumors initiated by M1 and M3 clone cells. The experiment was terminated 191 days post injection. **(G)** Tumor incidence of serial transplantation of fragments of tumors formed by M1 and M3 clone cells in the limiting dilution assay described in (F). Statistical significance was calculated using a Mann-Whitney *U* test. **, $P < 0.01$; ***, $P < 0.001$; ****, $P < 0.0001$.

3.1.5.3 HDAC inhibition causes a partial MET in M clones

Since the M clone cells underwent an irreversible EMT simply by manipulating the growth conditions, we speculated that the maintenance of their mesenchymal state depended on epigenetic regulators and modifications. We screened a number of epigenetic inhibitors to test whether any of those inhibitors would induce a reversion of the irreversible EMT clones to an epithelial state. In particular, we used 3-Deazaneplanocin A (DZNep), a pharmacological inhibitor of the Polycomb repressor complex component Ezh2 (Crea et al., 2012), a histone methyltransferase that trimethylates histone 3 lysine 27 (H3K27me3) and plays a key role in the initiation of an EMT (Tiwari et al., 2013b). We further used 5-Aza-2'-deoxycytidine (DAC) to inhibit DNA methylation by interfering with DNA methyltransferases (DNMTs). DNA methylation has been previously shown important in the reversion of an EMT in PC9, but not in A549 non-small-cell lung cancer cell lines (Zhang et al., 2017a). Finally, due to the reported roles of histone deacetylases (HDACs) in the reversion of an EMT in breast, ovarian, pancreatic and bladder carcinoma cells (Srivastava et al., 2010; Tang et al., 2016), we tested the HDAC inhibitor Trichostatin A (TSA) for its ability to revert mesenchymal M clone cells to an epithelial state.

Among the inhibitors tested, only TSA induced morphological changes towards an epithelial state in M clone cells, with a marked increase in the expression of the epithelial marker E-cad, yet no apparent change in the expression of the mesenchymal markers Fn1 and N-cad (Supplemental Figure S1A-D). These results indicate that histone deacetylation played a critical role in maintaining the mesenchymal phenotype of M clone cells. In contrast, treatment with DAC or DZNep did not change the mesenchymal phenotype of M clone cells. Bisulfite pyrosequencing of the E-cad gene promoter in reversible and irreversible EMT cells also did not show any significant change in the extent of methylated CpG islands (Supplemental Figure S1E), indicating that changes in DNA methylation were not accountable for the difference between a reversible and an irreversible EMT. The more specific inhibitor of Ezh2 methyltransferase activity EPZ005687 (Knutson et al., 2012) also did not elicit any changes in cell morphology or EMT marker expression (Supplemental Figure S1F,G).

Based on the effects observed with TSA and on the reported contribution of HDAC Class I inhibitors to the reversal of an EMT in pancreatic cancer cells (Meidhof et al., 2015), we treated Py2T-LT cells and M clone cells with two more HDAC inhibitors, the selective HDAC Class I inhibitor Tacedinaline (CI994) and the non-selective HDAC inhibitor Panobinostat (LBH589) (Beckers et al., 2007). Both inhibitors showed an efficient repression of HDAC activity in both M3 clone cells and Py2T-LT cells, as confirmed by immunoblotting analysis of H3 acetylation levels (Figure 3A). Consistent with a partial epithelial morphology, the inhibition of HDAC activities by CI994 and LBH589 provoked an increase in E-cad expression in M3 clone cells, yet without evident changes in N-cad and Vim expression (Figure 3A,B). Only a moderate loss of the mesenchymal marker Fn1 was observed in the presence of LBH589. Similar changes in expression patterns and cell morphology were observed in M1 and M2 clone cells treated with CI994 and LBH589 (Supplemental Figure S2A,B). In comparison, despite an efficient inhibition of HDAC activity, Py2T-LT cells showed no obvious alterations in E-cad, Fn1, N-cad and Vim expression upon treatment with CI994 or LBH589 (Figure 3A,B).

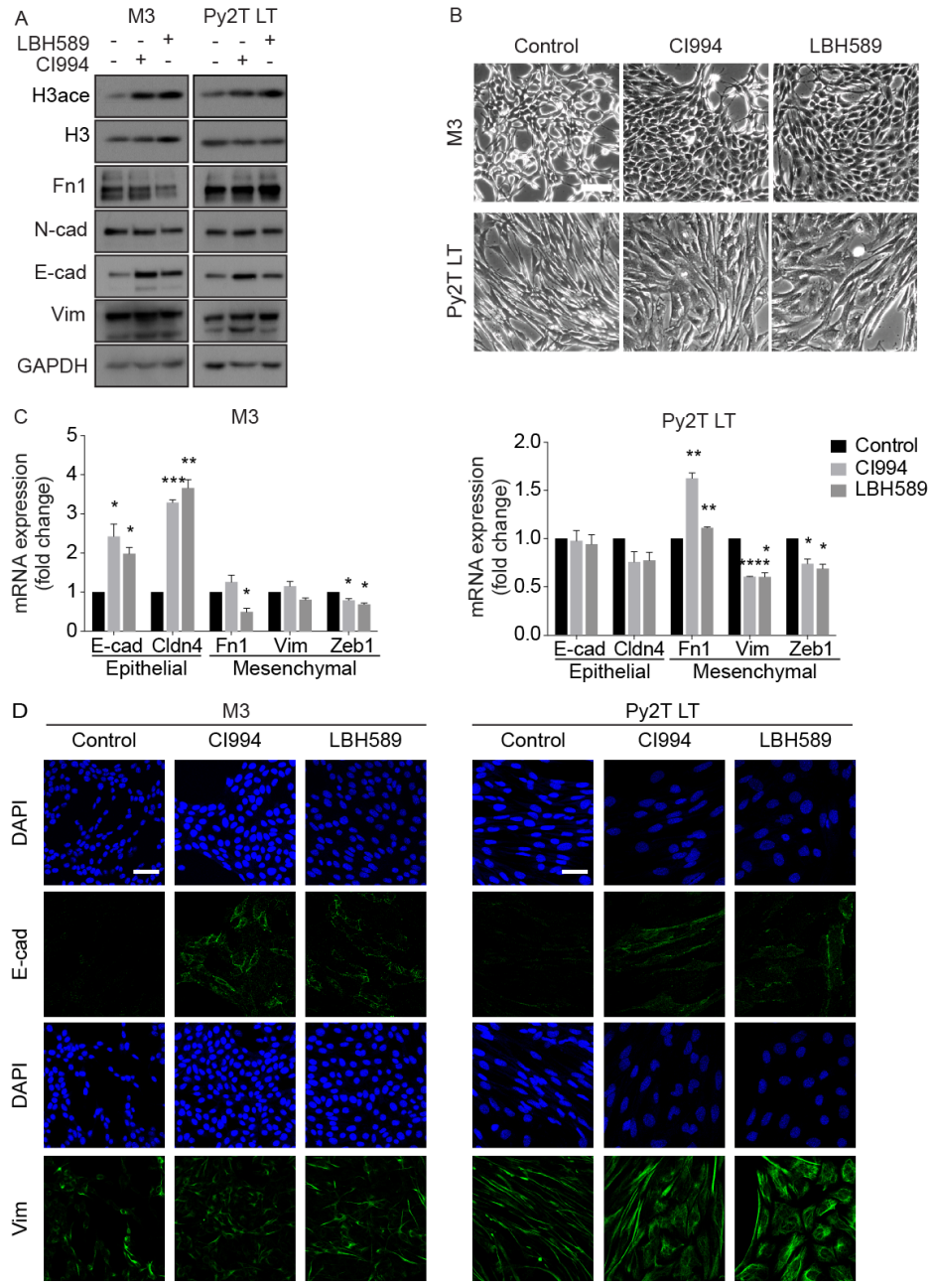

Figure 3. HDAC inhibition induces a partial MET in M clone cells (A) The protein levels of acetylated H3 (H3ace), fibronectin (Fn1), N-cadherin (N-cad), E-cadherin (E-cad), and vimentin (Vim) in M3 clones and Py2T-LT cells exposed or not to HDAC inhibitors (2μM Tacedinaline/CI994 or 10nM Panobinostat/LBH589) for 72 hours were determined by immunoblotting. Immunoblotting for total H3 and GAPDH was used as a loading control. **(B)** Morphology of M3 clone cells and Py2T-LT cells treated with 2μM CI994 and 10nM LBH589 for 72 hours as evaluated by phase contrast microscopy. Scale bar, 100μm. **(C)** Quantitative RT-PCR analysis of the mRNA levels of E-cadherin (E-cad), Claudin4 (Cldn4), fibronectin (Fn1), vimentin

(Vim), and Zeb1 in M3 clone cells and Py2T-LT cells treated with CI994 (2μM) and LBH589 (10nM) for 72 hours. Fold changes are related to mRNA levels in cells treated with DMSO diluent. **(D)** Confocal immunofluorescence microscopy analysis of the expression of the epithelial marker E-cadherin (E-cad) and the mesenchymal marker vimentin (Vim) in M3 clone cells and Py2T-LT cells in the absence and presence of HDAC inhibitors CI994 (2μM) and LBH589 (10nM) for 72 hours. Scale bar, 50μm. Data are displayed as mean ± SEM. Statistical values were calculated using a paired, two-tailed t-test. *, P < 0.05; **, P < 0.01, ***; P < 0.001; ****, P < 0.0001.

Quantitative RT-PCR analysis confirmed a MET in CI994 and LBH589-treated M clone cells with increased expression of the epithelial markers E-cad and Claudin4 (Cldn4), yet varying expression levels of the mesenchymal markers Fn1, Vim and Zeb1. In contrast, Py2T-LT cells remained unaffected by treatment with CI994 and LBH589 (Figure 3C, Supplemental Figure S2C). Immunofluorescence microscopy analysis revealed the specific localization of E-cad to cell membranes in M clone cells treated with CI994 and LBH589. In comparison, neither a gain of E-cad and nor a loss of Vim expression was observed in Py2T-LT cells treated with the HDAC inhibitors in the presence of TGFβ (Figure S3D, Supplemental Figure S2D).

Together, these results indicate that M clone cells can be partially reverted to an epithelial state by HDAC inhibition, while Py2T-LT cells only revert to an epithelial phenotype by the withdrawal of TGFβ.

3.1.5.4 The Mbd3/NuRD complex is critical for a mesenchymal state

The fact that HDAC inhibition only partially reverted mesenchymal M clone cells into an epithelial state motivated us to assess whether additional factors were involved in the regulation of epithelial-mesenchymal plasticity. It is well established that multimeric protein complexes facilitate HDAC functions (Hayakawa and Nakayama, 2011). For example, the Mbd3/NuRD complex exerts its activity at least in part via HDACs and plays a critical role in the efficient reprogramming of MEFs into iPS cells (Rais et al., 2013).

To test whether the Mbd3/NuRD complex was a critical component in the maintenance of a mesenchymal state, we ablated Mbd3 expression in M clone cells by the stable expression of shRNAs targeting Mbd3. Indeed, the efficient depletion of Mbd3 led to an epithelial morphology of M clone cells with increased expression of E-cad and Cldn4, accompanied by reduced expression of Vim, Fn1, N-cad and Zeb1 at both the protein and mRNA level, compared to shControl-transfected cells (Figure 4A,B). In contrast, the efficient depletion of Mbd3 in Py2T-LT cells failed to affect the expression of EMT markers (Figure 4A,B). SiRNA-mediated depletion of Mbd3 elicited similar changes in EMT marker expression, yet at lower efficiency (Supplemental Figure S3A,B). In contrast, shRNA-mediated depletion of Mbd3 in Py2T-LT cells rather led to increased E-cad mRNA levels and no change in Cldn4, Fn1, Vim and Zeb1 expression (Figure 4C).

Confocal immunofluorescence microscopy analysis indicated that shRNA and siRNA-mediated ablation of Mbd3 in M3 clone cells led to a localization of the epithelial marker proteins E-cad and ZO-1 to cell-cell junctions, to the conversion of mesenchymal stress fibers to epithelial cortical actin and to a reduction in Vim expression, compared to cells transfected with shControl (Figure 4D, Supplemental Figure S3C). In contrast, depletion of Mbd3 in Py2T-LT cells failed to induce a membrane localization of E-cad and ZO-1 and did not affect actin stress fibers or the expression of Vim (Figure 4D, Supplemental Figure S3C). Together, these results indicate that Mbd3 plays a critical role in sustaining the mesenchymal state of M clone cells.

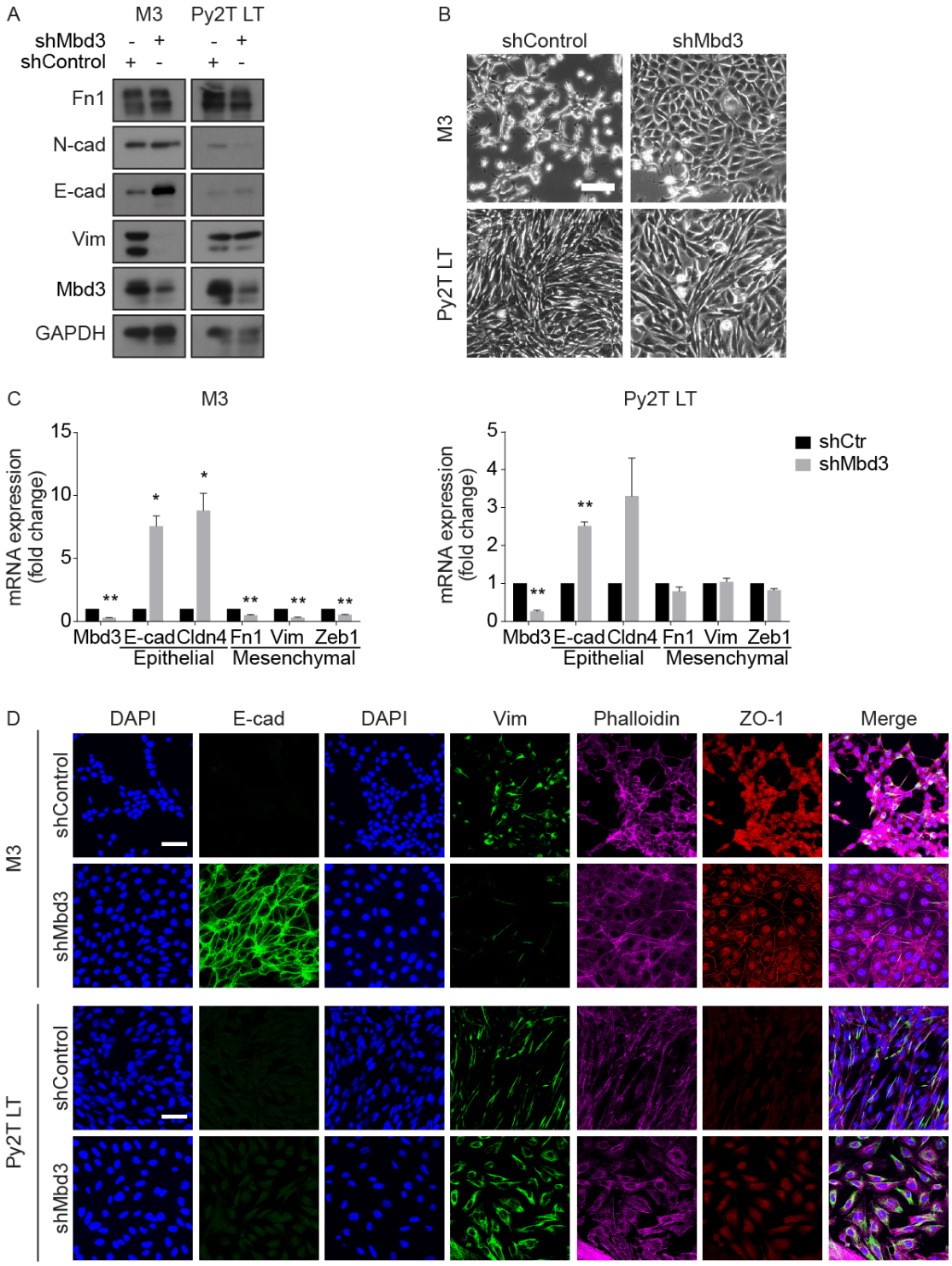

Figure 4. The Mbd3/NuRD complex is required for the maintenance of a mesenchymal cell state (A) The protein levels of fibronectin (Fn1), N-cadherin (N-cad), E-cadherin (E-cad), vimentin (Vim), and Mbd3 were evaluated by immunoblotting in M3 clone cells and in Py2T-LT cells expressing either shControl or shMbd3. Immunoblotting for GAPDH was used as a loading control. **(B)** Phase-contrast microscopy of M3 clone cells and Py2T-LT cells stably expressing shControl

or shMbd3. Scale bar, 100µm. **(C)** Quantitative RT-PCR analysis of the mRNA levels of Mbd3, E-cadherin (E-cad), Claudin4 (Cldn4), fibronectin (Fn1), vimentin (Vim), and Zeb1 in M3 clone cells and Py2T-LT cells expressing shMbd3. Fold changes are related to M3 clone cells and Py2T-LT cells expressing shControl. **(D)** Confocal immunofluorescence microscopy analysis of the expression and localization of the epithelial markers E-cadherin (E-cad) and ZO-1 and the mesenchymal marker vimentin (Vim) in M3 clone cells and Py2T-LT cells expressing either shControl or shMbd3. Phalloidin and DAPI staining visualize the actin cytoskeleton and nuclei, respectively. Scale bar, 50µm. Data are displayed as mean ± SEM. Statistical values were calculated using a paired, two-tailed t-test. *, $P < 0.05$; **, $P < 0.01$.

We next compared the genes differentially expressed between shControl and shMbd3-expressing M3 clone cells to the differentially expressed genes between Py2T-LT and M3 clone cells by RNA sequencing. 1351 genes were found to be specific for the Mbd3-dependent stable mesenchymal state (Supplemental Figure S3D). The majority of these genes (940 out of 1351) were differentially regulated by the depletion of Mbd3 (Supplemental Figure S3E), indicating that Mbd3 affects a wide range of genes to maintain the mesenchymal state of M clone cells.

3.1.5.5 Tet2 is required for the maintenance of the mesenchymal cell state

Based on reports that 5hmC was critical for the recruitment of the Mbd3/NuRD complex to its target genes in embryonic stem cells (ESCs) (Yildirim et al., 2011), we assessed whether Tet family hydroxylases played a role in maintaining the mesenchymal phenotype of M clone cells. Of the three family members, only the shRNA-mediated knock-down of Tet2 expression in M3 clone cells provoked a conversion to an epithelial cell morphology, an evident elevation of E-cad and Cldn4 expression and a reduced expression of Vim, Fn1, N-cad and Zeb1 at both the protein and mRNA level (Figure 5A-C). In contrast, knockdown of Tet2 expression in Py2T-LT cells did not affect cell morphology or EMT marker expression (Figure 5A-C).

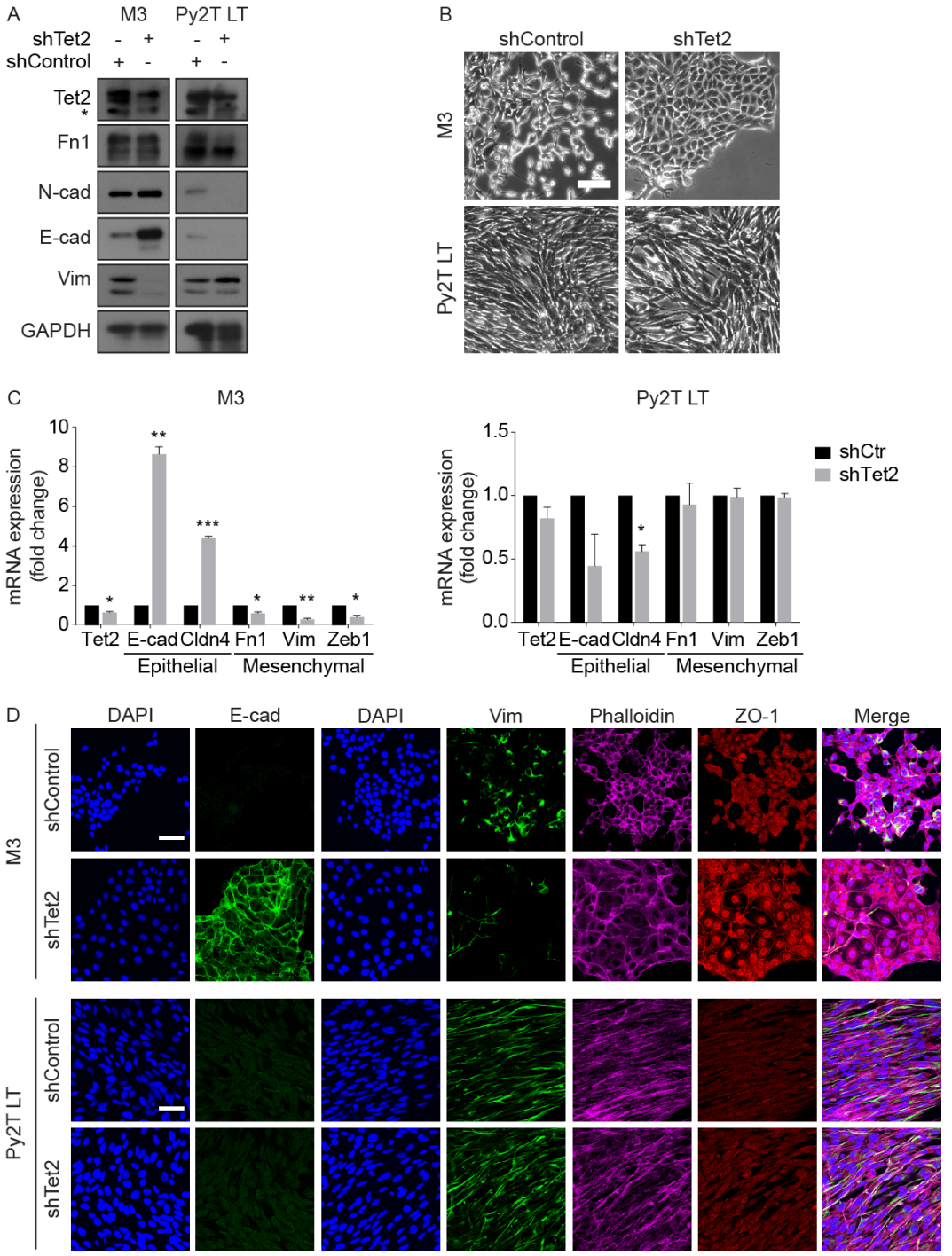

Figure 5. Tet2 is required for the maintenance of a mesenchymal cell state (A) Protein levels of Tet2, fibronectin (Fn1), N-cadherin (N-cad), E-cadherin (E-cad), and vimentin (Vim) were determined by immunoblotting in M3 clone cells and Py2T-LT cells expressing either shControl or shTet2. Immunoblotting for GAPDH was used as a loading control. * indicates a non-specific protein band stained by anti-Tet2 antibodies. **(B)** Phase-contrast microscopy of M3 clone cells and Py2T-LT cells expressing shControl or shTet2. Scale bar, 100μm. **(C)** Quantitative RT-PCR

analysis of the mRNA levels of Tet2, E-cadherin (E-cad), Claudin4 (Cldn4), fibronectin (Fn1), vimentin (Vim), and Zeb1 mRNA levels in M3 clone cells and Py2T-LT cells expressing shTet2. Fold changes are related to cells expressing shControl. **(D)** Confocal immunofluorescence microscopy analysis of the expression and localization of E-cadherin (E-cad) and ZO-1 and vimentin (Vim) in M3 clone cells and Py2T-LT cells expressing either shControl or shTet2. Phalloidin and DAPI staining visualize the actin cytoskeleton and nuclei, respectively. Scale bar, 50µm. Data are displayed as mean ± SEM. Statistical values were calculated using a paired, two-tailed t-test. *, $P < 0.05$; **, $P < 0.01$, ***; $P < 0.001$.

Comparable results were obtained with siRNA-mediated ablation of Tet2 expression in M3 clone cells and in Py2T-LT cells (Supplemental Figure S4A,B).

Confocal immunofluorescence microscopy analysis revealed the localization of E-cad and ZO-1 at cell-cell junctions, accompanied by cortical actin formation and reduced Vim expression in shTet2-expressing M3 clone cells (Figure 5D). In comparison, shRNA-mediated depletion of Tet2 in Py2T-LT cells did not show any effect (Figure 5D). The transient ablation of Tet2 expression by transfection of siRNAs confirmed these results (Figure S4C). Together, the results indicate that Tet2 is a critical player in the maintenance of a mesenchymal state in irreversible EMT cells.

Next generation RNA-sequencing revealed that 1116 were shared between the genes changed in their expression by depletion of Tet2 in M3 clone cells and genes differentially expressed between M3 clone cells and Py2T-LT cells (Supplemental Figure S4D). Similar to the depletion of Mbd3, the majority of these genes (760 out of 1116) were differentially regulated by the loss of Tet2 expression (Supplemental Figure S4E), indicating a profound function of Tet2 and Mbd3 in maintaining a mesenchymal cell state.

3.1.5.6 Combinatorial targeting of HDACs and Mbd3/Tet2

The above results indicate that the pharmacological inhibition of HDACs alone induces only a partial reversion of mesenchymal M clone cells to an epithelial state. By contrast, interfering with the Mbd3/NuRD complex, which may also involve HDAC and Tet2 activities, leads to an efficient reversion of M clone cells to an epithelial phenotype. Hence, we tested whether a combination of pharmacological HDAC inhibition with the ablation of Mbd3 or Tet2 provided an additive effect in reverting M clone cells to an epithelial state. M3 clone and Py2T-LT cells expressing shControl, shTet2 or shMbd3 were treated with CI994 or with solvent control. While the specific shRNAs efficiently depleted Mbd3 and Tet2 expression, respectively, CI994 efficiently inhibited HDAC enzymatic activity (Figure 6A). Interestingly, the ablation of both Tet2 and Mbd3 caused an apparent upregulation of H3 acetylation levels even in the absence of CI994, indicating the depletion of Tet2 and Mbd3 also affected HDAC activity (Figure 6A), likely by disrupting Mbd3/NuRD complexes. In combination with CI994 treatment, Tet2 and Mbd3-depleted M3 clone cells showed an increased expression of E-cad accompanied by the loss of Vim and Fn1 expression, as compared to the depletion of either Mbd3 or Tet2 alone or treatment with CI994 alone (Figure 6A). All treated cells showed an epithelial cell morphology which did not markedly increase upon combination treatment (Figure 6B). Notably, the combined ablation of Tet2 or Mbd3 with CI994 treatment also induced an increase in E-cad expression and reduced Fn1 and N-cad expression in Py2T-LT cells, in addition with a less elongated cellular phenotype (Figure 6B). The increased efficiency of a MET in M clone cells and Py2T-LT cells upon combinatorial treatment was also apparent by quantitative RT-PCR analysis of EMT marker expression (Supplemental Figure S5A).

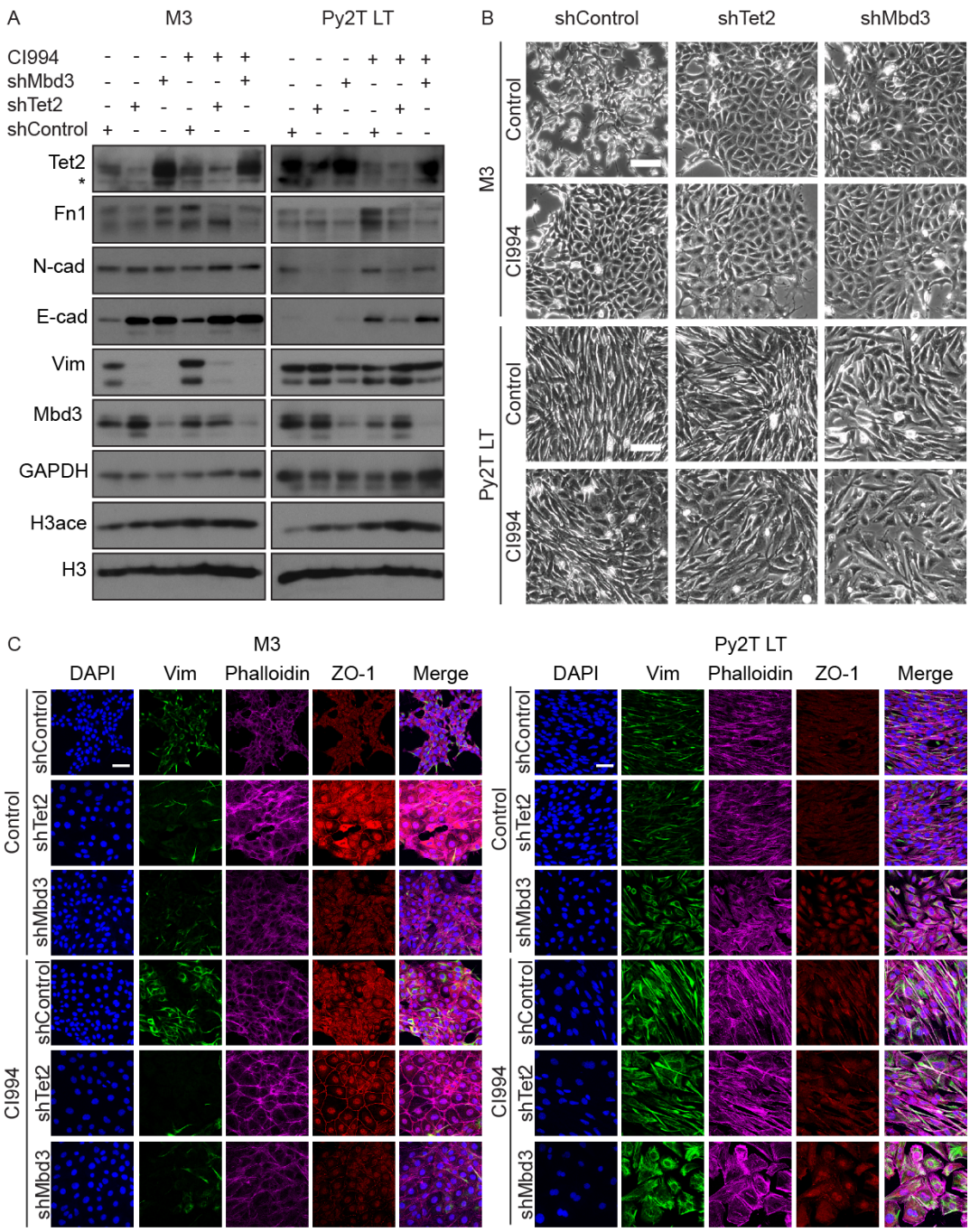

Figure 6. Combination of the depletion of Mbd3 or Tet2 expression with HDAC inhibition potentiates an MET of stable mesenchymal cells (A) Protein levels of Tet2, fibronectin (Fn1), N-cadherin (N-cad), E-cadherin (E-cad), vimentin (Vim) and Mbd3, as determined by immunoblotting of M3 clone cells and Py2T-LT cells stably expressing shControl, shTet2 or shMbd3 and cultured in the absence or presence of 2μM CI994 for 72 hours. Immunoblotting for GAPDH was used as a loading control. * indicates a non-specific protein band bound by anti-Tet2 antibodies. **(B)** Phase-contrast microscopy of M3 clones cells and Py2T-LT cells expressing shControl,

shTet2 or shMbd3 and cultured in the absence or presence of 2μM CI994. Scale bar, 100μm. **(C)** Confocal immunofluorescence microscopy analysis of the localization and expression of ZO-1 and vimentin (Vim) in M3 clone cells and Py2T-LT cells expressing shControl, shTet2 or shMbd3 and cultured in the absence or presence of 2μM CI994 for 72 hours. Phalloidin and DAPI staining visualize the actin cytoskeleton and nuclei, respectively. Scale bar, 50μm.

Immunofluorescence microscopy analysis confirmed these results. The depletion of Tet2 and Mbd3 in M3 clone cells in combination with CI994 treatment induced a more efficient localization of E-cad and ZO-1 at cell-cell junctions and the formation of cortical actin while enhancing a reduction in Vim expression, as compared to the ablation of either Mbd3 or Tet2 and CI994 treatment alone (Figure 6C, Supplemental Figure S5B). In contrast, the combinatorial treatment of Py2T-LT cells did neither provoke the localization of E-cad and ZO-1 at cell-cell junctions nor reduce mesenchymal Vim expression and actin stress fiber formation. Overall, these results underscore the observation that the combined inhibition of HDACs and the ablation of Mbd3 or Tet2 provides an additive effect in converting otherwise irreversible EMT cells to an epithelial state. The results also suggest that a functional Mbd3/NuRD complex together with HDAC and Tet2 hydroxylase activities is required for the maintenance of the mesenchymal cell state.

We further went on to identify the genes that are critical for the maintenance of the mesenchymal cell state in M clone cells. We first identified 367 genes that are differentially expressed upon treatment of M3 clone cells with the HDAC inhibitor CI994 or by the depletion of Mbd3 or Tet2 alone (Supplemental Figure S6A). We also identified 784 genes that are differentially regulated between Mbd3 or Tet2 depletion alone and Mbd3 or Tet2 depletion in combination with CI994 treatment (Figure S6A). Finally, we compared the 367 genes shared between CI994, shMbd3 and shTet2 treatments and the 784 genes that are assigned to the additive effect of HDAC inhibition in combination with Mbd3 and Tet2 depletion. This comparison identified 92 genes which change in their expression by all the treatments leading to an MET of M clone cells. We hypothesize that the 92 genes could be responsible for the additive effect of HDAC inhibition and

Mbd3 or Tet2 depletion during an MET of M clone cells and we refer to this list of genes as “induced MET (iMET)” gene signature (Figure S6A; Supplemental Table S1).

We next assessed whether the iMET genes were also differentially regulated during an MET of a reversible EMT system. RNA-sequencing was performed at early, middle and late time points of a MET of Py2T-LT cells upon TGFβ withdrawal (Py2T MET; Supplemental Table S1). Differentially expressed genes during the time course of Py2T MET cells were then compared to the 92-gene iMET signature (Supplemental Figure S6B). This analysis revealed not only common but also distinct gene expression patterns between the iMET gene signature and the genes changing during the reversible MET time course. The results further highlight the notion that, while sharing some regulatory pathways, an irreversible and a reversible EMT are distinct processes.

3.1.5.7 Tet2 and Mbd3 are required for primary tumor growth and metastasis

The critical role of Tet2 and the Mbd3/NuRD complex in an MET of M clone cells *in vitro* raised the question whether these epigenetic modifiers also play a role during metastasis formation *in vivo*. To address this question, M3 clone cells stably expressing shRNAs against Tet2 (shTet2), Mbd3 (shMbd3) and a non-targeting control-shRNA (shControl) were orthotopically implanted into the mammary fat pads of NSG mice. When the tumors were first palpable, daily treatment with CI994 was initiated (35 mg/kg; i.p.). The ablation of Tet2 and Mbd3 led to a significant decrease in primary tumor growth and tumor weights. The combination with CI994 treatment caused a further significant reduction in tumor growth and tumor weights as compared to the vehicle-treated cohorts (Figure 7A,B). The efficient depletion of Tet2 and Mbd3 expression and the efficacy of CI994-mediated inhibition of HDAC activity in the tumors were verified by immunoblotting (Figure 7C). Quantitative RT-PCR revealed that the combinatorial treatment with CI994 enhanced the

upregulation of epithelial markers and the downregulation of mesenchymal markers in Tet2 and Mbd3-depleted primary tumors (Figure 7D).

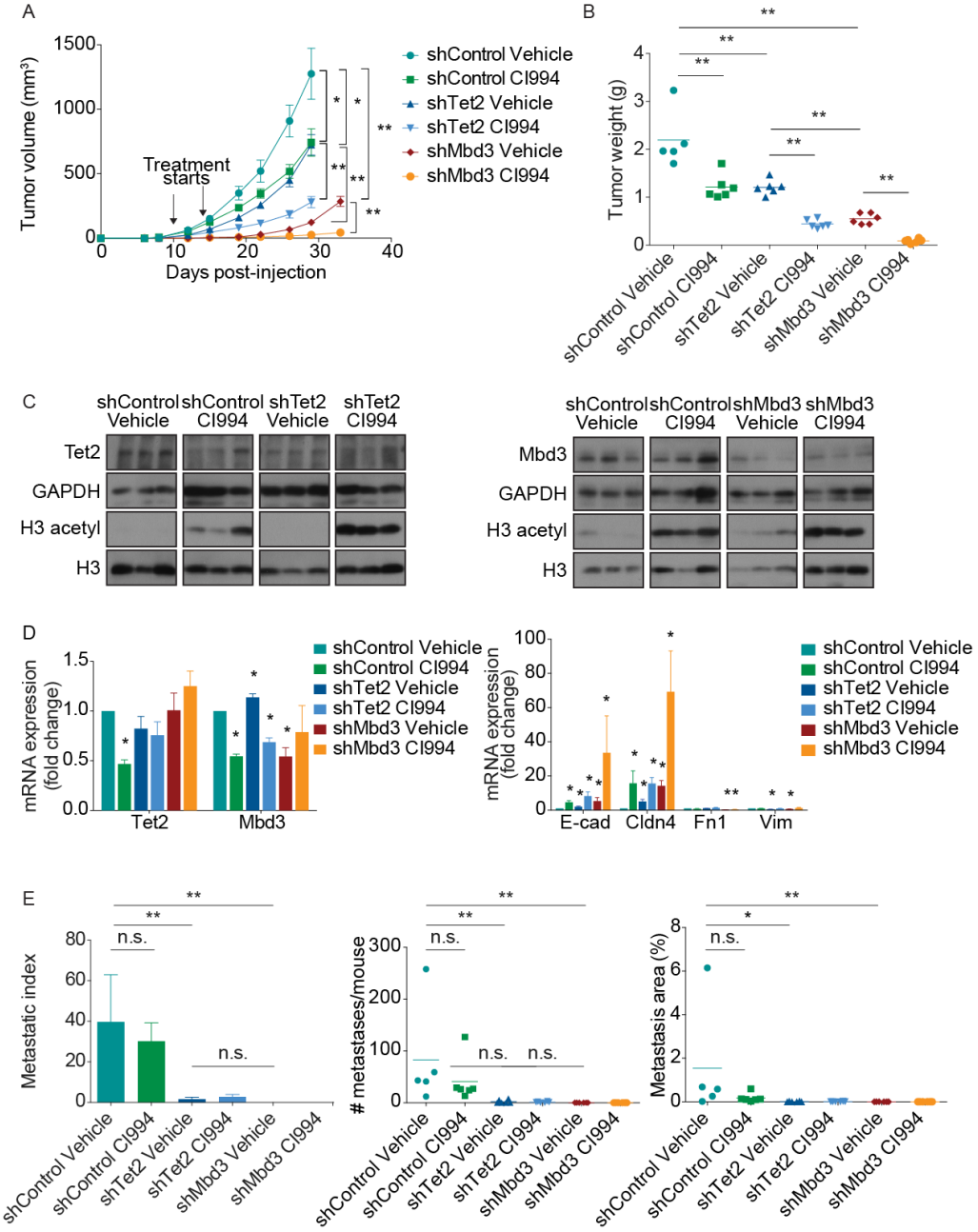

Figure 7. Depletion of Mbd3 or Tet2 expression in combination with HDAC inhibition efficiently represses primary tumor growth and lung metastasis (A) 10^5 shControl, shTet2, and shMbd3-expressing M3 clone cells were transplanted into the mammary fat pad of female NSG mice. When the tumors were palpable, mice were treated with HDAC inhibitor CI994 (35 mg/kg, i.p.), and tumor growth was measured over time. At least 5 mice were used for experimental cohort. Data are

displayed as mean tumor volumes ± SEM. **(B)** The mice described in (A) were sacrificed after 29 days of treatment and tumor weights were assessed. **(C)** The expression of Tet2 (left panel), Mbd3 (right panel), and acetylated H3 (H3 acetyl) in tumors of the mice described in (A and B) was analyzed by immunoblotting. Immunoblotting for GAPDH and total H3 was used as loading control. **(D)** Quantitative RT-PCR analysis of the mRNA levels of Tet2 and Mbd3 (left panel) and E-cadherin (E-cad), Claudin4 (Cldn4), fibronectin (Fn1) and vimentin (Vim) (right panel) in shTet2 or shMbd3 expressing tumors from mice described in (A and B). Fold changes relate to mRNA levels in tumors expressing shControl and treated with vehicle control. **(E)** Metastatic spread of shControl, shTet2 and shMbd3-expressing M3 clone tumors treated with vehicle or HDAC inhibitor CI994 was determined by serial sectioning of the lungs of mice described in (A and B). The metastatic index was calculated by the number of metastases divided by the primary tumor weights within the same mice (left panel). Mean of the number of metastases (middle panel) and metastatic area percentages per mouse were also quantified (right panel). Statistical significance was calculated using a Mann-Whitney *U* test. N.s., non-significant; *, $P< 0.05$; **, $P < 0.01$.

The ablation of Tet2 and Mbd3 also significantly reduced the number and the tissue area of metastasis in the lungs of transplanted mice, even when the number of metastases was normalized to the decreased primary tumor weights observed with the depletion of Tet2 or Mbd3 (metastatic index; Figure 7E). Remarkably, no metastatic lesions could be detected in mice implanted with shMbd3-expressing M3 clone cells with or without CI994 treatment. Notably, the inhibition of HDACs by itself did not cause a significant reduction in the number of lung metastasis, their surface area or metastatic index.

Altogether, these findings indicate that Tet2 and the Mbd3/NuRD complex play a pivotal role during primary tumor growth and metastasis formation. While a combinatorial treatment with HDAC inhibitors and the genetic depletion of Mbd3 or Tet2 shows an additive effect on MET of murine breast cancer cells *in vitro* and primary tumor growth *in vivo*, this additive effect is not apparent in the inhibition of tumor metastasis formation *in vivo*.

3.1.6 Discussion

We have set out to identify molecular pathways and mechanisms underlying the reversibility and irreversibility of an EMT in murine breast cancer cells. These pathways may serve as potential therapeutic targets to interfere with the metastatic dissemination and outgrowth of malignant cancer cells. Towards this goal, we have used Py2T murine breast cancer cells that undergo a reversible EMT upon stimulation with TGFβ to generate derivatives that maintain a stable mesenchymal phenotype upon normal culture conditions (M clones). We find that M clone cells can be forced to undergo an MET when treated with HDAC inhibitors or when depleted of Mbd3 or Tet2 expression. Notably, these pharmacological or genetic interferences, individually or in combination, efficiently repressed primary tumor growth and metastasis formation of highly tumorigenic and metastatic M clone cells. The results indicate that the Mbd3/NuRD complex containing HDACs and Tet2 may play a critical role in defining the epithelial-mesenchymal plasticity during an EMT and a MET and during the metastatic process. Combinatorial targeting of its components may thus offer an efficient approach to interfere with malignant disease.

Previous studies have mainly focused on HDACs' functional contributions to cancer cell apoptosis, proliferation and angiogenesis. The role of HDACs in epithelial-mesenchymal plasticity has remained unclear. Some reports show that HDAC inhibition induces an EMT in prostate, nasopharyngeal, colon and liver carcinoma cells (Kong et al., 2012); (Jiang et al., 2013). In contrast, other reports indicate that HDAC inhibition results in a partial MET state in breast, ovarian, bladder and pancreatic cancer cells (Tang et al., 2016; Tate et al., 2012). Finally, HDAC inhibition represses drug resistance of cancer cells forced to undergo an EMT by the expression of the transcription factor Zeb1 (Meidhof et al., 2015). Our results are consistent with the latter reports in that HDAC inhibition causes a partial MET phenotype in irreversible EMT cells, whereas no marked effects are observed in reversible EMT cells. In addition, we show that HDAC inhibition represses primary tumor growth with a significant upregulation of epithelial marker expression, yet with

no marked decrease in mesenchymal marker expression. Surprisingly, HDAC inhibition alone had no discernable effect on lung metastasis. Conflicting with our results, it has been reported that HDAC inhibition represses metastasis of hepatocellular carcinoma cells (Coradini et al., 2004).

A critical role for the HDAC1/2-containing Mi-2/NuRD complex during an EMT has been previously reported: it is recruited for the silencing of the E-cadherin (Cdh1) gene promoter by the EMT transcription factors Snail and Twist (Fujita et al., 2003); (Fu et al., 2011). The role of the Mbd3/NuRD complex as another type of NuRD complex during an EMT or a MET has remained elusive. Yet, the HDAC1/2- containing Mbd3/NuRD complex has been shown to act as a molecular block during ES cell differentiation and reprogramming of MEFs into iPS cells (Rais et al., 2013). We here report that Mbd3 is critical for the maintenance of a mesenchymal cell state and that its depletion results in a conversion to an epithelial cell phenotype. Moreover, the depletion of Mbd3 dramatically reduces primary tumor growth and completely abolishes the formation of metastasis.

Mbd3 interacts with Tet1 and regulate its target genes by recognizing 5hmC-rich DNA domains (Yildirim et al., 2011). On the other hand, it has been suggested that Mbd3 binding to DNA is independent of the presence of 5hmC and 5mC sites, even though Mbd3/NuRD co-exists with Tet1 and 5hmC positive sites (Baubec et al., 2013). Notably, DNA demethylation mediated by Tet hydroxylases and Tdg is required for a MET and the reprogramming of MEFs into iPS cells (Hu et al., 2014). In contrast, we here find that the ablation of Tet2 leads to a reversion of cells from a stable mesenchymal to an epithelial state. It has been recently reported that Tet2 could be de-acetylated by interacting with HDAC1 and HDAC2 and that interfering with their activities results into the repression of Tet2 activity and an increase in global 5hmC levels (Zhang et al., 2017b). Our results show that the inhibition of HDAC class I in combination with the depletion of Tet2 provides an additive effect to the reversion of mesenchymal M3 clone cells to an epithelial state.

Here, we demonstrate an important regulatory role of the epigenetic modifiers Mbd3/NuRD and Tet2 in the regulation of cell state transitions and of primary tumor growth and metastasis by their ability to affect the expression

of a wide range of genes. Notably, we have identified a 92 gene iMET signature representing genes that are differentially regulated during an MET of irreversible EMT cells induced by a combination of HDAC inhibition and depletion of Mbd3 and/or Tet2. Most importantly, our work identifies the inhibition of HDACs and of Tet2 and the Mbd3/NuRD complex as suitable therapeutic targets to interfere with primary tumor growth and metastasis formation. While potent pharmacological inhibitors against HDACs have been developed and are in clinical trials, their clinical efficacy appears sobering. Our work suggests that HDAC inhibition should be combined with the inhibition of Mbd3/NuRD and Tet hydroxylases. Unfortunately, efficient inhibitors of Tet hydroxylases and of the Mbd3/NuRD complex are only in development or are lacking (Scourzic et al., 2015). It has been reported that 2-hydroxyglutarate (2-HG) could inhibit Tet enzymes (Xu et al., 2011). However, many other α-ketoglutarate-dependent dioxygenases may be targeted as well (Xiao et al., 2012). Hence, specific inhibitors for Tet enzymes need to be developed to test their efficacy in repressing primary tumor growth and metastasis formation alone and in combination with HDAC inhibitors. Due to their pleiotropic mode of action and their reversible nature, these epigenetic modifiers are attractive targets for the development of novel cancer therapies.

3.1.7 Material and Methods

Reagents and antibodies

Reagents: recombinant human (rh) TGFβ1 (240-B, R&D Systems), DMEM (D5671, Sigma-Aldrich), MEGM (C-21010, PromoCell) with SupplementMix (C-39115, PromoCell), PBS (D8537, Sigma-Aldrich), trypsin (T4174, Sigma-Aldrich), FBS (F7524, Sigma-Aldrich), glutamine (G7513, Sigma-Aldrich), pencillin/streptomycin (P4333, Sigma-Aldrich), Opti-MEM (11058-021, Gibco), Lipofectamine RNAiMax (13778-150, Invitrogen), Alexa Fluor-488, 568, 633 (Invitrogen), Polybrene (107689, Sigma-Aldrich), Puromycin (ant-pr-5b, Invivogen), JetPEI (101-10, Polyplus), TRI Reagent® (T9424, Sigma-Aldrich), M-MLV reverse transcriptase (M314C, Promega), PowerUP™ SYBR® green Master Mix (A25743, ThermoFisher), Bradford reagent (500-0006, Biorad), protease inhibitor cocktail (P2714, Sigma-Aldrich).

Antibodies for immunoblotting: E-cadherin (610182, Transduction Laboratories), N-cadherin (M142, Takara), Fibronectin (F-3648, Sigma-Aldrich), GAPDH (ab9485, Abcam), Vimentin (5741, Cell Signaling), Mbd3 (14540, Cell Signaling), Tet2 (ab124297, Abcam), H3 acetyl (06-599, Millipore), H3K27me3 (07-449, Millipore), Histone H3 (ab1791, Abcam).
Antibodies for immunofluorescence: E-cadherin (13-1900, Zymed), Vimentin (V225, Sigma-Aldrich), Vimentin (NB300-223, Novus Biological, used in tissues), ZO-1 (617300, Zymed), Phalloidin (A12380, Invitrogen), N-Cadherin (610921, Transduction Laboratories).
siRNAs: siControl (ON-TARGET plus Non-Targeting pool, D-001810-10, Dharmacon), siTet2 (M-058965-01, Dharmacon), siMbd3 (M-047318-01, Dharmacon).
shRNAs: shControl (Mission Non-target shRNA control vector, SHC002), shTet2 (SHCLNG- NM_145989 Mouse, TRCN0000201087), shMbd3 (SHCLNG- NM_013595 Mouse, TRCN0000304501).
Pharmacological inhibitors: LBH589 (Panobinostat, S1030, Selleckchem), CI994 (Tacedinaline, S2818, Selleckchem, used for *in vitro* studies), CI994 (Tacedinaline, A4102, Apexbio, used for *in vivo* studies), Trichostatin A (TSA, T8552, Sigma-Aldrich), 3-Deazaneplanocin A (DZNep, 13828, Cayman Chemical), EPZ005687 (S7004, Selleckchem), 5-Aza-2'-deoxycytidine (Decitabine, A3656, Sigma-Aldrich).

Cell lines

Py2T cells (Waldmeier et al., 2012) and M clone cells were cultured in Dulbecco's modified Eagle's medium (DMEM) supplemented with glutamine, penicillin, streptomycin and 10% FBS (Sigma-Aldrich). Py2T cells were treated with 2ng/ml TGFβ1 and the medium was replenished every 3 days. All cells were cultured at 37°C with 5% CO_2 in a humid incubator.
In vitro irreversible EMT clones: M clones were generated by culturing in MEGM supplemented with SupplementMix (PromoCell) and glutamine, penicillin, streptomycin and 7% FBS (Sigma-Aldrich) for 3 months, when subpopulations of mesenchymal cells became apparent. Then, cells were transferred into DMEM supplemented with glutamine, penicillin, streptomycin

and 10% FBS (Sigma-Aldrich) and cultured for 2 months to select for stable mesenchymal subpopulations which were subsequently isolated as single cells and expanded as cell clones in 96-well plates.

Inhibitor treatments: Py2T-LT cells and M clone cells were treated with 2μM CI994 or 10nM LBH589 for 3 days. M2 and M3 clones were treated with 5μM DZNep, 2μM Decitabine, or 100nM TSA for 3 days. Py2T-LT cells and M3 clones were treated with 5μM CI994 or 5μM EPZ005687 for 6 days.

RNA isolation and quantitative RT-PCR

Total RNA was prepared using TRI Reagent (Sigma-Aldrich) for cultured cells or RNeasy mini kit (74104, Qiagen) for tissues and for RNA sequencing by using miRNeasy mini kit (217004, Qiagen). RNA was reverse transcribed with M-MLV reverse transcriptase (Promega), and transcripts were quantified by PCR using PowerUP SYBR green Master Mix (Thermo Fisher Scientific) in a StepOne Plus PCR machine (Applied Biosystems). Ribosomal protein L19 expression (RPL19) primers were used for normalization and fold changes were calculated using the comparative Ct method (ΔΔCt). Primers used for quantitative RT-PCR are listed in Supplemental Table S2.

Immunofluorescence staining of cultured cells

Cells were plated on glass coverslips, fixed with 4% paraformaldehyde/ PBS for 20 min and permeabilized with 0.5% NP-40 for 10 min at room temperature. Next, cells were rinsed and blocked using 3% BSA, 0.01% Triton X- 100 in PBS for 30 min at room temperature. Subsequently, cells were incubated with primary antibodies against E-cadherin, N-cadherin, ZO-1, Vimentin overnight at 4ºC. Cells were rinsed 3 times with blocking reagent followed by incubation with fluorochrome-labeled secondary antibodies or phalloidin-568 (Invitrogen) for 1 hour at room temperature. The coverslips were counterstained with DAPI (Sigma-Aldrich) for 5 min, rinsed 3 times, mounted (Fluorescent mounting medium, Dako) on microscope slides and imaged with a conventional immunofluorescence microscope (Leica DMI 4000) or a confocal laser scanning microscope (Leica SP5). Data were processed with Fiji Sofware.

Immunoblotting

Cells were lysed in RIPA buffer (150mM NaCl, 2mM $MgCl_2$, 2mM $CaCl_2$, 0.5% NaDOC, 1% NP40, 0.1% SDS, 10% Glycerol, 50mM Tris pH 8.0) containing 2mM Na_3VO_4, 10mM NaF, 1mM DTT, and a 1:200 dilution of stock protease inhibitor cocktail for mammalian cells (Roche). Protein concentration was determined using the Bradford assay (Bio-Rad). Equal amounts of protein were diluted in SDS-PAGE loading buffer (10% glycerol, 2% SDS, 65mM Tris, 1mg/100 ml bromophenol blue, 1% β-mercaptoethanol) and resolved by SDS-PAGE. Proteins were transferred to polyvinylidene fluoride (PVDF) membranes (Millipore) by wet transfer, blocked with 5% skim milk powder in TBS/0.05% Tween 20 and incubated with the indicated antibodies. HRP-conjugated secondary antibodies were detected by chemiluminescence with X-ray films (FUJIFILM).

Histone extraction

Cells were resuspended in lysis buffer (10mM HEPES, pH 7.9, 1.5mM $MgCl_2$, 10mM KCl, 0.5mM DTT) containing 1:200 dilution of protease inhibitor cocktail for mammalian cells (Roche). Acid extraction of histones from the nuclei was achieved by HCl to the final concentration of 0.2M and incubated for 30 min. Subsequently, the samples were centrifuged for 10 min and supernatant was neutralized with 5M NaOH.

Pyrosequencing of bisulfite-converted DNA

Genomic DNA was isolated from 10^6-10^7 cells by collection in 300µl Tris-EDTA buffer (10mM Tris-HCl pH 8.0, 1mM EDTA). Then, 300µl lysis buffer (20mM Tris-HCl pH 7.5, 4mM EDTA, 20mM NaCl, 1% SDS, 1mg/ml proteinase K) were added and incubated at 50°C for 5h. Subsequently, DNA was extracted by phenol/chloroform and precipitated by Na-acetate/ethanol. DNA pellets were resuspended in Tris-EDTA buffer pH 8.0, followed by RNase A (R6513, Sigma-Aldrich) at 37°C for 30min. Genomic DNA was treated with sodium bisulfite using the Epitect Bisulfite Kit (59104, Qiagen) according to the manufacturer´s instructions.

The bisulfite converted E-cadherin (E-cad) gene promoter region was PCR amplified by using methylation-specific primers with the biotin-labeled reverse primers at the 5'-end and HPLC-purified by using unconverted DNA as a negative control. PCR reactions were performed with 0.05 units JumpStart Taq DNA Polymerase (D4184, Sigma-Aldrich) per µl reaction volume 0.4µM primers and 2.5mM $MgCl_2$ in 50µl reactions. After 5 min of initial denaturation at 95°C, the cycling conditions of 35 cycles consisted of denaturation at 95°C for 30 s, annealing at 58°C for 30 s and elongation at 72°C for 2 min. Then, PCR products loaded on the gel and purified by using GenElute PCR Clean-up kit (NA1020, Sigma-Aldrich). 500ng of biotin-labeled PCR products were immobilized on streptavidin-coated sepharose beads (GE Healthcare) and sequenced with a PyroMark Q24 pyrosequencing system (Qiagen) according to the manufacturer´s instructions (adapted from (Noreen et al., 2014). The sequences of PCR and sequencing primers are given in Supplemental Table S3.

RNA-sequencing and data analysis:

Total RNA was isolated from cells of 2 independent experiments using the miRNeasy Mini Kit (Qiagen) according to the manufacturer's instruction. RNA quality control was performed with a fragment analyzer using the standard or high sensitivity RNA analysis kit (DNF-471-0500 or DNF-472-0500) from Labgene and RNA concentration was measured by using the Quanti-iT™ RiboGreen RNA assay kit (Life Technologies/Thermo Fisher Scientific). 200ng of RNA was utilized for library preparation with the TruSeq Stranded Total RNA LT Sample Prep Kit (Illumina). RNA-sequencing was carried out in the Genomics Facility (Basel) by HiSeq SBS kit v4 (Illumina) on an Illumina HiSeq 2500 and by NextSeq 500/550 High Output kit v2 (Illumina) on an Illumina NextSeq 500 according to manufacturer's instructions.

Obtained single-end RNA-seq reads were mapped to the mouse genome assembly, version mm10, with RNA-STAR (Dobin et al., 2013), with default parameters except for allowing only unique hits to genome (outFilterMultimapNmax=10) and filtering reads without evidence in spliced junction table (outFilterType="BySJout"). Using RefSeq mRNA coordinates from UCSC (genome.ucsc.edu, downloaded in December 2015) and the

qCount function from QuasR package (version 3.12.1) (Gaidatzis et al., 2015), we quantified gene expression as the number of reads that started within any annotated exon of a gene. The differentially expressed genes were identified using the edgeR package (version 1.10.1) (Robinson et al., 2010). Genes with p-value smaller than 0.05 and minimum log2 fold change of +/-0.584 were used for downstream analysis.

Batch effect correction and correlation analysis: Correlation analysis between MET, M3 clone (with CI994 inhibitor), depletion of Mbd3, Tet2 in M3 clone (with and without inhibitor) was performed on CPM (counts per million) data after correcting the batch effect using ComBat (Johnson et al., 2007). Correlation was computed using the Pearson method, and linkage criteria used was average. Hierarchical clustering was performed using “hclust” and heatmaps were generated using the heatmap2 function.

Lentiviral infection

Lentiviral plasmids containing short-hairpin RNAs (shRNA) against murine Tet2 and Mbd3 and the Non-Targeting shRNA control vector were purchased from Sigma. In order to produce lentiviral particles, HEK293T cells were transfected with the shRNA-encoding plasmids, the helper vectors pMDL and pREV and the envelope-encoding plasmid pVSV by JetPEI (Polyplus). Virus-containing supernatant was conditioned for 2 days. Viral supernatant was harvested and filtered (0.46µm), supplemented with polybrene (8ng/ml) and used to infect M3 clone cells and Py2T-LT cells. Infected cells were selected with 2µg/ml puromycin (Invitrogen).

siRNA-mediated knockdown

For a transient knockdown of Tet2 and Mbd3, 30nM and 40nM final concentrations of siGENOME smart pool siRNAs (Dharmacon) were used for M clone cells and Py2T-LT cells, respectively. A non-targeting pool was used as a negative control (Dharmacon). Reverse and forward transfections of siRNAs were performed with Lipofectamine RNAiMax reagent (Invitrogen) according to the manufacturer’s instructions.

Tumor transplantations

Mammary fat pad injection: 14-17 weeks old female NOD_scid_gamma (NSG mice; a kind gift from Nicola Aceto, University of Basel, Basel, Switzerland) were anaesthetized with isoflurane/oxygen and injected with $1x10^5$ Py2T-LT cells, M1 and M3 clones in 100µl PBS into mammary gland number 9. 10 mice were used per experimental cohort. Tumors were measured by digital caliper, and tumor volumes were calculated according to the formula $V = 0.543 \times l \times w^2$, where l represents length and w represents width of tumors measured by a digital caliper. When the tumors reached a maximal volume of 1 cm^3, mice were sacrificed by using CO_2, and tumors were isolated and further processed for further analysis.

CI994 treatment: 10^5 M3 cells (shControl, shTet2 and shMbd3) were orthotopically injected into the mammary fat pads of NSG mice as described above. 5-6 mice were used per treatment cohort. Once tumors were palpable, mice were treated daily with vehicle alone (5% DMSO, 30% Kolliphor, 65% Saline water) or with 35mg/kg CI994 (Tacedinaline, Apexbio) by i.p. injection. Mice were sacrificed 29 days post injection for shControl and shTet2, CI994 and vehicle-treated groups and 33 days for shMbd3, CI994 and vehicle-treated groups, due to the 4 days difference of the treatment start date.

Intra-venous injection: Py2T-LT cells, M1 and M3 clones were injected at a final concentration of 10^5 in 100µl PBS into the tail veins of 14-17 weeks old female NSG mice. Mice were sacrificed after 17 days, and lung metastasis was quantified by H&E staining of histological sections.

Tumor tissue transplantation: BALB/c $Rag2^{-/-}$;common γ $receptor^{-/-}$ (RG mice; a kind gift from A. Rolink, University of Basel, Basel, Switzerland) were transplanted with 1-2 mm^3 of M1 and M3 clones derived tumor into the mammary fat pads of 3 mice. Mice were sacrificed, when the tumors reached a maximal volume of 1 cm^3. Transplantation experiments were repeated for 2 generations. All experiments were performed following the rules and legislations of the Cantonal Veterinary Office and the Swiss Federal Veterinary Office (SFVO).

Haematoxylin & Eosin staining

For Haematoxylin & Eosin (H&E) staining, lungs were fixed at 4°C in 4%

phosphate buffered paraformaldehyde (PFA) for 12 hours and then embedded in paraffin after ethanol/xylene dehydration. H&E staining was performed as previously described (Wicki et al., 2006). Staining and metastasis number were evaluated in serial sections with an AxioScop 2 Plus microscope (Zeiss). Lung pictures were acquired with a Zeiss Axio Imager Z2 scanning microscope and metastases were quantified by Visiopharm application.

Immunofluorescence staining

For immunofluorescence analysis of frozen sections, organs were fixed at 4°C in 4% PFA for 2 hours, and cryopreserved for overnight in 20% sucrose in PBS prior to embedding in OCT freezing matrix. Cryosections were cut 7µm thick and dried for 30 min prior to rehydration in PBS. Slides were permeabilized with PBS/ 0.2% TritonX-100 and blocked for 30 min in PBS/5% normal goat serum and then incubated with the primary antibody in blocking buffer for 1 hour at room temperature. Immunofluorescence (IF) stainings were revealed by incubation with Alexa488 or Alexa568 labeled secondary antibodies (Invitrogen) and nuclei were stained with DAPI (Sigma-Aldrich). The stained slides were evaluated with a confocal laser scanning microscope (Leica SP5). Data were processed with Fiji Sofware.

Statistical analysis

Statistical analysis and graphs were generated using the GraphPad Prism software (GraphPad Software Inc, San Diego, CA). Statistical analyses were performed as indicated in the figure legends.

Ethics statement

Animal experiments were performed in strict accordance with the guidelines of the Swiss Federal Veterinary Office (SFVO) and the regulations of the Cantonal Veterinary Office of Basel-Stadt (license numbers 1878, 1907, and 1908). During the whole course of animal experiments, all efforts were made to minimize animal suffering.

Acknowledgments

We thank P. Schär and S. Weis (DBM Basel) for reagents and protocols, F. Noreen (DBM Basel) for pyrosequencing, D.I. Ronen for discussions, C. Beisel (D-BSSE, ETH Zürich) for next generation RNA sequencing, and P. Lorentz (DBM Basel) for excellent microscopy support.

Funding

This work was supported by the SystemsX.ch RTD project Cellplasticity, the SystemsX.ch MTD project MetastasiX, the Swiss National Science Foundation and the Swiss Cancer League.

Author contributions

A.N.K. designed and performed the experiments, analyzed the data and wrote the paper; R.K.R.K. performed bioinformatics analysis; H.A. performed animal experiments; H.B. analyzed animal experiments; and G.C. oversaw the project, designed experiments, analyzed the data and wrote the paper.

3.1.8 Supplemental data

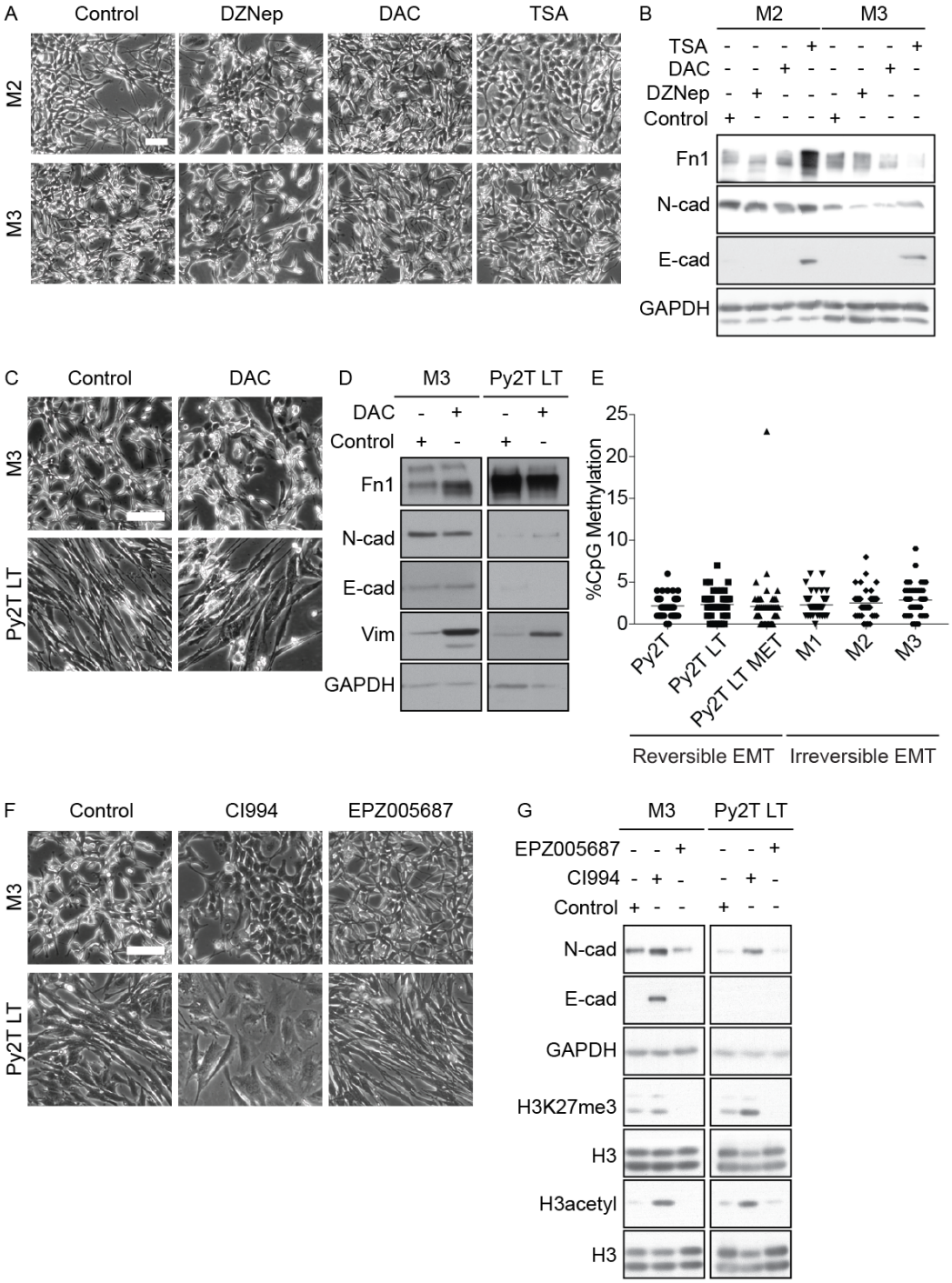

Supplemental Figure S1. Screening of epigenetic inhibitors for the reversion of M clone cells into an epithelial state (related to Figure 2) (A) Morphology of M2 and M3 clone cells treated with 2μM 3-Deazaneplanocin A (DZNep), 2μM 5-Aza-2'-deoxycytidine (DAC), and 100nM Trichostatin A (TSA), as evaluated by phase contrast microscopy. Scale bar, 100μm. **(B)** Immunoblotting analysis of the

expression of fibronectin (Fn1), N-cadherin (N-cad), and E-cadherin (E-cad) in M2 and M3 clone cells in the absence or presence of 2μM DZNep, 2μM DAC, and 100nM TSA for 72 hours. Immunoblotting for GAPDH was used as a loading. **(C)** Morphology of M3 clone cells and Py2T-LT cells treated with 2μM DAC, as visualized by phase contrast microscopy. Scale bar, 100μm. **(D)** Immunoblotting analysis of fibronectin (Fn1), N-cadherin (N-cad), E-cadherin (E-cad), and Vimentin (Vim) in M3 clones and Py2T-LT cells treated or not with 2μM DAC for 6 days. Immunoblotting for GAPDH was used as a loading control. **(E)** The percentage of CpG methylation of the E-cadherin (E-cad) gene promoter was analyzed by bisulfite pyrosequencing in Py2T, Py2T-LT, Py2T-LT MET cells (reversible EMT) and in M1, M2, M3 clone cells (irreversible EMT). **(F)** Morphology of M3 clone cells and Py2T-LT cells treated with 5μM CI994 and 5μM EPZ005687, as evaluated by phase contrast microscopy. Scale bar, 100μm. **(G)** Immunoblotting analysis of N-cadherin (N-cad), E-cadherin (E-cad), H3K27me3, and H3acetyl in M3 clone cells and in Py2T-LT cells treated or not with 5μM CI994 and 5μM EPZ005687 for 6 days. Immunoblotting for GAPDH was used as a loading control for EMT markers. Immunoblotting for H3 was used as loading control for H3K27me3 and H3acetyl.

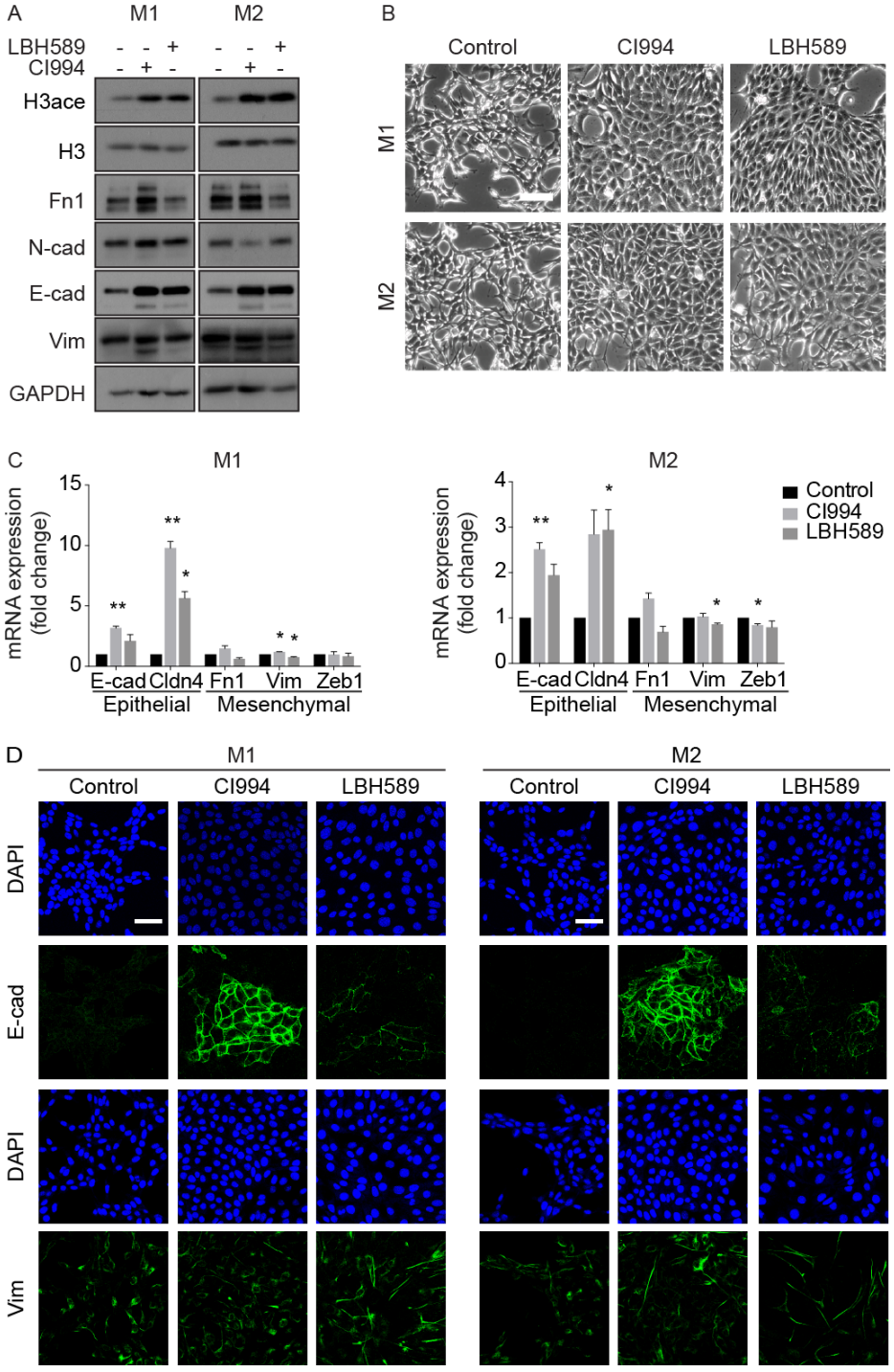

Supplemental Figure S2. HDAC inhibition causes a partial MET in M clone cells (related to Figure 3) (A) Immunoblotting analysis of H3 acetyl (H3ace), fibronectin (Fn1), N-cadherin (N-cad), E-cadherin (E-cad), and vimentin (Vim) in M1 and M2 clone cells cultured in the absence and presence of 2μM HDAC inhibitor (CI994) and 10nM Panobinostat (LBH589) for 72 hours. Immunoblotting for H3 was used as loading control for H3 acetyl and GAPDH was used as a loading control for EMT

markers. **(B)** The morphology of M1 and M2 clone cells treated with 2µM CI994 and 10nM LBH589 for 72 hours was evaluated by phase-contrast microscopy. Scale bar, 100µm. **(C)** Quantitative RT-PCR analysis of the mRNA levels of E-cadherin (E-cad), Claudin4 (Cldn4), fibronectin (Fn1), vimentin (Vim), and Zeb1 in M1 and M2 clone cells treated with CI994 (2µM) and LBH589 (10nM) for 72 hours. Fold changes are related to mRNA levels in cells treated with DMSO diluent. **(D)** Confocal immunofluorescence microscopy analysis of the expression levels and localization of the epithelial marker E-cadherin (E-cad) and the mesenchymal marker vimentin (Vim) in M1 and M2 clone cells cultured in the absence and presence of 2µM CI994 and 10nM LBH589 for 72 hours. Scale bar, 50µm. Data are displayed as mean ± SEM. Statistical values were calculated using a paired, two-tailed t-test. *, $P < 0.05$; **, $P < 0.01$.

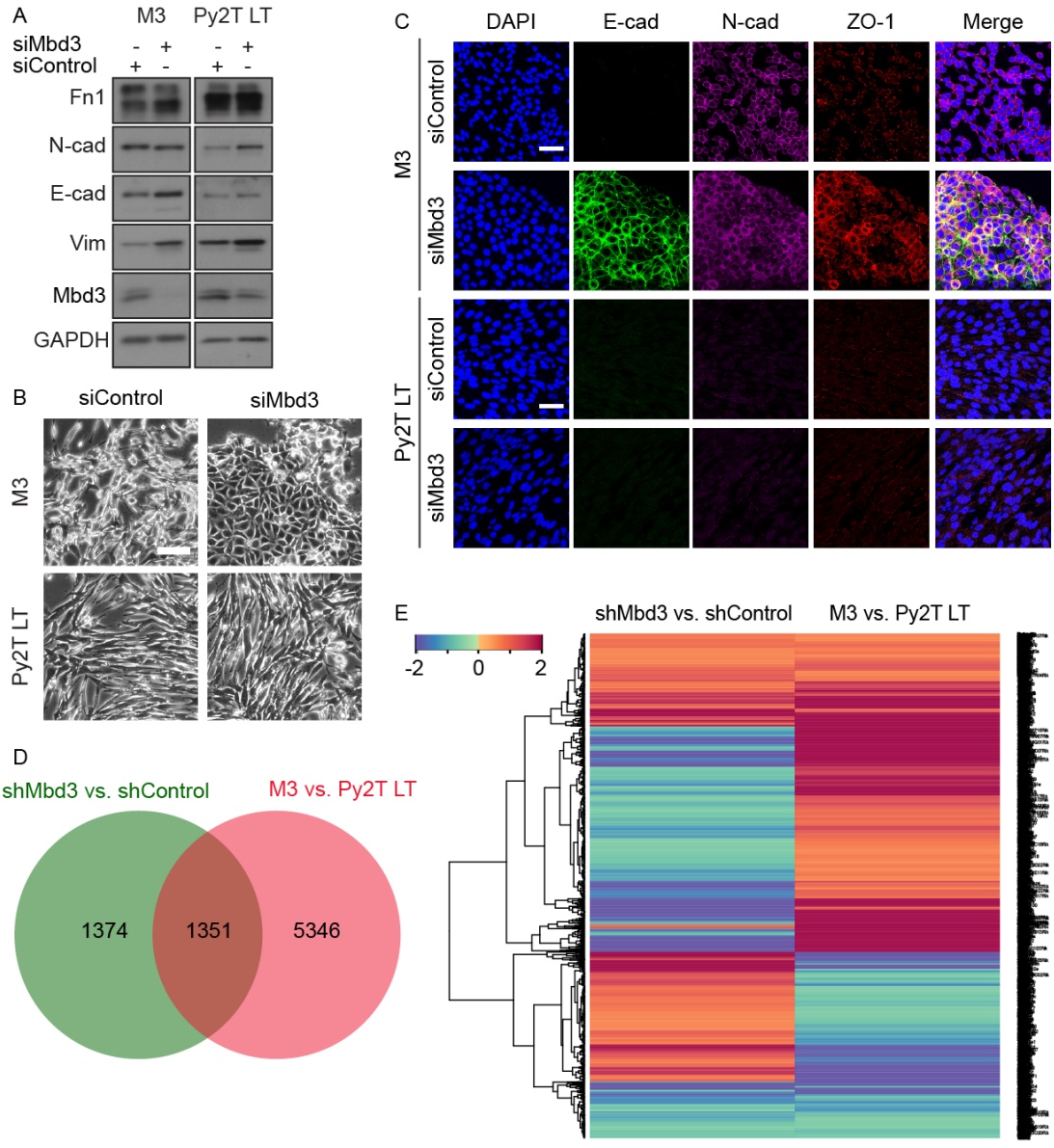

Supplemental Figure S3. The Mbd3/NuRD complex is involved in the maintenance of a mesenchymal state (related to Figure 4) (A) Expression of fibronectin (Fn1), N-cadherin (N-cad), E-cadherin (E-cad), vimentin (Vim) and Mbd3 in M3 clone cells and in Py2T-LT cells transfected with either siControl or siMbd3 was evaluated by immunoblotting. Immunoblotting for GAPDH was used as a loading control. **(B)** Phase-contrast microscopy of M3 clone cells and Py2T-LT cells transfected with either siControl or siMbd3. Scale bar, 100μm. **(C)** Localization and expression levels of the epithelial markers E-cadherin (E-cad) and ZO-1 and the mesenchymal marker N-cadherin (N-cad) in M3 clone cells and in Py2T-LT cells transfected with either siControl or siMbd3 were analyzed by confocal immunofluorescence microscopy. Scale bar, 50μm. **(D)** RNA extracted from shMbd3 or shControl-expressing cells and from M clone cells and Py2T-LT cells was extracted and sequenced by next generation sequencing. The Venn diagram represents the number of differentially regulated genes (*n*=1351; log2 fold change ≤-0.58 and ≥+0.58; p-value≤0.05) that are shared in their differential expression between shMbd3 vs. shControl M3 clone cells and between M3 clone cells vs. Py2T-LT cells. **(E)** The shared differently expressed genes (*n*=1351) identified in (D) were clustered in a heatmap. Columns and rows of the heatmap represent comparison and genes, respectively. Genes that are upregulated and downregulated are indicated by red and blue color code.

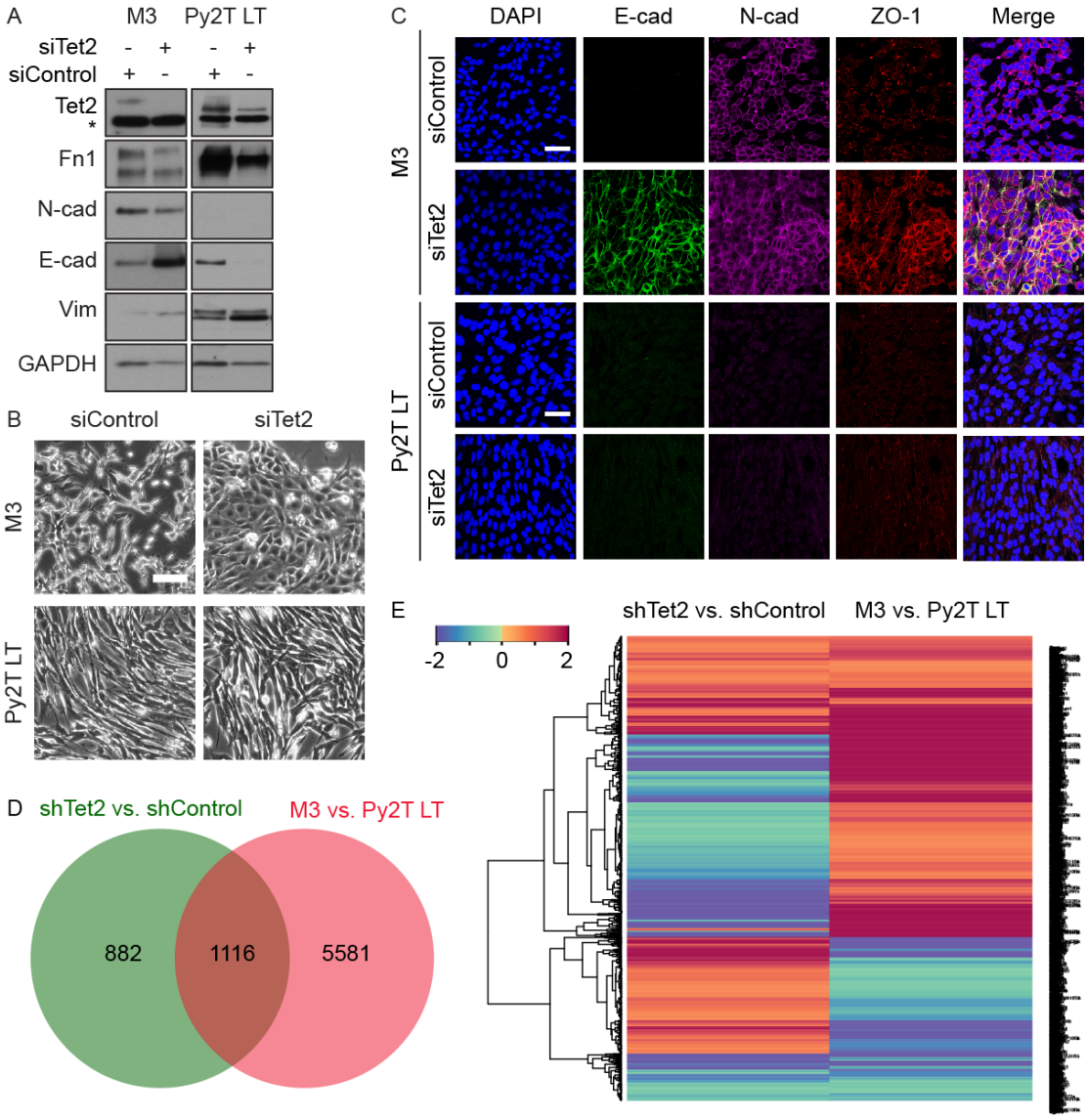

Supplemetal Figure S4. Loss of Tet2 induces a MET of M3 clone cells (related to Figure 5) (A) Tet2, fibronectin (Fn1), N-cadherin (N-cad), E-cadherin (E-cad), and Vimentin (Vim) protein expression levels in either siControl or siTet2-transfected M3 clone cells and in Py2T-LT cells were evaluated by immunoblotting. Immunoblotting for GAPDH was used as a loading control. * represents a non-specific protein band bound by binding for anti-Tet2 antibodies. **(B)** Phase-contrast microscopy of M3 clone cells and Py2T-LT cells transfected with either siControl or siTet2. Scale bar, 100μm. **(C)** Localization and expression levels of the epithelial markers E-cadherin (E-cad) and ZO-1 and the mesenchymal marker N-cadherin (N-cad) in M3 clone cells and in Py2T-LT cells transfected with either siControl or siTet2 were analyzed by confocal immunofluorescence microscopy. Scale bar, 50μm. **(D)** RNA extracted from shMbd3 or shCopntrol-expressing cells and from Ms clone cells and from Py2T-LT cells was extracted and sequenced by next generation sequencing. The Venn

diagram represents the number of differentially regulated genes (*n*=1116; log2 fold change ≤-0.58 and ≥+0.58; p-value≤0.05) that are are shared in their differential expression between shTet2 vs. shControl M3 clone cells and between M3 clone cells vs. Py2T-LT cells. **(E)** The shared differently expressed genes (*n*=1116) identified in (D) were clustered in a heatmap. Columns and rows of the heatmap represent comparison and genes, respectively. Genes that are upregulated and downregulated are indicated by red and blue color code.

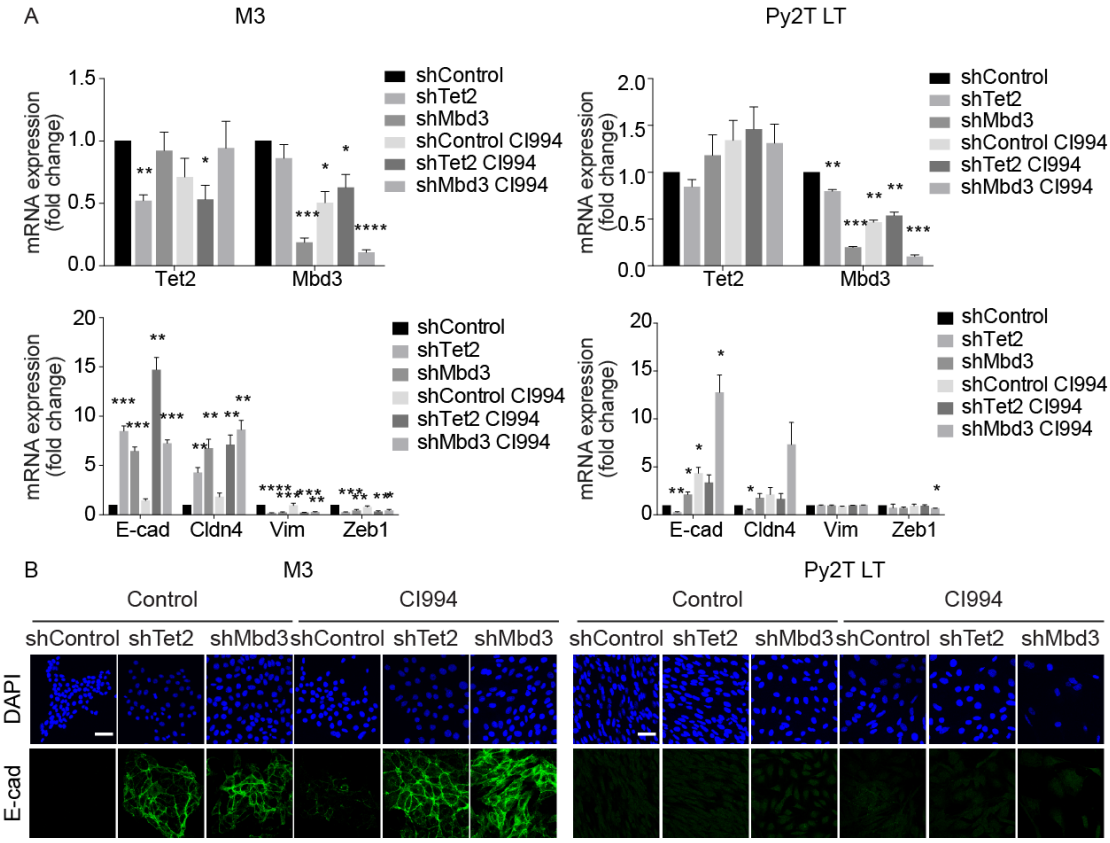

Supplemental Figure S5. HDAC inhibition improved MET in Mbd3 and Tet2-depleted M3 clone cells (related to Figure 6) (A) Quantitative RT-PCR analysis of the mRNA levels of Tet2 and Mbd3, as well as the epithelial genes E-cadherin (E-cad) and Claudin4 (Cldn4) and the mesenchymal genes fibronectin (Fn1), vimentin (Vim), and Zeb1 in Tet2 and Mbd3-depleted M3 clone cells and in Py2T-LT cells cultured for 72 hours in the absence and presence of 2μM HDAC inhibitor CI994. Fold changes are related to the cells stably expressing shControl in the absence of CI994. **(B)** Confocal immunofluorescence microscopy analysis of the localization and expression levels of the epithelial marker protein E-cadherin (E-cad) n M3 clone cells and Py2T-LT cells expressing either shControl, shTet2, or shMbd3 and cultured for 72 hours in the absence and presence of 2μM CI994. Scale bar, 50μm. Data are

displayed as mean ± SEM. Statistical values were calculated using a paired, two-tailed t-test. *, P < 0.05; **, P < 0.01, ***; P < 0.001; ****, P < 0.0001.

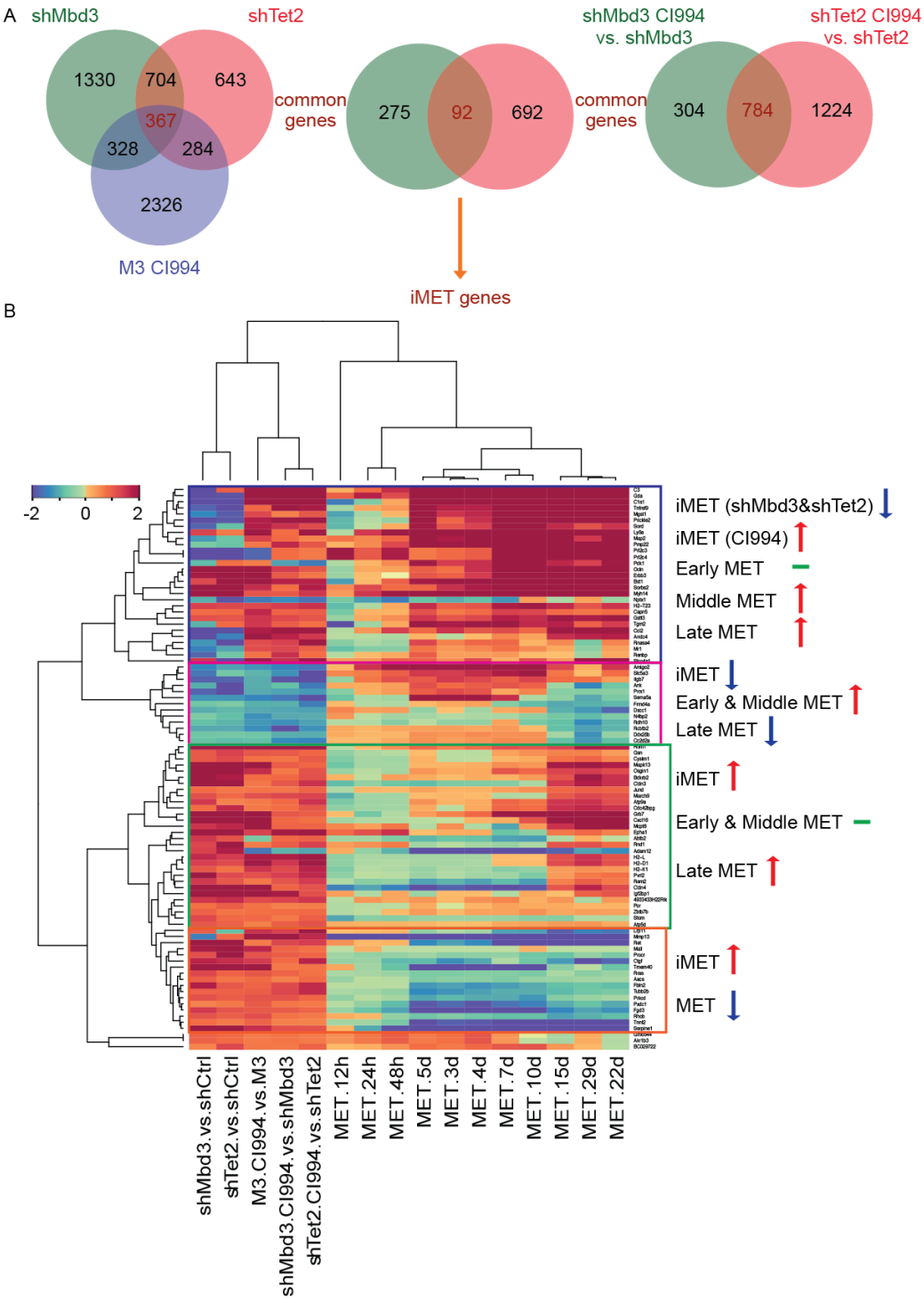

Supplemental Figure S6 (related to Figure 6) (A) The left Venn diagram represents the number of differentially regulated genes shared between the following three comparisons: shMbd3 vs. shControl, shTet2 vs. shControl and M3 clone cells control vs. M3 clone cells treated with CI994 for 72hr. The right Venn diagram

represents the number of differentially regulated genes shared between the comparisons: shMbd3 vs. shMbd3 + CI994 and shTet2 vs. shTet2 + CI994. The middle Venn diagram represents the number of differentially regulated genes that are common between the shared signatures of the left and the right Venn diagram. These common 92 genes are referred to as induced MET (iMET) genes. **(B)** Heatmap of the expression of the 92 shared differentially expressed iMET genes identified in (A) in the shRNA-manipulated and HDAC inhibitor treated M3 clone cells and during a time course of MET in Py2T-LT cells induced by the withdrawal of TGFβ. Columns and rows of the heatmap represent comparison and genes, respectively. Genes that are upregulated and downregulated are indicated by red and blue color code. MET: TGFβ was removed at different time points. These different time points were divided into three subcategories. Early MET (12h, 24h, 48h), Middle MET (3d, 4d, 5d, 7d, and 10d), Late MET (15d, 22d, 29d). Red arrows represent upregulated genes. Blue arrows represent downregulated genes. Green lines represent non-regulated genes.

Supplementary Table S1. List of the 92 genes that are shared in their differential expression between M3 clone cells either depleted of Mbd3 or depleted of Tet2 or inhibited in their HDAC activity. Numbers represent fold changes in expression.

Symbol	induced MET					reversible MET		
	M3.CI994 vs M3	**Tet2 vs Ctrl**	**Mbd3 vs Ctrl**	**shTet2.CI994 vs Tet2**	**Mbd3.CI994 vs Mbd3**	**Early**	**Middle**	**Late**
C3	2.87	0.99	-2.88	2.44	2.30	0.87	4.64	8.85
Myh14	1.11	3.27	2.73	1.49	1.08	1.34	4.96	8.36
Bst1	3.14	2.24	1.26	1.75	1.75	-0.05	3.13	7.03
Gda	2.01	-1.94	-5.32	2.36	2.77	1.33	5.00	6.97
Ocln	3.62	2.31	2.50	1.10	1.40	0.05	2.32	6.69
Sorbs2	1.61	1.98	3.52	1.78	0.79	0.88	2.12	5.68
Ly6a	1.99	0.69	1.32	1.97	0.81	1.23	4.86	5.24
Erbb3	2.41	2.19	1.91	0.71	1.05	-0.10	1.86	4.91
C1s1	2.70	-2.15	-3.52	4.21	3.16	-0.61	3.09	4.78
Grb7	4.29	3.08	3.43	1.01	1.08	-0.27	1.30	4.45
Tnfrsf9	0.88	-2.18	-1.79	1.87	2.11	0.16	2.00	3.52
Mgst1	1.29	-1.86	-1.39	1.09	0.63	-0.41	2.01	3.30
Cxcl16	2.36	2.21	3.19	0.77	0.86	-0.18	0.28	3.16
Prl2c3	-1.75	-3.17	-2.18	0.69	0.82	1.63	1.58	3.05
Prl2c4	-1.75	-3.18	-2.18	0.69	0.82	1.62	1.58	3.05
Prickle2	1.79	-1.89	-5.89	2.03	2.73	-0.47	1.97	2.83

Ccl2	1.81	-3.28	-2.57	3.17	3.59	0.58	1.12	2.57
Pmp22	0.71	-0.76	-0.63	1.09	1.64	0.66	2.44	2.22
Map2	1.32	-0.74	-1.21	0.59	0.82	0.74	2.70	2.18
Mcpt8	2.92	1.67	1.50	0.93	0.94	0.53	-0.10	2.12
Mapk13	2.44	3.02	2.09	0.91	1.02	-0.42	0.27	2.00
Gstt3	1.49	1.10	1.19	1.10	1.26	0.13	1.45	2.00
Slco4a1	2.03	-3.15	1.46	2.42	1.57	0.61	0.81	1.86
Arrdc4	2.09	-1.47	-2.04	1.45	1.72	-0.12	0.18	1.70
Pdk1	0.66	0.77	-0.86	-1.52	-1.13	0.16	1.89	1.66
Rom1	2.08	2.81	2.03	2.10	2.71	0.16	0.94	1.64
Cldn3	0.72	2.25	2.36	1.55	1.09	-0.66	-0.55	1.60
Cdc42bpg	0.69	1.66	0.79	1.09	0.80	-0.35	0.43	1.57
Bdkrb2	0.80	1.83	2.04	1.17	0.86	0.17	0.20	1.55
Sord	1.80	-0.80	-1.77	1.24	1.56	-0.23	1.83	1.43
Atp9a	0.66	0.62	1.45	1.52	0.83	-0.41	0.51	1.42
H2-T23	1.27	1.29	1.35	1.56	1.42	-0.26	1.52	1.41
Tgm2	1.48	0.83	-0.94	0.77	1.04	-0.69	2.06	1.38
Cldn4	2.70	2.87	3.50	1.14	0.92	-1.34	-2.00	1.34
H2-D1	1.97	1.25	1.40	1.95	1.48	-0.27	-0.12	1.33
Osgin1	1.61	2.11	1.98	1.15	0.67	-0.24	0.58	1.33
H2-L	1.85	1.42	1.62	2.34	1.81	-0.29	-0.14	1.28
MARCH9	1.18	0.87	1.16	1.33	1.29	-0.52	-0.02	1.18
Rnd1	0.67	1.98	1.30	1.37	1.04	0.51	-0.24	1.03
Amigo2	-1.27	-1.13	-1.41	-1.58	-1.42	1.21	2.58	1.01
Jund	0.72	0.70	0.82	0.93	0.71	0.00	0.29	0.93
Capn5	1.68	0.87	0.85	1.03	0.95	-0.12	1.08	0.81
Rem2	0.71	1.10	1.45	1.42	1.14	-0.36	-1.04	0.77
Cystm1	0.77	1.24	1.08	1.06	0.73	-0.37	0.09	0.76
Epha1	1.37	3.56	3.00	2.30	1.92	1.19	-0.16	0.74
Igf2bp1	2.90	2.01	2.01	1.19	1.88	0.15	-0.03	0.69
Itgb7	-1.01	-1.77	-1.80	-2.62	-1.96	0.50	1.24	0.66
Pvrl2	1.19	1.23	2.27	1.66	1.39	-0.19	-0.34	0.62
Gsn	1.09	1.35	1.06	0.92	1.06	-0.25	0.14	0.54
Slc5a3	-0.93	-0.69	-1.59	-2.28	-1.28	0.73	1.69	0.52
H2-K1	1.51	0.76	1.09	1.72	1.26	-0.30	-0.36	0.42
Atp5d	0.62	0.97	1.10	1.16	1.00	0.16	0.14	0.35
Zbtb7b	0.76	0.73	0.96	0.84	0.80	-0.04	0.31	0.32
4933433H22 Rik	1.25	1.61	1.50	1.49	1.33	0.21	0.35	0.20
Rnase4	1.22	-2.10	-1.24	2.48	1.36	-0.36	0.76	0.16
Por	0.76	1.04	0.76	0.65	0.61	-0.10	0.18	0.15
BC029722	0.71	1.30	0.60	0.95	0.70	0.25	0.92	0.15
Mr1	1.21	-1.09	-1.47	0.98	1.32	-0.62	0.61	0.04
Abtb2	-0.63	1.14	1.46	0.97	0.88	-0.38	-0.95	0.00
Mall	1.69	2.13	1.89	0.77	0.92	0.06	0.03	0.00
Renbp	0.75	-0.73	-1.75	0.80	1.56	0.06	0.43	-0.01
Gm6644	0.67	0.83	0.95	0.67	0.74	0.74	0.60	-0.05
Akr1b3	0.67	0.83	0.95	0.67	0.74	0.73	0.59	-0.06

Nptx1	-1.52	-1.93	-0.99	-1.63	-1.36	-1.10	-0.70	-0.07
Stom	0.87	0.87	1.28	0.98	0.68	-0.71	-0.39	-0.29
Aacs	0.85	0.73	1.04	0.86	0.61	-0.17	-0.51	-0.30
Rras	1.08	0.95	1.28	0.75	0.94	-0.27	-0.58	-0.36
Prkcd	1.13	1.00	1.17	0.88	1.15	-0.26	-1.05	-0.39
Tmem40	2.99	2.94	2.54	0.73	0.70	-0.26	-2.35	-0.42
Prrx1	-1.02	-3.33	-1.79	-1.20	-1.11	0.02	0.84	-0.52
Procr	1.14	2.46	1.20	0.91	1.02	-0.38	-0.47	-0.60
Ddx26b	-0.73	-0.69	-0.71	-0.98	-0.99	0.15	0.49	-0.65
N4bp2	-1.30	-0.83	-0.61	-1.00	-1.05	0.04	-0.27	-0.71
Sema5a	-1.42	-1.25	-1.24	-2.74	-1.56	-0.42	1.61	-0.71
Tubb2b	1.01	0.97	0.98	1.64	1.30	-0.30	-1.16	-0.74
Fbln2	0.92	1.10	1.79	1.63	1.25	-0.07	-1.17	-0.81
Ank	-0.99	-2.37	-0.98	-1.55	-0.81	0.26	1.03	-0.81
Pxdc1	1.05	0.68	0.62	0.67	0.71	-0.45	-1.73	-0.94
Cc2d2a	-0.82	-0.87	-0.79	-1.42	-1.36	0.11	0.46	-0.96
Rcbtb2	-1.32	-1.04	-1.03	-1.28	-2.05	0.21	0.28	-0.96
Rhob	1.21	1.01	1.13	0.69	0.75	-0.03	-0.72	-0.97
Frmd4a	-0.96	-0.61	-0.71	-1.51	-0.97	-0.09	-0.15	-0.98
Rdh10	-1.23	-0.92	-0.80	-1.13	-1.31	-0.27	-0.24	-1.04
Fgd3	1.06	1.13	1.45	0.94	1.05	-0.75	-2.37	-1.27
Dscc1	-1.05	-0.91	-1.01	-1.10	-1.08	0.44	-0.01	-1.31
Adam12	-1.58	1.80	1.35	-1.08	-0.93	-0.38	-3.91	-1.41
Lrp11	1.56	-0.79	1.03	2.37	1.37	0.07	-0.63	-1.62
Ctgf	1.44	1.59	1.70	1.71	0.84	-0.54	-0.83	-1.75
Tnnt2	0.92	0.69	0.82	0.61	0.64	-0.40	-2.28	-2.44
Ret	0.67	2.83	4.86	1.42	1.31	0.22	-1.71	-4.02
Mmp13	4.08	0.84	-1.49	1.65	3.07	-2.58	-4.54	-5.35
Serpine1	1.60	2.24	2.74	1.15	1.20	-0.97	-5.20	-5.82

Supplemental Table S2. Primers for quantitative RT-PCR

Primer name	Sequences (5'-3')
Rpl19 Forward primer	CTCGTTGCCGGAAAAACA
Rpl19 Reverse primer	TCATCCAGGTCACCTTCTCA
E-cadherin Forward primer	CGACCCTGCCTCTGAATCC
E-cadherin Reverse primer	TACACGCTGGGAAACATGAGC
Claudin4 Forward primer	GTCCTGGGAATCTCCTTGGC
Claudin4 Reverse primer	TCTGTGCCGTGACGATGTTG
Fibronectin Forward primer	CCCAGACTTATGGTGGCAATT
Fibronectin Reverse primer	AATTTCCGCCTCGAGTCTGA

Vimentin Forward primer	CCAACCTTTTCTTCCCTGAA
Vimentin Reverse primer	TTGAGTGGGTGTCAACCAGA
Snail Forward primer	CTCTGAAGATGCACATCCGAA
Snail Reverse primer	GGCTTCTCACCAGTGTGGGT
Zeb1 Forward primer	GCCAGCAGTCATGATGAAAA
Zeb1 Reverse primer	TATCACAATACGGGCAGGTG
Twist1 Forward primer	GCCGGAGACCTAGATGTCATTG
Twist1 Reverse primer	CACGCCCTGATTCTTGTGAA
Tet2 Forward primer	AGAGAAGACAATCGAGAAGTCGG
Tet2 Reverse primer	CCTTCCGTACTCCCAAACTCAT
Mbd3 Forward primer	GAAGCTAAGTGGATTGAGTGCC
Mbd3 Reverse primer	GACAGCAGCGTCTCATCTGTA

Supplemental Table S3. Primers for PCR and Pyrosequencing

Gene name	Sequences (5'-3')
E-cadherin	F: GTTTTTTGGTTGTTATTTGTAGGTG
	R: CTCTATCTCAAACAAAAACCCTACTC
	Seq1: GGTTGTTATTTGTAGGTG
	Seq2: AGAATTTTTGTTAGATTTT
	Seq3: GTGGAGGGTTTTGAT
	Seq4: TTTTTTAAGAAAGTTGGGATT

4 Conclusion and future plans

Epithelial-mesenchymal transition (EMT) represents cellular plasticity, which involves dynamic switches from epithelial to mesenchymal cell states. EMT is a process that endows stationary epithelial tumor cells with increased motility and invasiveness. The reverse process MET is required for the metastatic outgrowth in distant tissues. Hence, elucidating the regulatory mechanisms during epithelial-mesenchymal plasticity provides important insights to prevent metastasis.

In this study, we used a different approach to study the epithelial mesenchymal plasticity by comparing irreversible and reversible EMT model systems. During characterization of these two EMT systems, we noticed that irreversible and reversible EMT cells exhibit *in vitro* and *in vivo* differences. We observed different expression levels of EMT markers as well as differences in the whole transcriptome identified by RNA-sequencing. We determined 6624 differentially regulated genes in the irreversible EMT cells compared to the reversible EMT cells. Further, *in vivo* analysis indicated that the irreversible mesenchymal cells exhibit higher tumor initiation, tumor formation and ability to home in to the lungs than the reversible EMT cells. It is important to note that even though we observed mesenchymal primary tumors, we do not have evidence whether they retain their mesenchymal state in the metastatic site. These results may indicate the existence of the different mesenchymal cell types and states, with different EMT signatures and functional properties.

We provided evidence for the differences in epigenetic modifiers between the irreversible and reversible EMT cells. We showed that the Mbd3/NuRD complex involving histone deacetylases (HDACs) and Tet2 hydroxylase act in the maintenance of the mesenchymal state in the irreversible EMT cells. Additionally, we deduced a list of genes that are regulated by Mbd3, Tet2 in the absence and presence of HDACs in the irreversible EMT cells. We further reported the depletion of Mbd3, Tet2 in the absence and presence of HDAC inhibitor led to a mesenchymal-epithelial transition (MET), as well as diminishing the tumor growth and metastasis.

Deeper mechanistic details of the working principles and the regulatory networks of these molecules during the cell state transitions of EMT are required to be explained. This will give us a broad perspective to understand the genome-wide regulation of the cell plasticity by epigenetic regulators during malignant tumor progression and metastasis. Further studies could help to identify specific inhibitors for the TET enzymes and the combination treatments with HDAC inhibitors could open a new avenue for more effective therapy. Instead of the targeting single gene mutations, epigenetic modifiers are more attractive therapeutic targets due to their wide spread acting mechanisms and reversible nature.

5 References

1. Allis, C. D., and Jenuwein, T. (2016). The molecular hallmarks of epigenetic control. Nat Rev Genet *17*, 487-500.
2. Apostolou, E., and Hochedlinger, K. (2013). Chromatin dynamics during cellular reprogramming. Nature *502*, 462-471.
3. Araya, J., Cambier, S., Morris, A., Finkbeiner, W., and Nishimura, S. L. (2006). Integrin-Mediated Transforming Growth Factor-β Activation Regulates Homeostasis of the Pulmonary Epithelial-Mesenchymal Trophic Unit. The American Journal of Pathology *169*, 405-415.
4. Bannister, A. J., and Kouzarides, T. (2011). Regulation of chromatin by histone modifications. Cell Research *21*, 381-395.
5. Bartel, D. P. (2004). MicroRNAs: Genomics, Biogenesis, Mechanism, and Function. Cell *116*, 281-297.
6. Baubec, T., Ivánek, R., Lienert, F., and Schübeler, D. (2013). Methylation-Dependent and -Independent Genomic Targeting Principles of the MBD Protein Family. Cell *153*, 480-492.
7. Baum, B., Settleman, J., and Quinlan, M. P. (2008). Transitions between epithelial and mesenchymal states in development and disease. Seminars in Cell & Developmental Biology *19*, 294-308.
8. Beck, B., and Blanpain, C. (2013). Unravelling cancer stem cell potential. Nat Rev Cancer *13*, 727-738.
9. Beckers, T., Burkhardt, C., Wieland, H., Gimmnich, P., Ciossek, T., Maier, T., and Sanders, K. (2007). Distinct pharmacological properties of second generation HDAC inhibitors with the benzamide or hydroxamate head group. International Journal of Cancer *121*, 1138-1148.
10. Bedi, U., Mishra, V. K., Wasilewski, D., Scheel, C., and Johnsen, S. A. (2014). Epigenetic plasticity: A central regulator of epithelial-to-mesenchymal transition in cancer. Oncotarget *5*, 2016-2029.
11. Bernstein, B. E., Mikkelsen, T. S., Xie, X., Kamal, M., Huebert, D. J., Cuff, J., Fry, B., Meissner, A., Wernig, M., Plath, K.*, et al.* (2006). A Bivalent Chromatin Structure Marks Key Developmental Genes in Embryonic Stem Cells. Cell *125*, 315-326.
12. Bertos, N. R., and Park, M. (2011). Breast cancer — one term, many entities? The Journal of Clinical Investigation *121*, 3789-3796.
13. Berx, G., Raspé, E., Christofori, G., Thiery, J. P., and Sleeman, J. P. (2007). Pre-EMTing metastasis? Recapitulation of morphogenetic processes in cancer. Clinical & Experimental Metastasis *24*, 587-597.
14. Bill, R., and Christofori, G. (2015). The relevance of EMT in breast cancer metastasis: Correlation or causality? FEBS Letters *589*, 1577-1587.
15. Bird, A. (2002). DNA methylation patterns and epigenetic memory. Genes & Development *16*, 6-21.
16. Bonnans, C., Chou, J., and Werb, Z. (2014). Remodelling the extracellular matrix in development and disease. Nat Rev Mol Cell Biol *15*, 786-801.
17. Brabletz, T. (2012). To differentiate or not — routes towards metastasis. Nat Rev Cancer *12*, 425-436.

18. Brown, R. L., Reinke, L. M., Damerow, M. S., Perez, D., Chodosh, L. A., Yang, J., and Cheng, C. (2011). CD44 splice isoform switching in human and mouse epithelium is essential for epithelial-mesenchymal transition and breast cancer progression. J Clin Invest *121*, 1064-1074.
19. Burk, U., Schubert, J., Wellner, U., Schmalhofer, O., Vincan, E., Spaderna, S., and Brabletz, T. (2008). A reciprocal repression between ZEB1 and members of the miR-200 family promotes EMT and invasion in cancer cells. EMBO Reports *9*, 582-589.
20. Cano, A., Perez-Moreno, M. A., Rodrigo, I., Locascio, A., Blanco, M. J., del Barrio, M. G., Portillo, F., and Nieto, M. A. (2000). The transcription factor Snail controls epithelial-mesenchymal transitions by repressing E-cadherin expression. Nat Cell Biol *2*, 76-83.
21. Cao, Q., Yu, J., Dhanasekaran, S. M., Kim, J. H., Mani, R. S., Tomlins, S. A., Mehra, R., Laxman, B., Cao, X., Yu, J.*, et al.* (2008). Repression of E-cadherin by the polycomb group protein EZH2 in cancer. Oncogene *27*, 7274-7284.
22. Cardenas, H., Vieth, E., Lee, J., Segar, M., Liu, Y., Nephew, K. P., and Matei, D. (2014). TGF-beta induces global changes in DNA methylation during the epithelial-to-mesenchymal transition in ovarian cancer cells. Epigenetics *9*, 1461-1472.
23. Cavallaro, U., Schaffhauser, B., and Christofori, G. (2002). Cadherins and the tumour progression: is it all in a switch? Cancer Letters *176*, 123-128.
24. Chaffer, C. L., Marjanovic, N. D., Lee, T., Bell, G., Kleer, C. G., Reinhardt, F., D'Alessio, A. C., Young, R. A., and Weinberg, R. A. (2013). Poised chromatin at the ZEB1 promoter enables cell plasticity and enhances tumorigenicity. Cell *154*, 61-74.
25. Chambers, A. F., Groom, A. C., and MacDonald, I. C. (2002). Metastasis: Dissemination and growth of cancer cells in metastatic sites. Nat Rev Cancer *2*, 563-572.
26. Chang, R., Zhang, Y., Zhang, P., and Zhou, Q. (2017). Snail acetylation by histone acetyltransferase p300 in lung cancer. Thoracic Cancer *8*, 131-137.
27. Cheng, C. W., Wu, P. E., Yu, J. C., Huang, C. S., Yue, C. T., Wu, C. W., and Shen, C. Y. (2001). Mechanisms of inactivation of E-cadherin in breast carcinoma: modification of the two-hit hypothesis of tumor suppressor gene. Oncogene *20*, 3814-3823.
28. Christofori, G. (2003). Changing neighbours, changing behaviour: cell adhesion molecule‐mediated signalling during tumour progression. The EMBO Journal *22*, 2318-2323.
29. Christofori, G. (2006). New signals from the invasive front. Nature *441*, 444-450.
30. Cimmino, L., Abdel-Wahab, O., Levine, Ross L., and Aifantis, I. (2011). TET Family Proteins and Their Role in Stem Cell Differentiation and Transformation. Cell Stem Cell *9*, 193-204.
31. Collett, K., Eide, G. E., Arnes, J., Stefansson, I. M., Eide, J., Braaten, A., Aas, T., Otte, A. P., and Akslen, L. A. (2006). Expression of enhancer of zeste homologue 2 is significantly associated with increased tumor cell proliferation and is a marker of aggressive breast cancer. Clinical Cancer Research *12*, 1168-1174.

32. Coradini, D., Zorzet, S., Rossin, R., Scarlata, I., Pellizzaro, C., Turrin, C., Bello, M., Cantoni, S., Speranza, A., Sava, G.*, et al.* (2004). Inhibition of Hepatocellular Carcinomas in vitro and Hepatic Metastases in vivo in Mice by the Histone Deacetylase Inhibitor HA-But. Clinical Cancer Research *10*, 4822-4830.
33. Crea, F., Paolicchi, E., Marquez, V. E., and Danesi, R. (2012). Polycomb genes and cancer: Time for clinical application? Critical Reviews in Oncology/Hematology *83*, 184-193.
34. Davalos, V., Moutinho, C., Villanueva, A., Boque, R., Silva, P., Carneiro, F., and Esteller, M. (2012). Dynamic epigenetic regulation of the microRNA-200 family mediates epithelial and mesenchymal transitions in human tumorigenesis. Oncogene *31*, 2062-2074.
35. Davis, F. M., Stewart, T. A., Thompson, E. W., and Monteith, G. R. (2014). Targeting EMT in cancer: opportunities for pharmacological intervention. Trends in Pharmacological Sciences *35*, 479-488.
36. De Moerlooze, L., Spencer-Dene, B., Revest, J. M., Hajihosseini, M., Rosewell, I., and Dickson, C. (2000). An important role for the IIIb isoform of fibroblast growth factor receptor 2 (FGFR2) in mesenchymal-epithelial signalling during mouse organogenesis. Development *127*, 483-492.
37. De Raedt, T., Beert, E., Pasmant, E., Luscan, A., Brems, H., Ortonne, N., Helin, K., Hornick, J. L., Mautner, V., Kehrer-Sawatzki, H.*, et al.* (2014). PRC2 loss amplifies Ras-driven transcription and confers sensitivity to BRD4-based therapies. Nature *514*, 247-251.
38. Denslow, S. A., and Wade, P. A. (2007). The human Mi-2/NuRD complex and gene regulation. Oncogene *26*, 5433-5438.
39. Di Croce, L., and Helin, K. (2013). Transcriptional regulation by Polycomb group proteins. Nat Struct Mol Biol *20*, 1147-1155.
40. Diepenbruck, M., and Christofori, G. (2016). Epithelial-mesenchymal transition (EMT) and metastasis: yes, no, maybe? Curr Opin Cell Biol *43*, 7-13.
41. Dobin, A., Davis, C. A., Schlesinger, F., Drenkow, J., Zaleski, C., Jha, S., Batut, P., Chaisson, M., and Gingeras, T. R. (2013). STAR: ultrafast universal RNA-seq aligner. Bioinformatics *29*, 15-21.
42. Dong, C., Wu, Y., Wang, Y., Wang, C., Kang, T., Rychahou, P. G., Chi, Y.-I., Evers, B. M., and Zhou, B. P. (2013). Interaction with Suv39H1 is Critical for Snail-mediated E-cadherin Repression in Breast Cancer. Oncogene *32*, 1351-1362.
43. Dong, C., Wu, Y., Yao, J., Wang, Y., Yu, Y., Rychahou, P. G., Evers, B. M., and Zhou, B. P. (2012). G9a interacts with Snail and is critical for Snail-mediated E-cadherin repression in human breast cancer. The Journal of Clinical Investigation *122*, 1469-1486.
44. Dumont, N., Wilson, M. B., Crawford, Y. G., Reynolds, P. A., Sigaroudinia, M., and Tlsty, T. D. (2008). Sustained induction of epithelial to mesenchymal transition activates DNA methylation of genes silenced in basal-like breast cancers. Proceedings of the National Academy of Sciences *105*, 14867-14872.

45. Eberharter, A., and Becker, P. B. (2002). Histone acetylation: a switch between repressive and permissive chromatin: Second in review series on chromatin dynamics. EMBO Reports *3*, 224-229.
46. Elloul, S., Elstrand, M. B., Nesland, J. M., Trope, C. G., Kvalheim, G., Goldberg, I., Reich, R., and Davidson, B. (2005). Snail, Slug, and Smad-interacting protein 1 as novel parameters of disease aggressiveness in metastatic ovarian and breast carcinoma. Cancer *103*, 1631-1643.
47. Ellsworth, R. E., Blackburn, H. L., Shriver, C. D., Soon-Shiong, P., and Ellsworth, D. L. (2017). Molecular heterogeneity in breast cancer: State of the science and implications for patient care. Seminars in Cell & Developmental Biology *64*, 65-72.
48. Eswarakumar, V. P., Monsonego-Ornan, E., Pines, M., Antonopoulou, I., Morriss-Kay, G. M., and Lonai, P. (2002). The IIIc alternative of Fgfr2 is a positive regulator of bone formation. Development *129*, 3783-3793.
49. Ferrari-Amorotti, G., Chiodoni, C., Shen, F., Cattelani, S., Soliera, A. R., Manzotti, G., Grisendi, G., Dominici, M., Rivasi, F., Colombo, M. P.*, et al.* (2014). Suppression of Invasion and Metastasis of Triple-Negative Breast Cancer Lines by Pharmacological or Genetic Inhibition of Slug Activity. Neoplasia *16*, 1047-1058.
50. Ferrari-Amorotti, G., Fragliasso, V., Esteki, R., Prudente, Z., Soliera, A. R., Cattelani, S., Manzotti, G., Grisendi, G., Dominici, M., Pieraccioli, M.*, et al.* (2013). Inhibiting Interactions of Lysine Demethylase LSD1 with Snail/Slug Blocks Cancer Cell Invasion. Cancer Research *73*, 235-245.
51. Fici, P., Gallerani, G., Morel, A.-P., Mercatali, L., Ibrahim, T., Scarpi, E., Amadori, D., Puisieux, A., Rigaud, M., and Fabbri, F. (2017). Splicing factor ratio as an index of epithelial-mesenchymal transition and tumor aggressiveness in breast cancer. Oncotarget *8*, 2423-2436.
52. Fraga, M. F., Ballestar, E., Montoya, G., Taysavang, P., Wade, P. A., and Esteller, M. (2003). The affinity of different MBD proteins for a specific methylated locus depends on their intrinsic binding properties. Nucleic Acids Research *31*, 1765-1774.
53. Friedman, R. C., Farh, K. K.-H., Burge, C. B., and Bartel, D. P. (2009). Most mammalian mRNAs are conserved targets of microRNAs. Genome Research *19*, 92-105.
54. Fu, J., Qin, L., He, T., Qin, J., Hong, J., Wong, J., Liao, L., and Xu, J. (2011). The TWIST/Mi2/NuRD protein complex and its essential role in cancer metastasis. Cell Res *21*, 275-289.
55. Fujita, N., Jaye, D. L., Kajita, M., Geigerman, C., Moreno, C. S., and Wade, P. A. (2003). MTA3, a Mi-2/NuRD Complex Subunit, Regulates an Invasive Growth Pathway in Breast Cancer. Cell *113*, 207-219.
56. Gaidatzis, D., Lerch, A., Hahne, F., and Stadler, M. B. (2015). QuasR: quantification and annotation of short reads in R. Bioinformatics *31*, 1130-1132.
57. Giepmans, B. N. G., and van Ijzendoorn, S. C. D. (2009). Epithelial cell–cell junctions and plasma membrane domains. Biochimica et Biophysica Acta (BBA) - Biomembranes *1788*, 820-831.
58. Gjorevski, N., Boghaert, E., and Nelson, C. M. (2012). Regulation of Epithelial-Mesenchymal Transition by Transmission of Mechanical Stress through Epithelial Tissues. Cancer Microenvironment *5*, 29-38.

59. Glozak, M. A., and Seto, E. (2007). Histone deacetylases and cancer. Oncogene *26*, 5420-5432.
60. Grady, W. M., Willis, J., Guilford, P. J., Dunbier, A. K., Toro, T. T., Lynch, H., Wiesner, G., Ferguson, K., Eng, C., Park, J.-G.*, et al.* (2000). Methylation of the CDH1 promoter as the second genetic hit in hereditary diffuse gastric cancer. Nat Genet *26*, 16-17.
61. Graff, J. R., Herman, J. G., Lapidus, R. G., Chopra, H., Xu, R., Jarrard, D. F., Isaacs, W. B., Pitha, P. M., Davidson, N. E., and Baylin, S. B. (1995). E-Cadherin Expression Is Silenced by DNA Hypermethylation in Human Breast and Prostate Carcinomas. Cancer Research *55*, 5195-5199.
62. Gregory, P. A., Bert, A. G., Paterson, E. L., Barry, S. C., Tsykin, A., Farshid, G., Vadas, M. A., Khew-Goodall, Y., and Goodall, G. J. (2008). The miR-200 family and miR-205 regulate epithelial to mesenchymal transition by targeting ZEB1 and SIP1. Nat Cell Biol *10*, 593-601.
63. Grozinger, C. M., and Schreiber, S. L. (2002). Deacetylase Enzymes: Biological Functions and the Use of Small-Molecule Inhibitors. Chemistry & Biology *9*, 3-16.
64. Haberland, M., Montgomery, R. L., and Olson, E. N. (2009). The many roles of histone deacetylases in development and physiology: implications for disease and therapy. Nat Rev Genet *10*, 32-42.
65. Hanahan, D., and Weinberg, Robert A. (2011). Hallmarks of Cancer: The Next Generation. Cell *144*, 646-674.
66. Hay, E. D. (1995). An overview of epithelio-mesenchymal transformation. Acta Anat (Basel) *154*, 8-20.
67. Hayakawa, T., and Nakayama, J. (2011). Physiological roles of class I HDAC complex and histone demethylase. J Biomed Biotechnol *2011*, 129383.
68. Hendrich, B., Guy, J., Ramsahoye, B., Wilson, V. A., and Bird, A. (2001). Closely related proteins MBD2 and MBD3 play distinctive but interacting roles in mouse development. Genes & Development *15*, 710-723.
69. Hendrich, B., and Tweedie, S. (2003). The methyl-CpG binding domain and the evolving role of DNA methylation in animals. Trends in Genetics *19*, 269-277.
70. Herranz, N., Pasini, D., Díaz, V. M., Francí, C., Gutierrez, A., Dave, N., Escrivà, M., Hernandez-Muñoz, I., Di Croce, L., Helin, K.*, et al.* (2008). Polycomb Complex 2 Is Required for E-cadherin Repression by the Snail1 Transcription Factor. Molecular and Cellular Biology *28*, 4772-4781.
71. Hoot, K. E., Lighthall, J., Han, G., Lu, S.-L., Li, A., Ju, W., Kulesz-Martin, M., Bottinger, E., and Wang, X.-J. (2008). Keratinocyte-specific Smad2 ablation results in increased epithelial-mesenchymal transition during skin cancer formation and progression. The Journal of Clinical Investigation *118*, 2722-2732.
72. Hsu, Dennis S.-S., Wang, H.-J., Tai, S.-K., Chou, C.-H., Hsieh, C.-H., Chiu, P.-H., Chen, N.-J., and Yang, M.-H. (2014). Acetylation of Snail Modulates the Cytokinome of Cancer Cells to Enhance the Recruitment of Macrophages. Cancer Cell *26*, 534-548.
73. Hsu, Y.-L., Huang, M.-S., Yang, C.-J., Hung, J.-Y., Wu, L.-Y., and Kuo, P.-L. (2011). Lung Tumor-associated Osteoblast-derived Bone Morphogenetic Protein-2 Increased Epithelial-to-Mesenchymal Transition of Cancer by

Runx2/Snail Signaling Pathway. Journal of Biological Chemistry *286*, 37335-37346.
74. Hu, X., Zhang, L., Mao, S.-Q., Li, Z., Chen, J., Zhang, R.-R., Wu, H.-P., Gao, J., Guo, F., Liu, W.*, et al.* (2014). Tet and TDG Mediate DNA Demethylation Essential for Mesenchymal-to-Epithelial Transition in Somatic Cell Reprogramming. Cell Stem Cell *14*, 512-522.
75. Huang, R. Y.-J., Guilford, P., and Thiery, J. P. (2012). Early events in cell adhesion and polarity during epithelial-mesenchymal transition. Journal of Cell Science *125*, 4417-4422.
76. Hynes, R. O. (2002). Integrins: Bidirectional, Allosteric Signaling Machines. Cell *110*, 673-687.
77. Iwano, M., Plieth, D., Danoff, T. M., Xue, C., Okada, H., and Neilson, E. G. (2002). Evidence that fibroblasts derive from epithelium during tissue fibrosis. The Journal of Clinical Investigation *110*, 341-350.
78. Jaffe, A. B., and Hall, A. (2005). RHO GTPASES: Biochemistry and Biology. Annual Review of Cell and Developmental Biology *21*, 247-269.
79. Jiang, G.-M., Wang, H.-S., Zhang, F., Zhang, K.-S., Liu, Z.-C., Fang, R., Wang, H., Cai, S.-H., and Du, J. (2013). Histone deacetylase inhibitor induction of epithelial–mesenchymal transitions via up-regulation of Snail facilitates cancer progression. Biochimica et Biophysica Acta (BBA) - Molecular Cell Research *1833*, 663-671.
80. Johnson, W. E., Li, C., and Rabinovic, A. (2007). Adjusting batch effects in microarray expression data using empirical Bayes methods. Biostatistics *8*, 118-127.
81. Jordan, V. C., and Brodie, A. M. H. (2007). Development and evolution of therapies targeted to the estrogen receptor for the treatment and prevention of breast cancer. Steroids *72*, 7-25.
82. Kaji, K., Caballero, I. M., MacLeod, R., Nichols, J., Wilson, V. A., and Hendrich, B. (2006). The NuRD component Mbd3 is required for pluripotency of embryonic stem cells. Nat Cell Biol *8*, 285-292.
83. Kaji, K., Nichols, J., and Hendrich, B. (2007). Mbd3, a component of the NuRD co-repressor complex, is required for development of pluripotent cells. Development *134*, 1123-1132.
84. Kallergi, G., Papadaki, M. A., Politaki, E., Mavroudis, D., Georgoulias, V., and Agelaki, S. (2011). Epithelial to mesenchymal transition markers expressed in circulating tumour cells of early and metastatic breast cancer patients. Breast Cancer Research *13*, R59.
85. Kalluri, R., and Weinberg, R. A. (2009). The basics of epithelial-mesenchymal transition. The Journal of Clinical Investigation *119*, 1420-1428.
86. Kirchner, T., and Brabletz, T. (2000). Patterning and Nuclear β-Catenin Expression in the Colonic Adenoma-Carcinoma Sequence: Analogies with Embryonic Gastrulation. The American Journal of Pathology *157*, 1113-1121.
87. Kleer, C. G., Cao, Q., Varambally, S., Shen, R., Ota, I., Tomlins, S. A., Ghosh, D., Sewalt, R. G. A. B., Otte, A. P., Hayes, D. F.*, et al.* (2003). EZH2 is a marker of aggressive breast cancer and promotes neoplastic transformation of breast epithelial cells. Proceedings of the National Academy of Sciences *100*, 11606-11611.

88. Klein, C. A. (2009). Parallel progression of primary tumours and metastases. Nat Rev Cancer *9*, 302-312.
89. Knutson, S. K., Wigle, T. J., Warholic, N. M., Sneeringer, C. J., Allain, C. J., Klaus, C. R., Sacks, J. D., Raimondi, A., Majer, C. R., Song, J.*, et al.* (2012). A selective inhibitor of EZH2 blocks H3K27 methylation and kills mutant lymphoma cells. Nat Chem Biol *8*, 890-896.
90. Kong, D., Ahmad, A., Bao, B., Li, Y., Banerjee, S., and Sarkar, F. H. (2012). Histone Deacetylase Inhibitors Induce Epithelial-to-Mesenchymal Transition in Prostate Cancer Cells. PLoS ONE *7*, e45045.
91. Korpal, M., Lee, E. S., Hu, G., and Kang, Y. (2008). The miR-200 family inhibits epithelial-mesenchymal transition and cancer cell migration by direct targeting of E-cadherin transcriptional repressors ZEB1 and ZEB2. The Journal of biological chemistry *283*, 14910-14914.
92. Kouzarides, T. (2007). Chromatin Modifications and Their Function. Cell *128*, 693-705.
93. Lai, A. Y., and Wade, P. A. (2011). Cancer biology and NuRD: a multifaceted chromatin remodelling complex. Nat Rev Cancer *11*, 588-596.
94. Lamouille, S., Xu, J., and Derynck, R. (2014). Molecular mechanisms of epithelial–mesenchymal transition. Nature reviews Molecular cell biology *15*, 178-196.
95. Lapidus, R. G., Ferguson, A. T., Ottaviano, Y. L., Parl, F. F., Smith, H. S., Weitzman, S. A., Baylin, S. B., Issa, J. P., and Davidson, N. E. (1996). Methylation of estrogen and progesterone receptor gene 5' CpG islands correlates with lack of estrogen and progesterone receptor gene expression in breast tumors. Clinical Cancer Research *2*, 805-810.
96. Lee, M. G., Wynder, C., Cooch, N., and Shiekhattar, R. (2005). An essential role for CoREST in nucleosomal histone 3 lysine 4 demethylation. Nature *437*, 432-435.
97. Li, R., Liang, J., Ni, S., Zhou, T., Qing, X., Li, H., He, W., Chen, J., Li, F., Zhuang, Q.*, et al.* (2010). A Mesenchymal-to-Epithelial Transition Initiates and Is Required for the Nuclear Reprogramming of Mouse Fibroblasts. Cell Stem Cell *7*, 51-63.
98. Li, Y., Wan, X., Wei, Y., Liu, X., Lai, W., Zhang, L., Jin, J., Wu, C., Shao, Q., Shao, G., and Lin, Q. (2016). LSD1-mediated epigenetic modification contributes to ovarian cancer cell migration and invasion. Oncology reports *35*, 3586-3592.
99. Lim, S., Janzer, A., Becker, A., Zimmer, A., Schüle, R., Buettner, R., and Kirfel, J. (2010). Lysine-specific demethylase 1 (LSD1) is highly expressed in ER-negative breast cancers and a biomarker predicting aggressive biology. Carcinogenesis *31*, 512-520.
100. Lin, T., Ponn, A., Hu, X., Law, B. K., and Lu, J. (2010a). Requirement of the histone demethylase LSD1 in Snai1-mediated transcriptional repression during epithelial-mesenchymal transition. Oncogene *29*, 4896-4904.
101. Lin, Y., Wu, Y., Li, J., Dong, C., Ye, X., Chi, Y. I., Evers, B. M., and Zhou, B. P. (2010b). The SNAG domain of Snail1 functions as a molecular hook for recruiting lysine‐specific demethylase 1. The EMBO Journal *29*, 1803-1816.

102. Liu, B., Pan, C.-F., He, Z.-C., Wang, J., Wang, P.-L., Ma, T., Xia, Y., and Chen, Y.-J. (2016). Long Noncoding RNA-LET Suppresses Tumor Growth and EMT in Lung Adenocarcinoma. BioMed Research International *2016*, 4693471.
103. Liu, Y.-N., Lee, W.-W., Wang, C.-Y., Chao, T.-H., Chen, Y., and Chen, J. H. (2005). Regulatory mechanisms controlling human E-cadherin gene expression. Oncogene *24*, 8277-8290.
104. Luo, H., Shenoy, Anitha K., Li, X., Jin, Y., Jin, L., Cai, Q., Tang, M., Liu, Y., Chen, H., Reisman, D*., et al.* (2016). MOF Acetylates the Histone Demethylase LSD1 to Suppress Epithelial-to-Mesenchymal Transition. Cell Reports *15*, 2665-2678.
105. Malouf, G. G., Taube, J. H., Lu, Y., Roysarkar, T., Panjarian, S., Estecio, M. R., Jelinek, J., Yamazaki, J., Raynal, N. J.-M., Long, H*., et al.* (2013). Architecture of epigenetic reprogramming following Twist1-mediated epithelial-mesenchymal transition. Genome Biology *14*, R144.
106. Martin, T. A., Goyal, A., Watkins, G., and Jiang, W. G. (2005). Expression of the transcription factors snail, slug, and twist and their clinical significance in human breast cancer. Annals of surgical oncology *12*, 488-496.
107. Maschler, S., Wirl, G., Spring, H., Bredow, D. v., Sordat, I., Beug, H., and Reichmann, E. (2005). Tumor cell invasiveness correlates with changes in integrin expression and localization. *24*, 2032-2041.
108. McDonald, O. G., Wu, H., Timp, W., Doi, A., and Feinberg, A. P. (2011). Genome-scale epigenetic reprogramming during epithelial-to-mesenchymal transition. Nat Struct Mol Biol *18*, 867-874.
109. Mehlen, P., and Puisieux, A. (2006). Metastasis: a question of life or death. Nat Rev Cancer *6*, 449-458.
110. Meidhof, S., Brabletz, S., Lehmann, W., Preca, B. T., Mock, K., Ruh, M., Schüler, J., Berthold, M., Weber, A., Burk, U*., et al.* (2015). ZEB1‐associated drug resistance in cancer cells is reversed by the class I HDAC inhibitor mocetinostat. EMBO Molecular Medicine *7*, 831-847.
111. Mendell, J. T. (2005). MicroRNAs: critical regulators of development, cellular physiology and malignancy. Cell Cycle *4*, 1179-1184.
112. Metzger, E., Wissmann, M., Yin, N., Muller, J. M., Schneider, R., Peters, A. H. F. M., Gunther, T., Buettner, R., and Schule, R. (2005). LSD1 demethylates repressive histone marks to promote androgen-receptor-dependent transcription. Nature *437*, 436-439.
113. Miettinen, P. J., Ebner, R., Lopez, A. R., and Derynck, R. (1994). TGF-beta induced transdifferentiation of mammary epithelial cells to mesenchymal cells: involvement of type I receptors. The Journal of Cell Biology *127*, 2021-2036.
114. Mills, A. A. (2010). Throwing the cancer switch: reciprocal roles of polycomb and trithorax proteins. Nat Rev Cancer *10*, 669-682.
115. Mottamal, M., Zheng, S., Huang, T. L., and Wang, G. (2015). Histone Deacetylase Inhibitors in Clinical Studies as Templates for New Anticancer Agents. Molecules (Basel, Switzerland) *20*, 3898-3941.
116. Nass, S. J., Herman, J. G., Gabrielson, E., Iversen, P. W., Parl, F. F., Davidson, N. E., and Graff, J. R. (2000). Aberrant Methylation of the

Estrogen Receptor and E-Cadherin 5′ CpG Islands Increases with Malignant Progression in Human Breast Cancer. Cancer Research *60*, 4346-4348.

117. Nelson, W. J. (2009). Remodeling Epithelial Cell Organization: Transitions Between Front–Rear and Apical–Basal Polarity. Cold Spring Harbor Perspectives in Biology *1*, a000513.

118. Neves, R., Scheel, C., Weinhold, S., Honisch, E., Iwaniuk, K. M., Trompeter, H.-I., Niederacher, D., Wernet, P., Santourlidis, S., and Uhrberg, M. (2010). Role of DNA methylation in miR-200c/141 cluster silencing in invasive breast cancer cells. BMC Research Notes *3*, 219.

119. Nieto, M. A. (2011). The Ins and Outs of the Epithelial to Mesenchymal Transition in Health and Disease. Annual Review of Cell and Developmental Biology *27*, 347-376.

120. Nieto, M. A. (2013). Epithelial Plasticity: A Common Theme in Embryonic and Cancer Cells. Science *342*.

121. Nieto, M. A., Huang, Ruby Y.-J., Jackson, Rebecca A., and Thiery, Jean P. (2016). EMT: 2016. Cell *166*, 21-45.

122. Noreen, F., Röösli, M., Gaj, P., Pietrzak, J., Weis, S., Urfer, P., Regula, J., Schär, P., and Truninger, K. (2014). Modulation of Age- and Cancer-Associated DNA Methylation Change in the Healthy Colon by Aspirin and Lifestyle. JNCI: Journal of the National Cancer Institute *106*, dju161-dju161.

123. Ocaña, Oscar H., Córcoles, R., Fabra, Á., Moreno-Bueno, G., Acloque, H., Vega, S., Barrallo-Gimeno, A., Cano, A., and Nieto, M. A. (2012). Metastatic Colonization Requires the Repression of the Epithelial-Mesenchymal Transition Inducer Prrx1. Cancer Cell *22*, 709-724.

124. Oktyabri, D., Tange, S., Terashima, M., Ishimura, A., and Suzuki, T. (2014). EED regulates epithelial–mesenchymal transition of cancer cells induced by TGF-β. Biochemical and Biophysical Research Communications *453*, 124-130.

125. Ottaviano, Y. L., Issa, J.-P., Parl, F. F., Smith, H. S., Baylin, S. B., and Davidson, N. E. (1994). Methylation of the Estrogen Receptor Gene CpG Island Marks Loss of Estrogen Receptor Expression in Human Breast Cancer Cells. Cancer Research *54*, 2552-2555.

126. Paranjape, A. N., Balaji, S. A., Mandal, T., Krushik, E. V., Nagaraj, P., Mukherjee, G., and Rangarajan, A. (2014). Bmi1 regulates self-renewal and epithelial to mesenchymal transition in breast cancer cells through Nanog. BMC Cancer *14*, 785.

127. Peinado, H., Ballestar, E., Esteller, M., and Cano, A. (2004). Snail Mediates E-Cadherin Repression by the Recruitment of the Sin3A/Histone Deacetylase 1 (HDAC1)/HDAC2 Complex. Molecular and Cellular Biology *24*, 306-319.

128. Phillips, S., Prat, A., Sedic, M., Proia, T., Wronski, A., Mazumdar, S., Skibinski, A., Shirley, Stephanie H., Perou, Charles M., Gill, G.*, et al.* (2014). Cell-State Transitions Regulated by SLUG Are Critical for Tissue Regeneration and Tumor Initiation. Stem Cell Reports *2*, 633-647.

129. Pino, M. S., Balsamo, M., Di Modugno, F., Mottolese, M., Alessio, M., Melucci, E., Milella, M., McConkey, D. J., Philippar, U., Gertler, F. B.*, et al.* (2008). Human Mena+11a isoform serves as a marker of epithelial

phenotype and sensitivity to epidermal growth factor receptor inhibition in human pancreatic cancer cell lines. Clin Cancer Res *14*, 4943-4950.
130. Polo, J. M., and Hochedlinger, K. (2010). When Fibroblasts MET iPSCs. Cell Stem Cell *7*, 5-6.
131. Prat, A., Parker, J. S., Karginova, O., Fan, C., Livasy, C., Herschkowitz, J. I., He, X., and Perou, C. M. (2010). Phenotypic and molecular characterization of the claudin-low intrinsic subtype of breast cancer. Breast Cancer Research *12*, R68.
132. Puppe, J., Drost, R., Liu, X., Joosse, S. A., Evers, B., Cornelissen-Steijger, P., Nederlof, P., Yu, Q., Jonkers, J., van Lohuizen, M., and Pietersen, A. M. (2009). BRCA1-deficient mammary tumor cells are dependent on EZH2 expression and sensitive to Polycomb Repressive Complex 2-inhibitor 3-deazaneplanocin A. Breast Cancer Research *11*, R63.
133. Radisky, D. C. (2005). Epithelial-mesenchymal transition. Journal of Cell Science *118*, 4325-4326.
134. Rais, Y., Zviran, A., Geula, S., Gafni, O., Chomsky, E., Viukov, S., Mansour, A. A., Caspi, I., Krupalnik, V., Zerbib, M., *et al.* (2013). Deterministic direct reprogramming of somatic cells to pluripotency. Nature *502*, 65-70.
135. Robertson, K. D. (2005). DNA methylation and human disease. Nat Rev Genet *6*, 597-610.
136. Robinson, M. D., McCarthy, D. J., and Smyth, G. K. (2010). edgeR: a Bioconductor package for differential expression analysis of digital gene expression data. Bioinformatics *26*, 139-140.
137. Rodriguez-Boulan, E., and Macara, I. G. (2014). Organization and execution of the epithelial polarity programme. Nat Rev Mol Cell Biol *15*, 225-242.
138. Roth, S. Y., Denu, J. M., and Allis, C. D. (2001). Histone Acetyltransferases. Annual Review of Biochemistry *70*, 81-120.
139. Saito, M., and Ishikawa, F. (2002). The mCpG-binding Domain of Human MBD3 Does Not Bind to mCpG but Interacts with NuRD/Mi2 Components HDAC1 and MTA2. Journal of Biological Chemistry *277*, 35434-35439.
140. Samavarchi-Tehrani, P., Golipour, A., David, L., Sung, H.-k., Beyer, T. A., Datti, A., Woltjen, K., Nagy, A., and Wrana, J. L. (2010). Functional Genomics Reveals a BMP-Driven Mesenchymal-to-Epithelial Transition in the Initiation of Somatic Cell Reprogramming. Cell Stem Cell *7*, 64-77.
141. Schnitt, S. J. (2010). Classification and prognosis of invasive breast cancer: from morphology to molecular taxonomy. Mod Pathol *23*, S60-S64.
142. Schubeler, D. (2015). Function and information content of DNA methylation. Nature *517*, 321-326.
143. Scourzic, L., Mouly, E., and Bernard, O. A. (2015). TET proteins and the control of cytosine demethylation in cancer. Genome Med *7*, 9.
144. Serresi, M., Gargiulo, G., Proost, N., Siteur, B., Cesaroni, M., Koppens, M., Xie, H., Sutherland, K. D., Hulsman, D., Citterio, E., *et al.* (2016). Polycomb Repressive Complex 2 Is a Barrier to KRAS-Driven Inflammation and Epithelial-Mesenchymal Transition in Non-Small-Cell Lung Cancer. Cancer Cell *29*, 17-31.

145. Shi, Y., Lan, F., Matson, C., Mulligan, P., Whetstine, J. R., Cole, P. A., Casero, R. A., and Shi, Y. (2004). Histone Demethylation Mediated by the Nuclear Amine Oxidase Homolog LSD1. Cell *119*, 941-953.
146. Shi, Y., and Massagué, J. (2003). Mechanisms of TGF-β Signaling from Cell Membrane to the Nucleus. Cell *113*, 685-700.
147. Shi, Y.-J., Matson, C., Lan, F., Iwase, S., Baba, T., and Shi, Y. (2005). Regulation of LSD1 Histone Demethylase Activity by Its Associated Factors. Molecular Cell *19*, 857-864.
148. Shirakihara, T., Saitoh, M., and Miyazono, K. (2007). Differential Regulation of Epithelial and Mesenchymal Markers by δEF1 Proteins in Epithelial–Mesenchymal Transition Induced by TGF-β. Molecular Biology of the Cell *18*, 3533-3544.
149. Song, Su J., Poliseno, L., Song, Min S., Ala, U., Webster, K., Ng, C., Beringer, G., Brikbak, Nicolai J., Yuan, X., Cantley, Lewis C.*, et al.* (2013). MicroRNA-Antagonism Regulates Breast Cancer Stemness and Metastasis via TET-Family-Dependent Chromatin Remodeling. Cell *154*, 311-324.
150. Spaderna, S., Schmalhofer, O., Wahlbuhl, M., Dimmler, A., Bauer, K., Sultan, A., Hlubek, F., Jung, A., Strand, D., Eger, A.*, et al.* (2008). The Transcriptional Repressor ZEB1 Promotes Metastasis and Loss of Cell Polarity in Cancer. Cancer Research *68*, 537-544.
151. Srivastava, R. K., Kurzrock, R., and Shankar, S. (2010). MS-275 Sensitizes TRAIL-Resistant Breast Cancer Cells, Inhibits Angiogenesis and Metastasis, and Reverses Epithelial-Mesenchymal Transition In vivo. Molecular Cancer Therapeutics *9*, 3254-3266.
152. Sun, B. O., Fang, Y., Li, Z., Chen, Z., and Xiang, J. (2015). Role of cellular cytoskeleton in epithelial-mesenchymal transition process during cancer progression. Biomedical Reports *3*, 603-610.
153. Tahiliani, M., Koh, K. P., Shen, Y., Pastor, W. A., Bandukwala, H., Brudno, Y., Agarwal, S., Iyer, L. M., Liu, D. R., Aravind, L., and Rao, A. (2009). Conversion of 5-Methylcytosine to 5-Hydroxymethylcytosine in Mammalian DNA by MLL Partner TET1. Science *324*, 930-935.
154. Tam, W. L., and Weinberg, R. A. (2013). The epigenetics of epithelial-mesenchymal plasticity in cancer. Nat Med *19*, 1438-1449.
155. Tang, H. M., Kuay, K. T., Koh, P. F., Asad, M., Tan, T. Z., Chung, V. Y., Lee, S. C., Thiery, J. P., and Huang, R.-J. (2016). An epithelial marker promoter induction screen identifies histone deacetylase inhibitors to restore epithelial differentiation and abolishes anchorage independence growth in cancers. Cell Death Discovery *2*, 16041.
156. Tarin, D. (2005). The Fallacy of Epithelial Mesenchymal Transition in Neoplasia. Cancer Research *65*, 5996-6001.
157. Tate, C. R., Rhodes, L. V., Segar, H. C., Driver, J. L., Pounder, F. N., Burow, M. E., and Collins-Burow, B. M. (2012). Targeting triple-negative breast cancer cells with the histone deacetylase inhibitor panobinostat. Breast Cancer Research *14*, R79.
158. Thiery, J. P. (2002). Epithelial-mesenchymal transitions in tumour progression. Nat Rev Cancer *2*, 442-454.
159. Thiery, J. P., Acloque, H., Huang, R. Y. J., and Nieto, M. A. (2009). Epithelial-Mesenchymal Transitions in Development and Disease. Cell *139*, 871-890.

160. Thiery, J. P., and Sleeman, J. P. (2006). Complex networks orchestrate epithelial-mesenchymal transitions. Nat Rev Mol Cell Biol *7*, 131-142.
161. Thomson, S., Buck, E., Petti, F., Griffin, G., Brown, E., Ramnarine, N., Iwata, K. K., Gibson, N., and Haley, J. D. (2005). Epithelial to Mesenchymal Transition Is a Determinant of Sensitivity of Non–Small-Cell Lung Carcinoma Cell Lines and Xenografts to Epidermal Growth Factor Receptor Inhibition. Cancer Research *65*, 9455-9462.
162. Tiwari, N., Gheldof, A., Tatari, M., and Christofori, G. (2012). EMT as the ultimate survival mechanism of cancer cells. Seminars in Cancer Biology *22*, 194-207.
163. Tiwari, N., Meyer-Schaller, N., Arnold, P., Antoniadis, H., Pachkov, M., van Nimwegen, E., and Christofori, G. (2013a). Klf4 Is a Transcriptional Regulator of Genes Critical for EMT, Including Jnk1 (Mapk8). PLOS ONE *8*, e57329.
164. Tiwari, N., Tiwari, Vijay K., Waldmeier, L., Balwierz, Piotr J., Arnold, P., Pachkov, M., Meyer-Schaller, N., Schübeler, D., van Nimwegen, E., and Christofori, G. (2013b). Sox4 Is a Master Regulator of Epithelial-Mesenchymal Transition by Controlling Ezh2 Expression and Epigenetic Reprogramming. Cancer Cell *23*, 768-783.
165. Tsai, Jeff H., Donaher, Joana L., Murphy, Danielle A., Chau, S., and Yang, J. (2012). Spatiotemporal Regulation of Epithelial-Mesenchymal Transition Is Essential for Squamous Cell Carcinoma Metastasis. Cancer Cell *22*, 725-736.
166. Tsai, J. H., and Yang, J. (2013). Epithelial–mesenchymal plasticity in carcinoma metastasis. Genes & Development *27*, 2192-2206.
167. Turner, B. M. (2007). Defining an epigenetic code. Nat Cell Biol *9*, 2-6.
168. Varambally, S., Dhanasekaran, S. M., Zhou, M., Barrette, T. R., Kumar-Sinha, C., Sanda, M. G., Ghosh, D., Pienta, K. J., Sewalt, R. G. A. B., Otte, A. P.*, et al.* (2002). The polycomb group protein EZH2 is involved in progression of prostate cancer. Nature *419*, 624-629.
169. Venables, J. P., Brosseau, J.-P., Gadea, G., Klinck, R., Prinos, P., Beaulieu, J.-F., Lapointe, E., Durand, M., Thibault, P., Tremblay, K.*, et al.* (2013). RBFOX2 Is an Important Regulator of Mesenchymal Tissue-Specific Splicing in both Normal and Cancer Tissues. Molecular and Cellular Biology *33*, 396-405.
170. Vincent, T., Neve, E. P. A., Johnson, J. R., Kukalev, A., Rojo, F., Albanell, J., Pietras, K., Virtanen, I., Philipson, L., Leopold, P. L.*, et al.* (2009). A SNAIL1-SMAD3/4 transcriptional repressor complex promotes TGF-[beta] mediated epithelial-mesenchymal transition. Nat Cell Biol *11*, 943-950.
171. Vrba, L., Jensen, T. J., Garbe, J. C., Heimark, R. L., Cress, A. E., Dickinson, S., Stampfer, M. R., and Futscher, B. W. (2010). Role for DNA Methylation in the Regulation of miR-200c and miR-141 Expression in Normal and Cancer Cells. PLOS ONE *5*, e8697.
172. Waldmeier, L., Meyer-Schaller, N., Diepenbruck, M., and Christofori, G. (2012). Py2T Murine Breast Cancer Cells, a Versatile Model of TGFβ-Induced EMT In Vitro and In Vivo. PLOS ONE *7*, e48651.

173. Wang, J., Scully, K., Zhu, X., Cai, L., Zhang, J., Prefontaine, G. G., Krones, A., Ohgi, K. A., Zhu, P., Garcia-Bassets, I.*, et al.* (2007). Opposing LSD1 complexes function in developmental gene activation and repression programmes. Nature *446*, 882-887.
174. Wang, M., Liu, X., Guo, J., Weng, X., Jiang, G., Wang, Z., and He, L. (2015). Inhibition of LSD1 by Pargyline inhibited process of EMT and delayed progression of prostate cancer in vivo. Biochemical and Biophysical Research Communications *467*, 310-315.
175. Wang, Y., Zhang, H., Chen, Y., Sun, Y., Yang, F., Yu, W., Liang, J., Sun, L., Yang, X., Shi, L.*, et al.* (2009). LSD1 Is a Subunit of the NuRD Complex and Targets the Metastasis Programs in Breast Cancer. Cell *138*, 660-672.
176. Wang, Y., and Zhou, B. P. (2011). Epithelial-mesenchymal transition in breast cancer progression and metastasis. Chinese Journal of Cancer *30*, 603-611.
177. Warzecha, C. C., Sato, T. K., Nabet, B., Hogenesch, J. B., and Carstens, R. P. (2009). ESRP1 and ESRP2 Are Epithelial Cell-Type-Specific Regulators of FGFR2 Splicing. Molecular Cell *33*, 591-601.
178. Wicki, A., Lehembre, F., Wick, N., Hantusch, B., Kerjaschki, D., and Christofori, G. (2006). Tumor invasion in the absence of epithelial-mesenchymal transition: Podoplanin-mediated remodeling of the actin cytoskeleton. Cancer Cell *9*, 261-272.
179. Wolffe, A. P., Jones, P. L., and Wade, P. A. (1999). DNA demethylation. Proceedings of the National Academy of Sciences *96*, 5894-5896.
180. Xia, R., Jin, F.-y., Lu, K., Wan, L., Xie, M., Xu, T.-p., De, W., and Wang, Z.-x. (2015). SUZ12 promotes gastric cancer cell proliferation and metastasis by regulating KLF2 and E-cadherin. Tumor Biology *36*, 5341-5351.
181. Xiao, M., Yang, H., Xu, W., Ma, S., Lin, H., Zhu, H., Liu, L., Liu, Y., Yang, C., Xu, Y.*, et al.* (2012). Inhibition of α-KG-dependent histone and DNA demethylases by fumarate and succinate that are accumulated in mutations of FH and SDH tumor suppressors. Genes & Development *26*, 1326-1338.
182. Xu, W., Yang, H., Liu, Y., Yang, Y., Wang, P., Kim, S.-H., Ito, S., Yang, C., Wang, P., Xiao, M.-T.*, et al.* (2011). Oncometabolite 2-Hydroxyglutarate Is a Competitive Inhibitor of α-Ketoglutarate-Dependent Dioxygenases. Cancer Cell *19*, 17-30.
183. Xu, Z. Y., Yu, Q. M., Du, Y. A., Yang, L. T., Dong, R. Z., Huang, L., Yu, P. F., and Cheng, X. D. (2013). Knockdown of long non-coding RNA HOTAIR suppresses tumor invasion and reverses epithelial-mesenchymal transition in gastric cancer. International journal of biological sciences *9*, 587-597.
184. Yanagisawa, M., Huveldt, D., Kreinest, P., Lohse, C. M., Cheville, J. C., Parker, A. S., Copland, J. A., and Anastasiadis, P. Z. (2008). A p120 catenin isoform switch affects Rho activity, induces tumor cell invasion, and predicts metastatic disease. The Journal of biological chemistry *283*, 18344-18354.

185. Yang, J., and Weinberg, R. A. (2008). Epithelial-Mesenchymal Transition: At the Crossroads of Development and Tumor Metastasis. Developmental Cell *14*, 818-829.
186. Yang, M.-H., Hsu, D. S.-S., Wang, H.-W., Wang, H.-J., Lan, H.-Y., Yang, W.-H., Huang, C.-H., Kao, S.-Y., Tzeng, C.-H., Tai, S.-K*., et al.* (2010). Bmi1 is essential in Twist1-induced epithelial-mesenchymal transition. Nat Cell Biol *12*, 982-992.
187. Yang, X., Pursell, B., Lu, S., Chang, T.-K., and Mercurio, A. M. (2009). Regulation of β4-integrin expression by epigenetic modifications in the mammary gland and during the epithelial-to-mesenchymal transition. Journal of Cell Science *122*, 2473-2480.
188. Yang, X. J., and Seto, E. (2007). HATs and HDACs: from structure, function and regulation to novel strategies for therapy and prevention. Oncogene *26*, 5310-5318.
189. Yildirim, O., Li, R., Hung, J.-H., Chen, Poshen B., Dong, X., Ee, L.-S., Weng, Z., Rando, Oliver J., and Fazzio, Thomas G. (2011). Mbd3/NURD Complex Regulates Expression of 5-Hydroxymethylcytosine Marked Genes in Embryonic Stem Cells. Cell *147*, 1498-1510.
190. Yilmaz, M., and Christofori, G. (2009). EMT, the cytoskeleton, and cancer cell invasion. Cancer and Metastasis Reviews *28*, 15-33.
191. Yokomizo, C., Yamaguchi, K., Itoh, Y., Nishimura, T., Umemura, A., Minami, M., Yasui, K., Mitsuyoshi, H., Fujii, H., Tochiki, N*., et al.* (2011). High expression of p300 in HCC predicts shortened overall survival in association with enhanced epithelial mesenchymal transition of HCC cells. Cancer Letters *310*, 140-147.
192. Yu, M., Bardia, A., Wittner, B. S., Stott, S. L., Smas, M. E., Ting, D. T., Isakoff, S. J., Ciciliano, J. C., Wells, M. N., Shah, A. M*., et al.* (2013). Circulating Breast Tumor Cells Exhibit Dynamic Changes in Epithelial and Mesenchymal Composition. Science *339*, 580-584.
193. Yuan, J.-h., Yang, F., Wang, F., Ma, J.-z., Guo, Y.-j., Tao, Q.-f., Liu, F., Pan, W., Wang, T.-t., Zhou, C.-c*., et al.* (2014). A Long Noncoding RNA Activated by TGF-β Promotes the Invasion-Metastasis Cascade in Hepatocellular Carcinoma. Cancer Cell *25*, 666-681.
194. Zavadil, J., and Bottinger, E. P. (2005). TGF-[beta] and epithelial-to-mesenchymal transitions. Oncogene *24*, 5764-5774.
195. Zhang, N., Liu, Y., Wang, Y., Zhao, M., Tu, L., and Luo, F. (2017a). Decitabine reverses TGF-β1-induced epithelial–mesenchymal transition in non-small-cell lung cancer by regulating miR-200/ZEB axis. Drug Design, Development and Therapy *11*, 969-983.
196. Zhang, Y., and Reinberg, D. (2001). Transcription regulation by histone methylation: interplay between different covalent modifications of the core histone tails. Genes & Development *15*, 2343-2360.
197. Zhang, Y. W., Wang, Z., Xie, W., Cai, Y., Xia, L., Easwaran, H., Luo, J., Yen, R. C., Li, Y., and Baylin, S. B. (2017b). Acetylation Enhances TET2 Function in Protecting against Abnormal DNA Methylation during Oxidative Stress. Mol Cell *65*, 323-335.

6 Acknowledgments

At the end of my dissertation I would like to thank all those people who made this thesis possible and unforgettable experience for me.

First and foremost, I would like to express my sincere gratitude to my advisor Prof. Gerhard Christofori for his continuous support, encouragement and patience. I am thankful that when I spontaneously walked into his office all the way from Turkey, he gave me an opportunity to make this thesis possible. I feel very lucky to have him as my advisor because of his extensive knowledge, inspiring discussions and giving me the freedom to be independent but being there whenever I need the guidance.

Besides my advisor, I would like to thank to the rest of my committee members Prof. Dirk Schübeler and Prof. Lukas Sommer for their insightful comments and encouragement.

I am thankful to all former and present Christofori group members for the great atmosphere in the lab, all the stimulating discussions, skills, support and for all the fun throughout this thesis. In particular, Helena, Ravi, Dana, Hüseyin, Beena, Maren, Nathalie, Feng, Nami, Agathe, Laura, Marco for their contribution to this thesis and their precious support.

I am grateful to Helena for being such a nice colleague and friend with all her help and support throughout my thesis and for making my past years in Basel lot fun.

I would like to thank to all my great friends Gokce, Tuba, Busra, Esen, Merve, Anina who I know were always there for me with their great support.

My very sincere thanks goes to Petra for all her support and for spending her time to improve my German and Erica for helping me in many aspects during my stay in Basel.

Special thanks goes to my friend/collaborator Amar for cherishing my life, inspiring scientific discussions and for his selfless support, patience, encouragement, love, motivation and precious friendship throughout past years.

Finally, this thesis would not happen without my beloved family, dad, mom, Caglar and Tugce for always being there for me, for their endless love, support, motivation and patience throughout this thesis and my life.
THANK YOU ALL!